





# Seventh Framework Programme FP7-SPACE-2010-1 Stimulating the development of downstream GMES services

Grant agreement for: Collaborative Project. Small- or medium scale focused research project

Project acronym: **SIDARUS** 

Project title: Sea Ice Downstream services for Arctic and Antarctic Users

and Stakeholders

Grant agreement no. 262922
Start date of project: 01.01.11
Duration: 36 months

Project coordinator: Nansen Environmental and Remote Sensing Center, Bergen, Norway

## D4.4: Albedo and meltpond analysis

"Validation and calibration of the MPD retrieval using sea ice and melt pond albedo spectra measured during Polarstern cruise IceArc2012"

Due date of deliverable: 31.12.2013

Actual submission date: 20.01.2014

Organization name of lead contractor for this deliverable: UB

	Project co-funded by the European Commission				
	within the Seventh Framework Programme, Theme 6 SPACE				
	Dissemination Level				
PU	Public	X			
PP	Restricted to other programme participants (including the Commission)				
RE	Restricted to a group specified by the consortium (including the Commission)				
СО	Confidential, only for members of the consortium (including the Commission)				

ISSUE	DATE	CHANGE RECORDS	AUTHOR
1	17/01/2014	Version 0.1	Larysa Istomina/
			Georg Heygster
			/Eleonora Zege/
			Alexei Malinka/
			Aleksander
			Prikhach/ Ilja Katsev

### SIDARUS CONSORTIUM

Participant no.	Participant organisation name	Short name	Country
1 (Coordinator)	Nansen Environmental and Remote Sensing Center	NERSC	NO
2	Alfred-Wegener-Institut für Polar-und Meeresforschung	AWI	DE
3	Collecte Localisation Satellites SA	CLS	FR
4	University of Bremen, Institute of Environmental Physics	UB	DE
5	The Chancellor, Masters and Scholars of the University of Cambridge	UCAM	UK
6	Norwegian Meteorological Institute, Norwegian Ice Service	Met.no	NO
7	Scientific foundation Nansen International Environmental and Remote Sensing Centre	NIERSC	RU
8	B.I. Stepanov Institute of Physics of the National Academy of Sciences of Belarus	IPNASB	BR

No part of this work may be reproduced or used in any form or by any means (graphic, electronic, or mechanical including photocopying, recording, taping, or information storage and retrieval systems) without the written permission of the copyright owner(s) in accordance with the terms of the SIDARUS Consortium Agreement (EC Grant Agreement 262922).

All rights reserved.

This document may change without notice

## **Table of Contents**

1	PAR	RT I: MELT POND FRACTION AND SEA ICE ALBEDO: PRODUCT ANALYSIS	8
	1.1	INTRODUCTION	8
	1.2	Data used	9
	1.2.1	Cloud screening	9
	1.2.2	P Validation	9
	1.2.3	Gridding	11
	1.2.4	4 Averaging	12
	1.3	CASE STUDIES	13
	1.3.1		
	1.3.2	Comparison to MPF by A. Roesel et al. for the second week of June 2009	14
	1.4	TEMPORAL AND SPATIAL ANALYSIS OVER THE WHOLE MERIS DATASET	
	1.4.1	, 0 ,	
	1.4.2		
	1.4.3		
	1.5	CONCLUSIONS	22
2	PAR	RT II: VALIDATION AND CALIBRATION OF THE MPD RETRIEVAL USING SEA ICE AND MELT	
- P		LBEDO SPECTRA MEASURED DURING POLARSTERN CRUISE ICEARC2012	24
	2.1	INTRODUCTION	
	2.2	Undiagnosed situations	
	2.2.1		
	2.2.2	POLARSTERN FIELD DATA. MODELS VS. EXPERIMENTS	
	2.3 2.4	ANGLE OF INCIDENCE	
	2.4	ANALYSIS OF THE FIELD SPECTRAL MEASUREMENTS	
	2.6	BORDERS TO VARIATIONS OF MELTING ICE PARAMETERS FOR THE ITERATION PROCEDURE IN THE MPD SOFTWARE	
	2.6.1		
	2.6.2	· · · · · · · · · · · · · · · · · · ·	
	2.0.2	New in version 1.50	
	2.8	CONCLUSION	
R	EFERE	NCES	47
3	APP	PENDIX A	48
4	A DD	PENDIX B	111
5	APP	PENDIX C	131
	5.1	INTRODUCTION	131
	5.2	NEW FEATURES	131
	5.2.1	New features in version 1.55	131
	5.2.2	New features in version 1.50	132
	5.2.3	New features in version 1.20	133
	5.2.4	New features in version 1.10	133
	5.3	HOW TO INSTALL	
	5.4	How to run	134
	5.5	CONTROL FILES	135
	5.5.1	Control file to configure run parameters	135
	5.5.2	[atmo] section	135

5.5.	B [MERIS_data] section	136
5.5.	f [run] section	137
5.5.	5 [albedo] section	137
5.5.	[RAY_preferences] section	137
5.5.	7 [save] section	138
5.5.	B [boundaries] section	139
5.6	CONTROL FILE TO SET AEROSOL ATMOSPHERE MODEL STRATIFICATION	139
5.6.	[atmo] section	140
5.7	CONTROL FILE TO SET MODEL OF MOLECULAR-GASEOUS ATMOSPHERE	140
5.7.	1	
5.7.	1 -0 3	
5.8	MPD.INI CONTROL FILE	
5.9	MPD_XSECT.INI CONTROL FILE	142
5.10	OUTPUT FILE	142
	List of Figures	
	O - 4 - 1 P - 4 P - 4 P - 4 P - 4 P - 4 P - 1 P	0
	Spatial distribution of the validation data. The data includes FYI and MYI 1 Validation of the MPD algorithm against the in situ pond fraction measurement	
_	: Example image for aerial campaign MELTEX 2008, 06.06.2008. Field value:	
_	6 melt ponds1	_
	Example image for aerial campaign NOGRAM 2011, 21.07.2011. Field values	
	6 melt ponds1	
	Comparison of daily average (right) to the weekly average. Notice the missing	
	uds in the daily average	
	Locations on first year (left) and multiyear ice (right)	
	Time sequence of melt pond fraction, broadband albedo and NCEP air tempe	
	face for area in Beaufort sea near Barrow, May to September 20091. Time sequence of melt pond fraction, broadband albedo and NCEP air tempe	
_	face for area around North Greenland, May to September 2009	
	Comparison of the MPD product from MERIS data (right) to the pond fraction	
	II., 2011, (MODIS data) for the second week of June 2009.	
	Da: Comparison of the weekly average pond fraction for the first week of Ju	
	1 (top row, left and right correspondingly) and for the second week of June 20	
	ttom row, left and right correspondingly)1	
Figur 1	1b: Comparison of the weekly average pond fraction for the third week of Ju	ne 2007 and
<b>20</b> 1	1 (top row, left and right correspondingly) and for the fourth week of June 20	07 and 2011
(bo	ttom row, left and right correspondingly)1	8
Figur 1	2: Melt pond fraction trends (trend in MPF %) for the four weeks of June 2002-2	<b>2011.</b> 19
	2: Broadband sea ice albedo trends (trend in albedo %) for the four weeks o	
<b>20</b> 1	<b>1.</b> 2	0

### **SUMMARY**

The current deliverable addresses the analysis of the sea ice albedo and pond fraction products on various scales, from regional to global, from daily to trends over 10 years. This study has been performed with an updated version of the MPD retrieval after additional analysis done with in situ data (see Part II). The cloud screening has been improved as well.

Analysis of trends showed distinct spatial patterns of positive and negative trends of both products. The possible reason for them needs to be clarified via further studies.

### 1 Part I: Melt pond fraction and sea ice albedo: product analysis

### 1.1 Introduction

The current deliverable addresses the analysis of the sea ice albedo and pond fraction products on various scales, from regional to global, from daily to trends over 10 years. This study has been performed with an updated version of the MPD retrieval after additional analysis done with in situ data (see Part II). The cloud screening has been improved as well.

The products have been analyzed for consistency by comparing with the ground based and airborne data, via comparison with another remote sensing retrieval of melt pond fraction from MODIS data (by Roesel et al., 2011). Weekly averages for June of two years – 2007 and 2011 – have been analyzed. Spatial trends of melt pond fraction and sea ice albedo have been produced for June of each year of the whole MERIS dataset.

Currently, three summers of MERIS data (May to September 2009-2011) are processed and stored as daily averages. In addition, June of every year of the MERIS dataset (2002-2011) is processed and available as daily averages.

### 1.2 Data used

The data used for the present study are the pond fraction and broadband sea ice albedo products retrieved from MERIS data over the ice covered Arctic Ocean using the MPD retrieval (see earlier deliverables for more details on the basis of the algorithm. For the analysis done to update the algorithm up to the current stage, please see Part II, which is complementary to the research presented in Part I, i.e. all studies shown here are done with the latest version of the MPD retrieved described in the Part II).

### 1.2.1 Cloud screening

In addition to cloud screening described in earlier deliverables, we have employed two new criteria of cloud free snow/ice covered pixel:

- 1. Oxygen A band threshold on TOA reflectances: MERIS level 1b product contains reflectances at wavelengths 753nm and 760nm. These are bands 10 oxygen A reference and 11 band within the oxygen A absorption line. To detect cloud free pixels, we need to detect pixels where oxygen absorbed within the whole column as opposed to cloudy pixels, where the absorption happened only within small fraction of a whole column, namely, above the cloud. For this, we use a ratio of band 11 and 10 and manually derived threshold of 0.27. Visual analysis of several dozen daily averages showed improved cloud screening and decreased amount of cloud edges and high thin clouds within the resulting product as opposed to the product without this threshold.
- 2. Threshold on retrieved broadband albedo: due to very high and almost constant albedo of clouds within the MERIS spectral range, it is possible to detect clouds also using limitation on retrieved average of spectral albedo within MERIS spectral range 400...900nm, as no Arctic surface, whether melting sea ice or snow covered ice, can have broadband albedo higher than 0.95. This thresholds has also been visually checked over several dozen of daily averages in different stages of melt.

#### 1.2.2 Validation

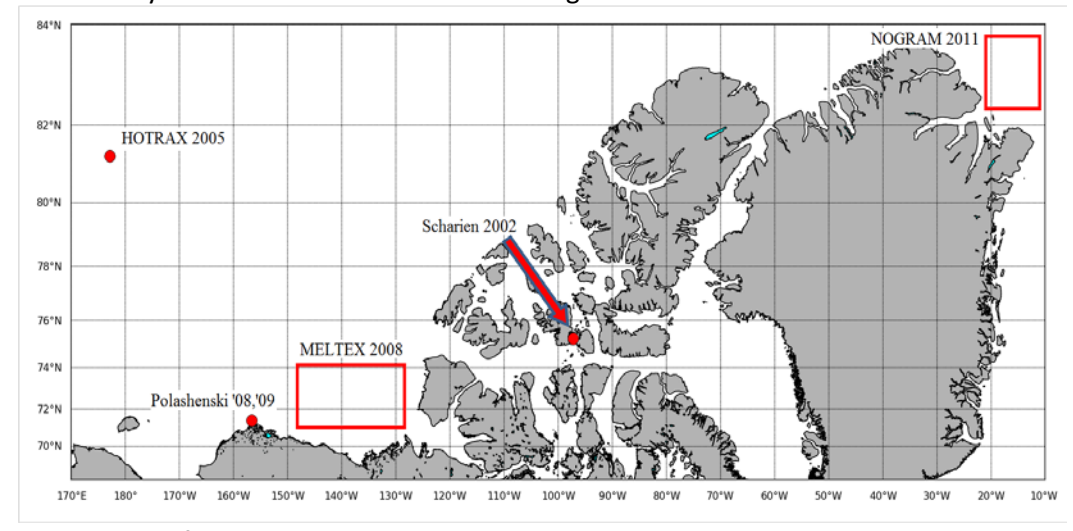
The validation of the MPD algorithm has been done using the datasets shown in Table 1.

Table 1: Datasets used for validation of the MPD algorithm (Authors, location, year, method)

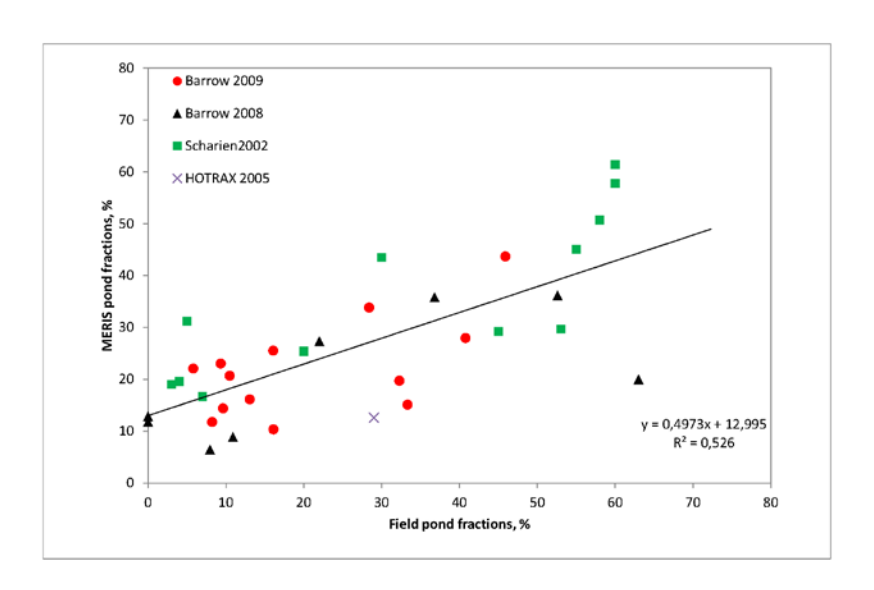
Polashenski, Barrow 2008	In situ field campaign, visual estimation
Polashenski, Barrow 2009	In situ field campaign, fractions along a 200m transect
Birnbaum, MELTEX 2008	Airborne measurements, supervised classification algorithm applied to geolocated quality assured aerial pictures
Birnbaum, NOGRAM 2011	Airborne measurements, supervised classification algorithm applied to geolocated

	quality assured aerial pictures
Scharien, Canadian Arctic 2002	In situ field campaign, visual estimation
Perovich, HOTRAX 2005	Ship cruise, hourly bridge observations, visual estimation

In addition, the summary of dataset locations is shown in Fig. 1.



Figur 1: Spatial distribution of the validation data. The data includes FYI and MYI.

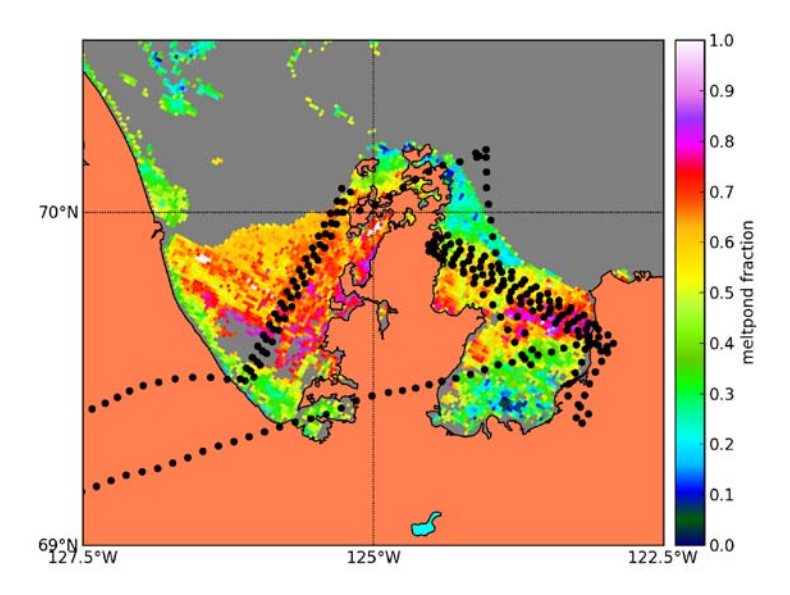


Figur 2: Validation of the MPD algorithm against the in situ pond fraction measurements.

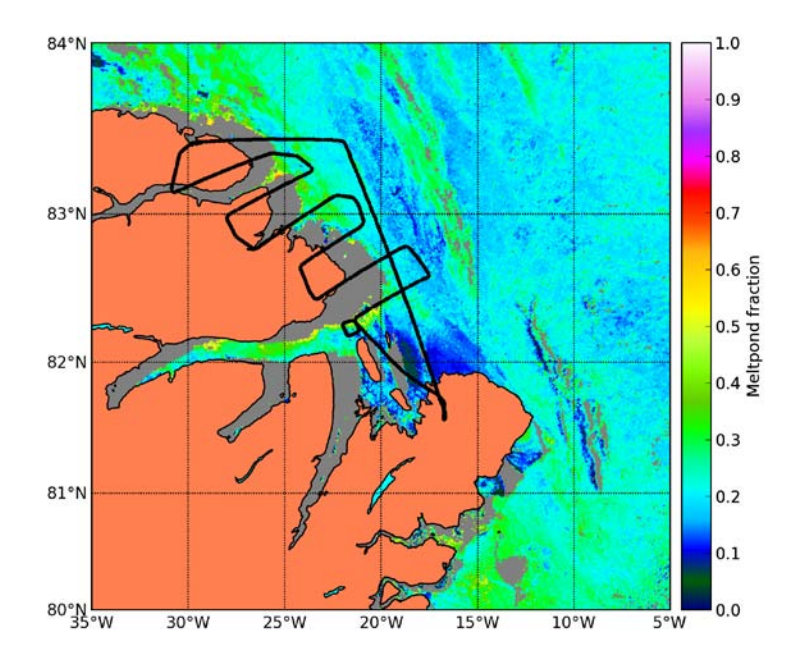
The results of validation against in situ data is shown in Fig. 2.

The two airborne campaigns were analyzed separately from the in situ data due to different resolution and observation method (i.e. different accuracy). Examples of comparison to airborne data are shown below (Fig. 3

and 4). The correspondence of the retrieved values to the validation data is reasonably good in both cases of in situ and airborne campaigns.



Figur 3: Example image for aerial campaign MELTEX 2008, 06.06.2008. Field value: on average 40% melt ponds.



Figur 4: Example image for aerial campaign NOGRAM 2011, 21.07.2011. Field values: on average 19% melt ponds.

### 1.2.3 Gridding

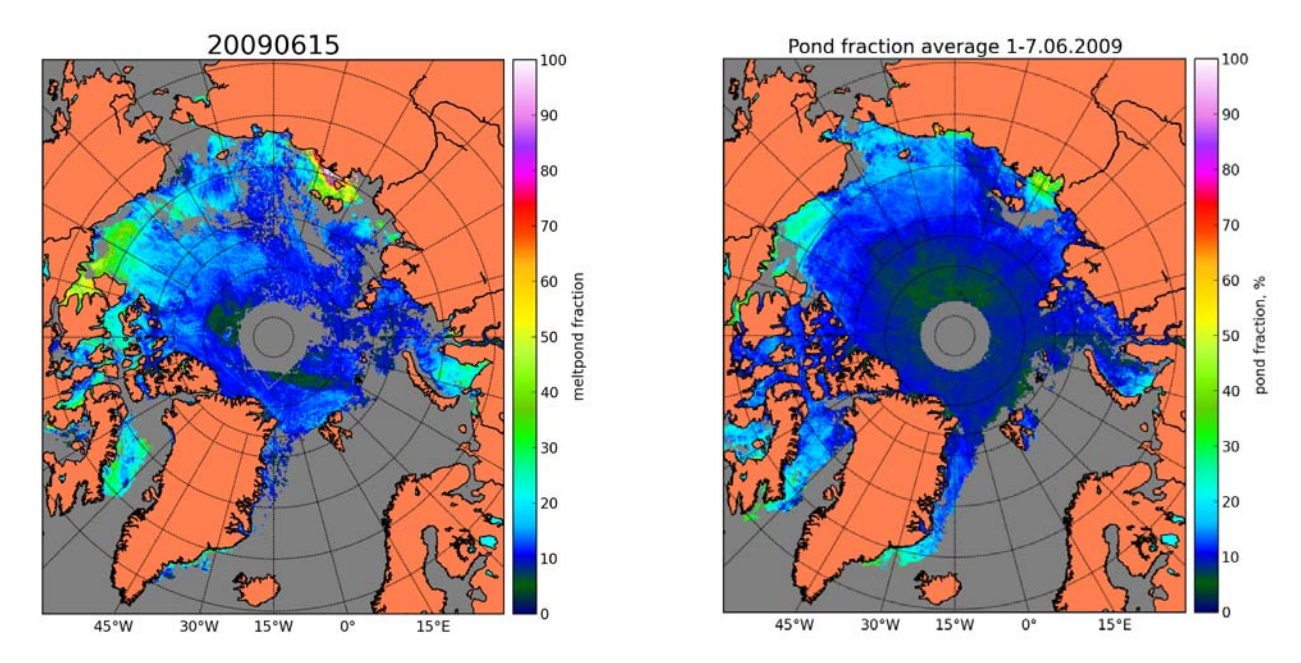
The processed swath MERIS level 1b data have been gridded into 12.5 km NSIDC grid with the criteria of more than half valid pixels (both spatially and temporally) within a grid cell to produce a valid grid cell. Standard deviation of such a mixed spatial and temporal average is also provided. Thus, the resulting NetCDF contains four

datasets: MPF, broadband albedo and their STDs. On average, there were around 13 overflights per day, with the density of overlapping overflights increasing to the center of the grid.

### 1.2.4 Averaging

Gridded daily products are then used to produce averages of higher order, e.g. weekly averages. Here again, more than half of available pixels have to be valid numbers to obtain a valid averaged value for a given grid cell. No weight or threshold on STDs is applied. The resulting STD is then written into the resulting NetCDF file together with the averaged value for the broadband albedo and melt pond fraction.

The essential difference in daily and e.g. weekly averages is the data coverage due to cloudiness and smoothness of the resulting product (see Fig. 5)

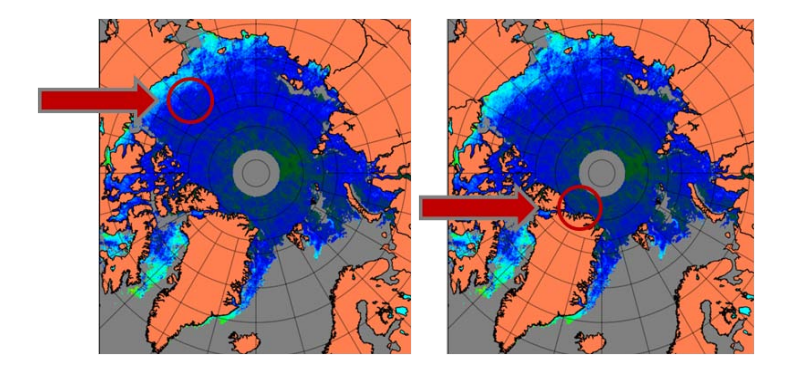


Figur 5: Comparison of daily average (right) to the weekly average. Notice the missing data due to clouds in the daily average.

### 1.3 Case studies

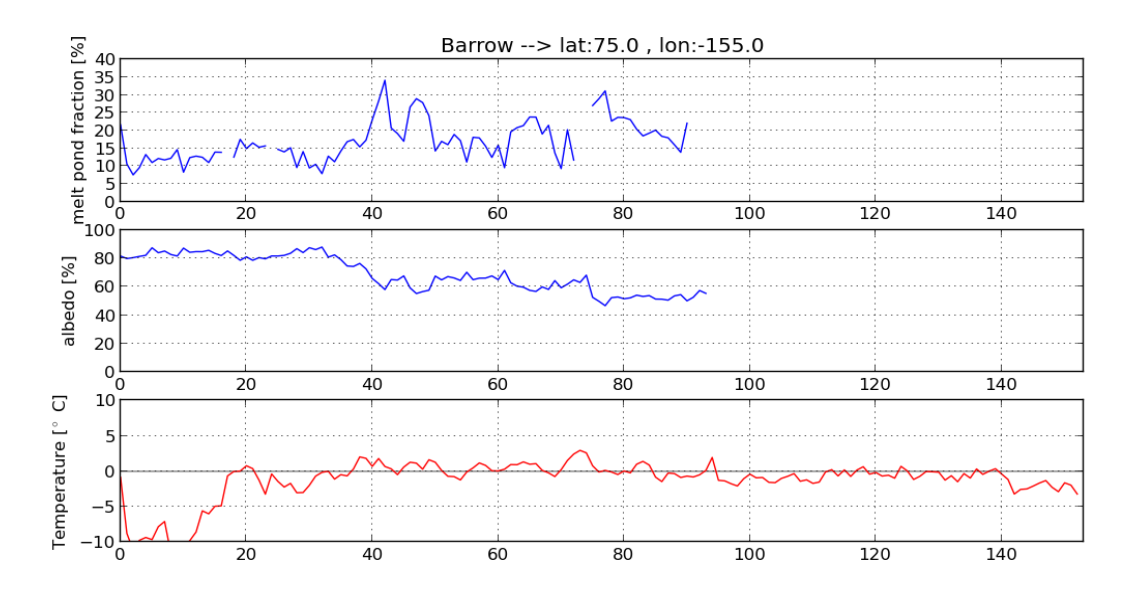
### 1.3.1 Time sequences of MPF and albedo for FYI and MYI

In order to illustrate the feasibility of the algorithm on FYI and MYI, time sequences over the summer 2009 have been produced for Beaufort sea (Fig 6, left) and North Greenland (Fig 6, right).



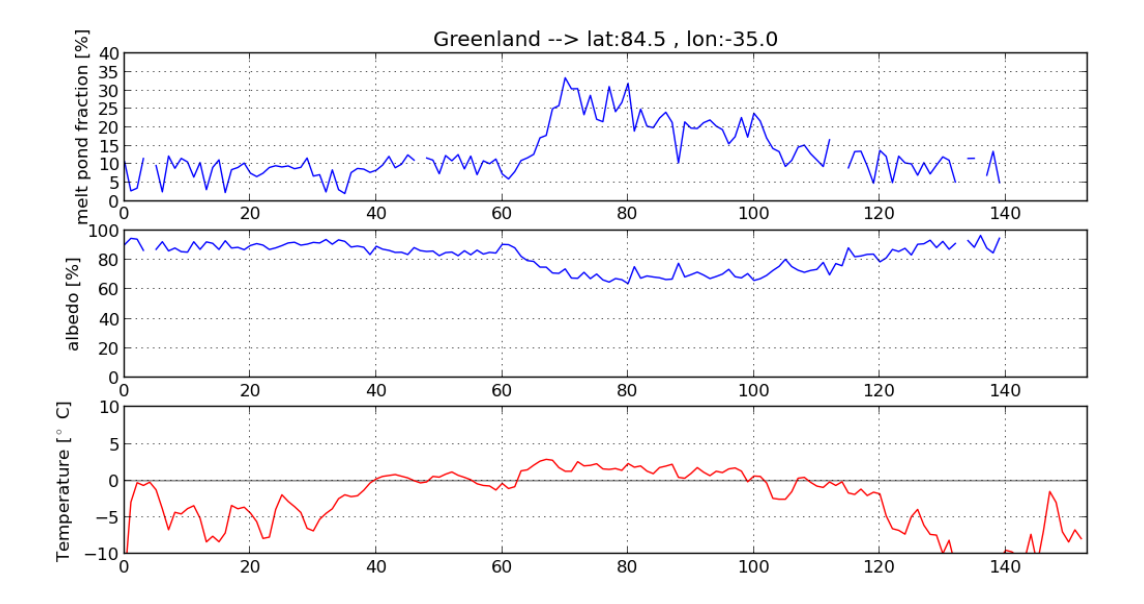
Figur 6: Locations on first year (left) and multiyear ice (right).

For this study, daily averaged product was taken in the area 75N, 155W and 84.5N, 35W and it was compared to the time sequence of air temperature at the surface from NCEP reanalysis data. The difference between melt evolution in the selected location is mainly in the fact that melt onset happens about a month earlier in lower latitudes: beginning of June on FYI as opposed to beginning of July for MYI. Then, the maximum melt pond fraction on FYI can be much about 4 times higher than that on MYI (maximum melt 0.2 on MYI as opposed to up to 0.8 on MYI). While the melt onset happens fast on both ice types, the later stage of melt - drainage of melt ponds - happens much faster on FYI than on MYI.



Figur 7: Time sequence of melt pond fraction, broadband albedo and NCEP air temperature at the surface for area in Beaufort sea near Barrow, May to September 2009.

One more difference between the two chosen locations is the sea ice concentration: for the MYI the ice concentration stays very high throughout the whole summer, whereas for the FYI region the effect of ice concentration and also ice drift (in the swath data for consecutive days separate floes and their drift is clearly visible) can affect the time sequence analysis. This affects the noisiness of the retrieved values.



Figur 8: Time sequence of melt pond fraction, broadband albedo and NCEP air temperature at the surface for area around North Greenland, May to September 2009.

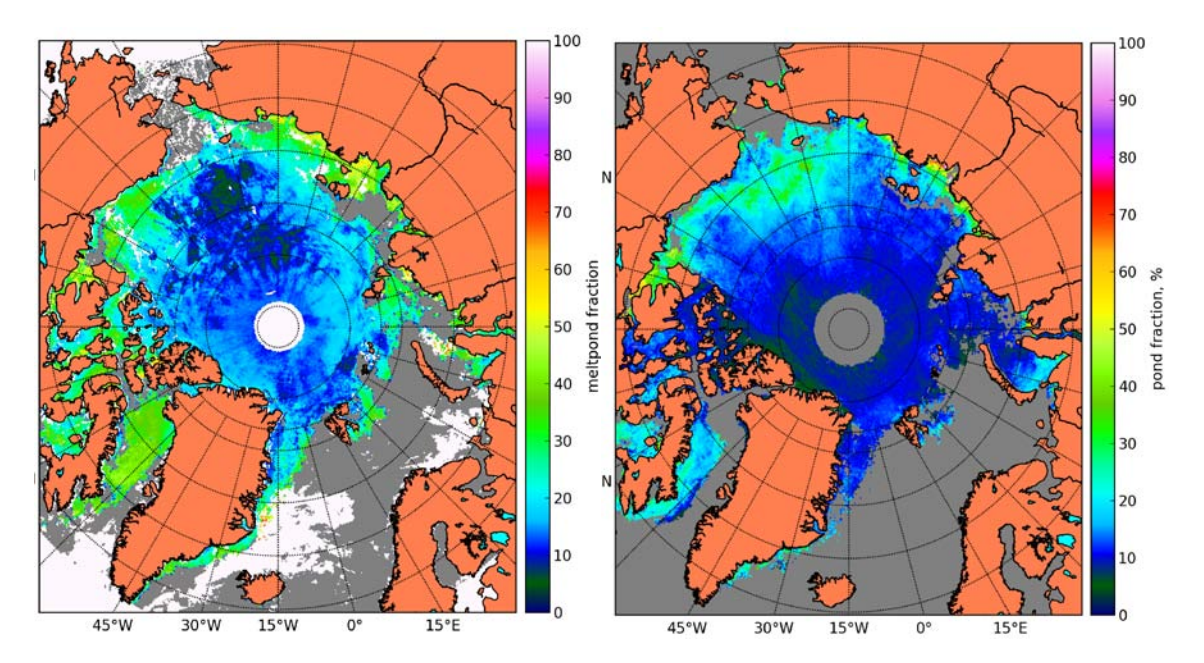
٧

Overall, the comparison of the retrieved MPFs and albedos to the surface air temperature (Fig. 7 and 8) shows clear connection between these during the melt onset: as soon as air temperature assumes positive values, sea ice albedo drops down and melt pond fraction increases sharply. For the both FYI and MYI the maximum melt pond fraction is around 0.35, with melt onset happening in the beginning of June for FYI and beginning of July for MYI. This corresponds to the knowledge about melt onset and dynamics from field measurements. The evolution of melt on MYI follows the air temperature dynamics and is ongoing till first snowfalls and freezing temperatures around end of August. The FYI region, however, is more affected by ice drift and varying ice concentration within the study area, therefore the curve appears noisier and interrupts with the ice melt in the area around end of July 2009. For periods before melt onset, the retrieved melt pond fractions range from 0% to 10-15% with relatively high albedos; this might be the effect of unscreened clouds which tend to increase retrieved pond fraction in case of small true pond fraction and decrease it in case of high true pond fractions.

### 1.3.2 Comparison to MPF by A. Roesel et al. for the second week of June 2009

The algorithm by Roesel et al, 2011, employs MODIS level 3 surface reflectance product as an input to the melt pond fraction retrieval, which retrieves sea ice concentration simultaneously, as opposed to the MPD algorithm which is not sensitive to sea ice concentration. Therefore it is feasible to start the comparison for the areas of

100% sea ice concentration, to avoid possible non-melt state induced inconsistencies. As seen from Fig. 9, even for High Arctic (area around the Pole, ice concentration around 100%) the discrepancy between the two retrievals is significant, with the MPD retrieval showing around 10% melt ponds and algorithm by Roesel et al. shows values up to two times higher, which is also valid for lower latitudes. In addition, the spatial pattern of melt pond fractions of the MPD retrieval does not resemble that of the algorithm by Roesel et al.: MPD retrieval (right) shows melt onset starting at Alaska, point Barrow, Beaufort Sea in the second week of June 2009, with the areas of the Arctic Ocean closer to the Pole relatively melt free. The MODIS data based product (left) shows almost the opposite spatial pattern.



Figur 9: Comparison of the MPD product from MERIS data (right) to the pond fractions by Roesel et al., 2011, (MODIS data) for the second week of June 2009.

To conclude about the reason of such discrepancy, more case studies have to be analyzed.

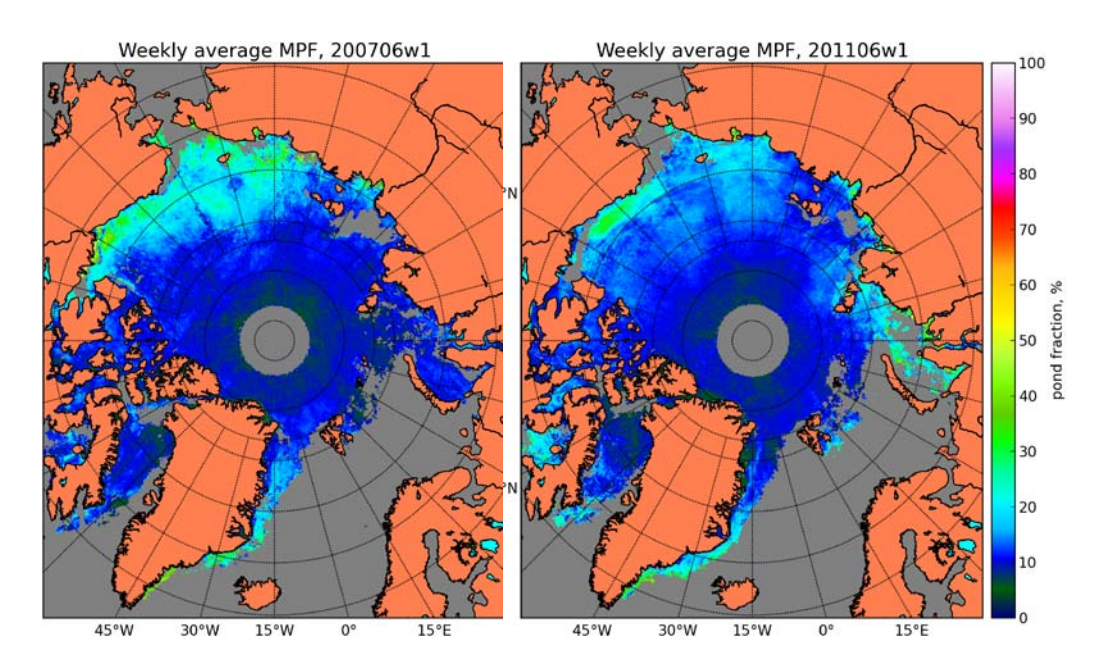
### 1.4 Temporal and spatial analysis over the whole MERIS dataset

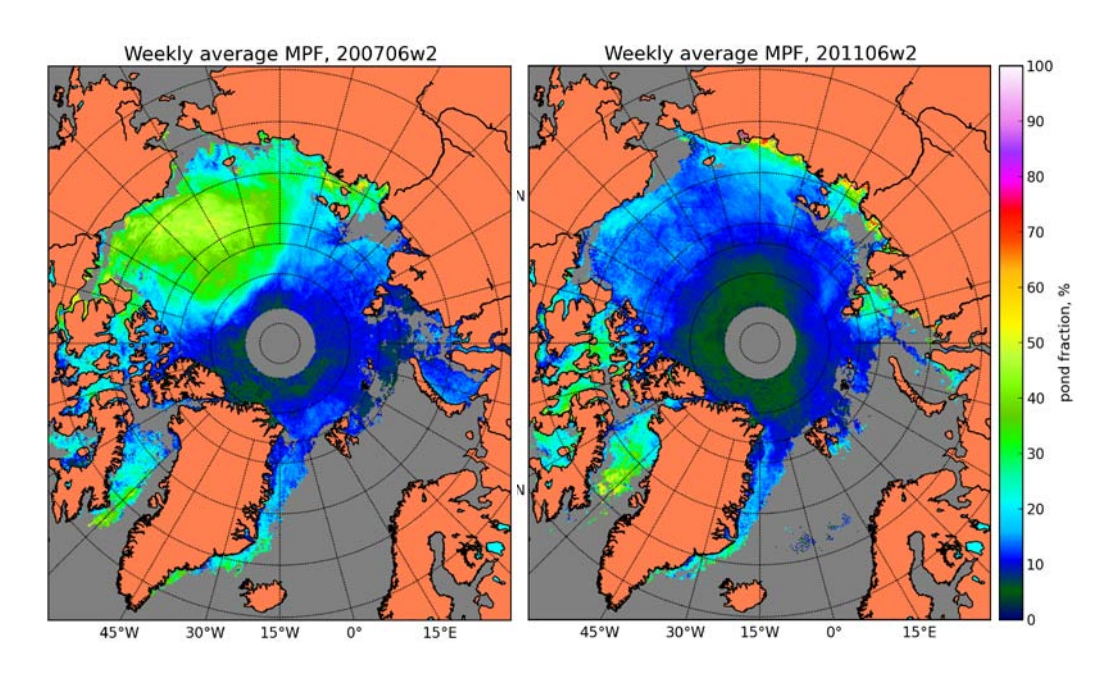
This chapter presents the main highlights of the processed MERIS data for 2002-2011. Weekly averages have been used for this study due to better data coverage; therefore the shown trends are produced with the weekly resolution.

The most speaking and characteristic stage of melting season is the melt onset and the first stage of melt evolution. Such dynamics is ice type specific, e.g. on FYI this is the rapid melt pond formation with the rapid drainage, during which the melt pond fraction changes drastically up and down within a scale of days to weeks. MYI features later (starts in July) and slower melt onset, less extreme pond fractions with the absence of rapid melt evolution stages. Because the FYI is most vulnerable to melting and during the ice minimum the fraction of FYI decreases drastically, we took June of each year of the available MERIS dataset to study the difference of melt onset date and melt evolution pond fraction mostly on FYI, and melt onset on MYI.

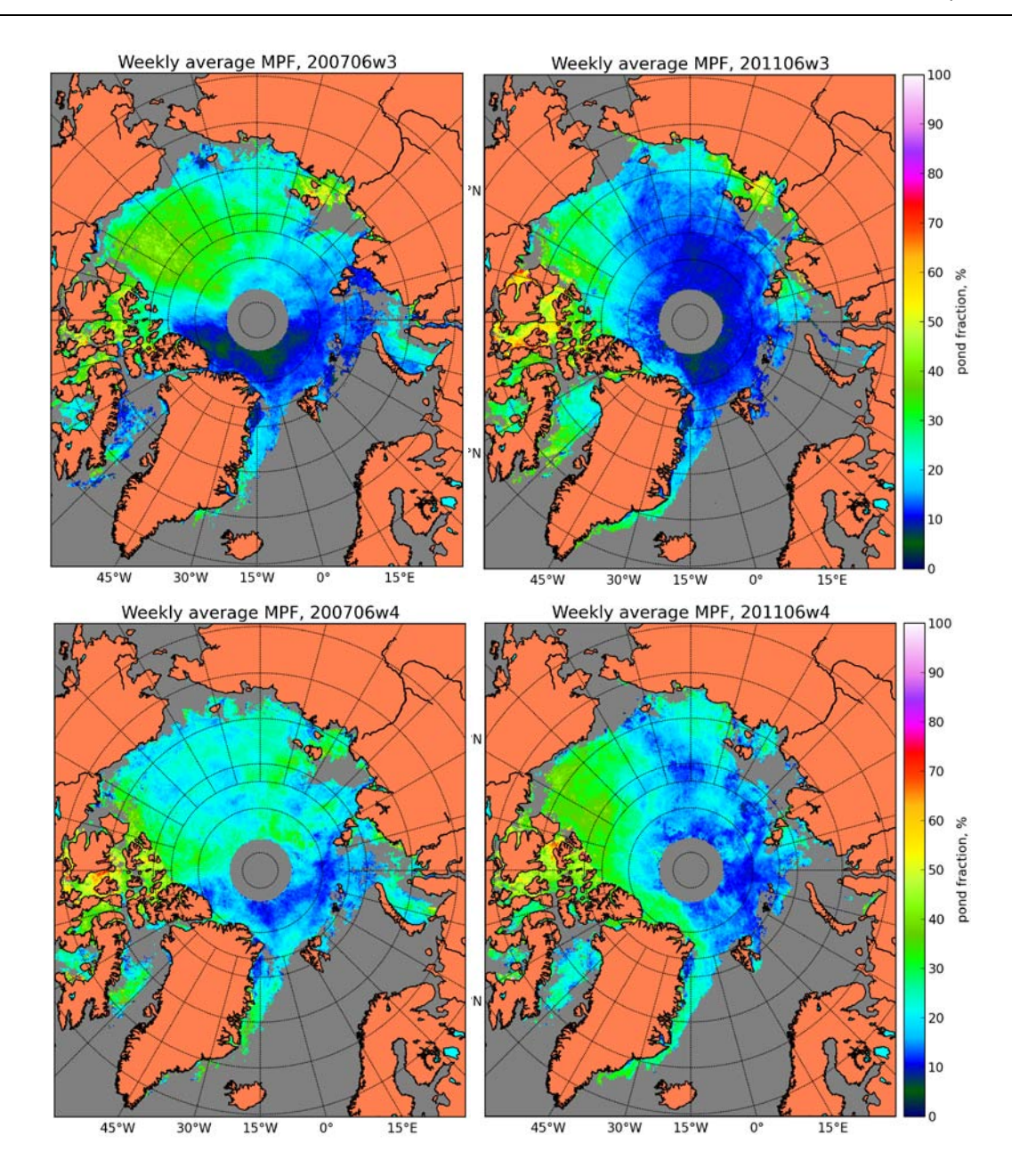
### 1.4.1 Weekly averages of June 2007 and 2011: how the record ice minimum in 2007 started.

It is interesting to compare the evolution of melt right after the onset of melt for the year of the record ice minimum 2007 and a similar by the ice minimum extent year 2011, to see how the patterns of melt changed within these 5 years to reach the same "resulting" ice extent during the sea ice minimum. In Fig. 10a the first two weeks of June are shown for the both years. It is visible that the melt onset during the first week of June has much more local character in 2011 than in 2007. It was localized near point Barrow and the shore of Beaufort Sea, as opposed to 2007 when the melt onset started already at a more global scale. The second week of June 2007 featured drastic melt in the Beaufort sea and the western part of the FYI covered Arctic Ocean, whereas in 2011 the situation was more or less stable relative to first week of June.





Figur 10a: Comparison of the weekly average pond fraction for the first week of June 2007 and 2011 (top row, left and right correspondingly) and for the second week of June 2007 and 2011 (bottom row, left and right correspondingly)

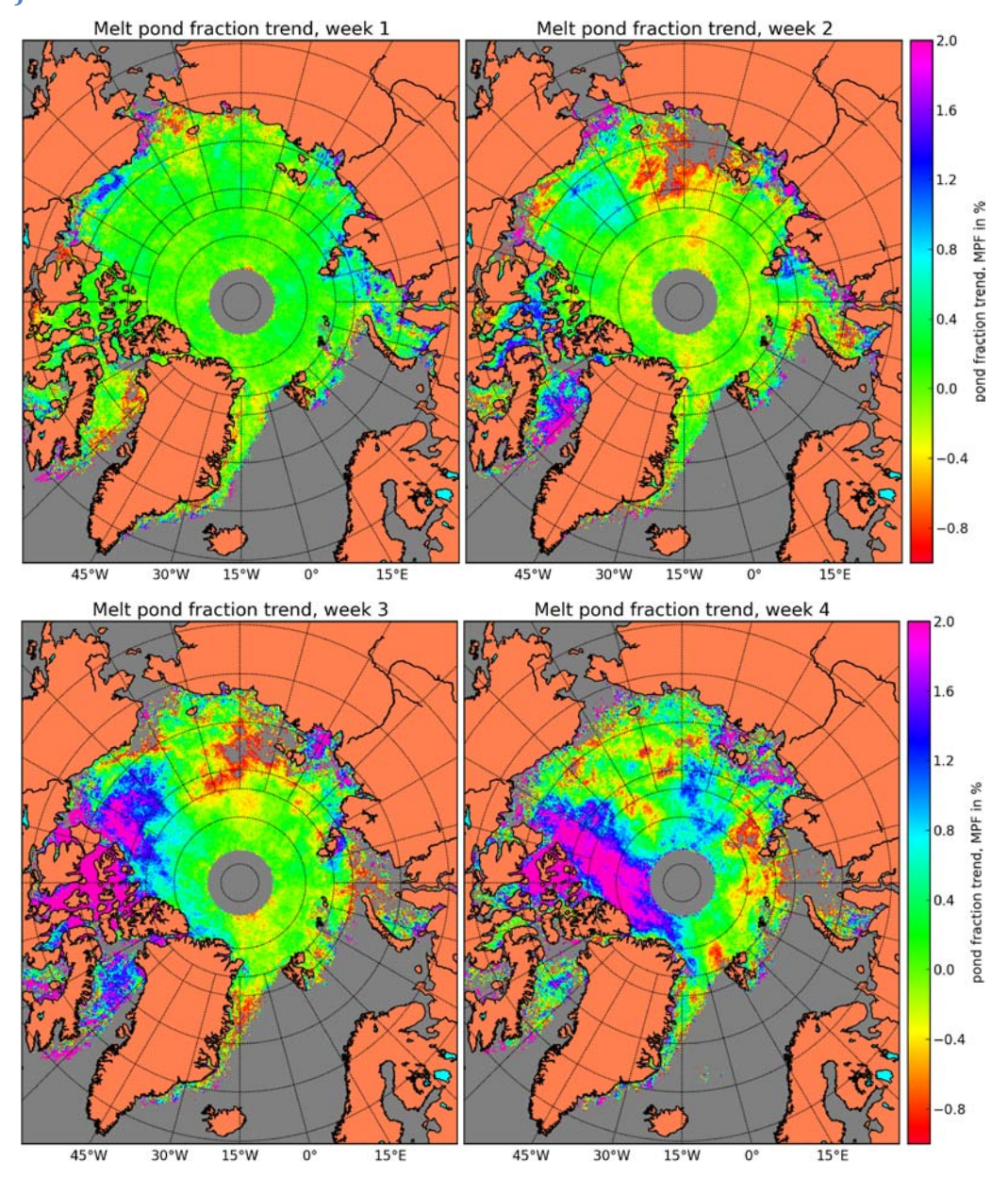


Figur 11b: Comparison of the weekly average pond fraction for the third week of June 2007 and 2011 (top row, left and right correspondingly) and for the fourth week of June 2007 and 2011 (bottom row, left and right correspondingly)

In Fig. 10b, the third and the forth weeks of June 2007 and 2011 are shown (order of plots same as in Fig. 10a). Here finally (one week delay as compared to June 2007) melt started during the third week of June 2011, but it is centered around Queen Elizabeth Islands. The fourth week of June 2011 shows that melting spreads from there over the FYI covered ocean, whereas in 2007 at this time same areas have already experienced maximum of melt and are now draining. MYI areas of both years display start of melting, which evolves and reaches maximum in July (not shown here).

To conclude: years 2007 and 2011 feature different time of melt onset and also different spatial patterns of melt pond fractions, however the ice extent near ice minimum is close. Analysis of further months of data is needed to find out which of the regions was responsible for the main ice cover decline and whether some characteristic dynamics of melt pond evolution was prominent in those areas.

# 1.4.2 Spatial trends of melt pond fractions for the Arctic Ocean over the whole MERIS dataset (2002-2011)

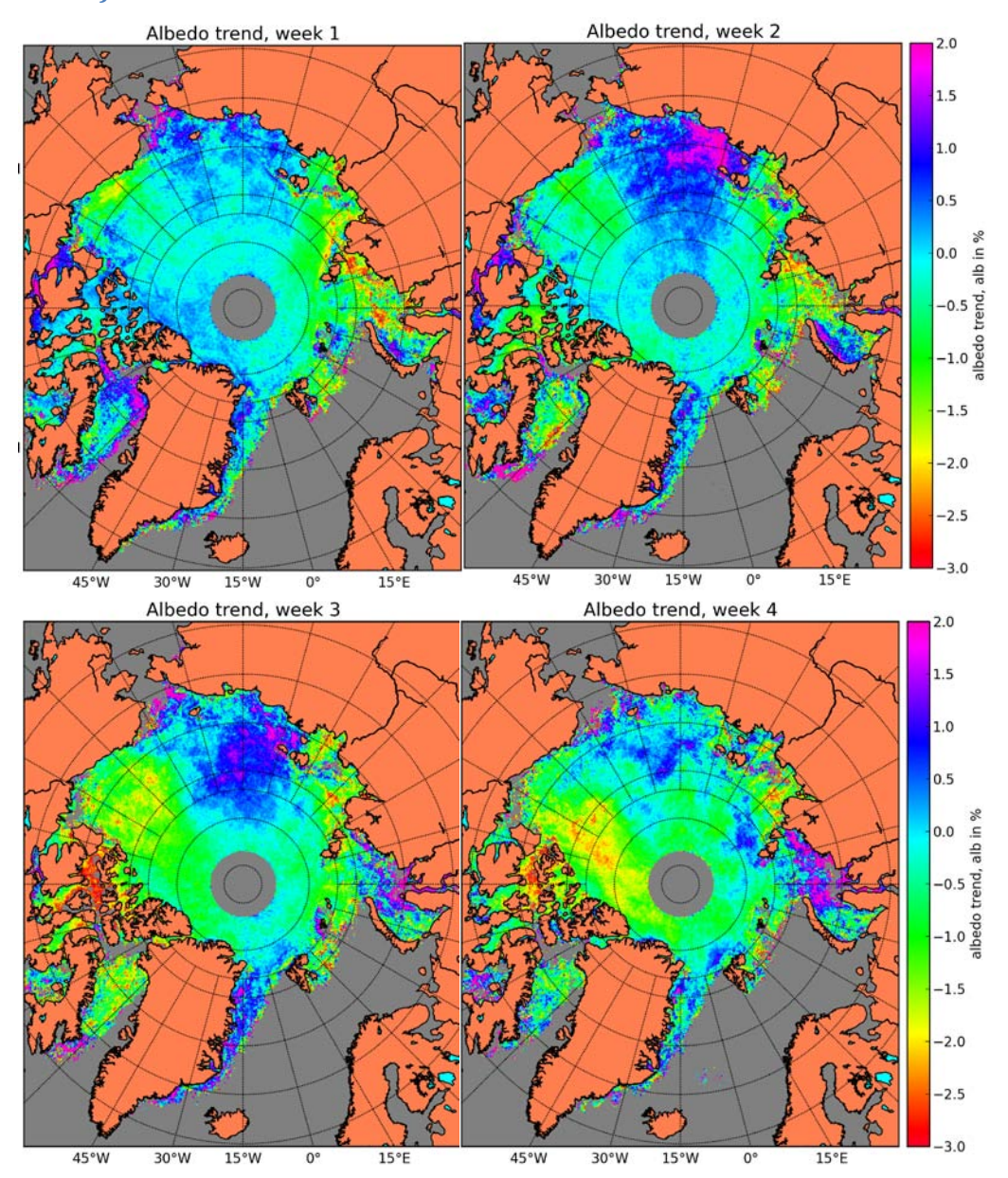


Figur 12: Melt pond fraction trends (trend in MPF %) for the four weeks of June 2002-2011.

There is no trend for the first week of June throughout the years (Fig. 11), except for a slight positive trend of melt pond fraction near point Barrow. This feature disappears for the second week, and a positive trend of 1-2 % is located within Queen Elizabeth Islands. This trend exists for the whole June. Possible explanation for it is not the increased absolute value melt pond fraction, but earlier melt onset for these areas a related to the beginning of

the dataset. A negative trend in the East-Siberian Sea has yet to be explained: either it is the opposite temporal shift of melt evolution towards summer, or an outlier in the weather conditions within the studied years, or a true trend due to changed climatic balance of the region. The melt pond fraction trend for the 4<sup>th</sup> week of June has a complicated pattern, which resembles spatial oscillations. Further analysis is needed to clarify these spatial and temporal pattern.

# 1.4.3 Spatial trends of broadband sea ice albedo for the Arctic Ocean over the whole MERIS dataset (2002-2011)



Figur 13: Broadband sea ice albedo trends (trend in albedo %) for the four weeks of June 2002-2011.

The melt pond fraction and the broadband albedo of the pixel are joint products, i.e. increasing trend of melt pond fraction should in principle give a decreasing trend of the albedo. Decreasing albedo trend around Queen Elizabeth Islands and increasing trend in the East-Siberian Sea (see Fig. 12) correspond well to already seen

dynamics of the melt pond fraction weekly trends, with slight differences in spatial patterns which can be explained by different sensitivity of both retrievals to open water and melt ponds.

### 1.5 Conclusions

An updated version of the MPD algorithm comprises improved retrieval procedure (see Part II), improved cloud screening and advanced gridding for the mass processing of MERIS data. With these updated methods, the validation effort has been redone, three years of MERIS data has been processed (2009-2011) and stored as daily averages and each June of years 2002-2011 has been processed as well and stored and daily and weekly averages. From these products, extensive time sequence and trend study has been performed for selected time ranges, regions and global Arctic Ocean. Comparison of weekly melt evolution for June 2007 and 2011 has been performed and showed different spatial and temporal dynamics of melt, which in the end gave similar ice extent near the ice minimum.

Analysis of trends showed distinct spatial patterns of positive and negative trends of both products. The possible reason for them needs to be clarified via further studies.

# 2 Part II: Validation and calibration of the MPD retrieval using sea ice and melt pond albedo spectra measured during Polarstern cruise IceArc2012

### 2.1 Introduction

In the process of the deployment of the MPD code to retrieve the spectral albedo of Arctic Ice and melt pond fraction (developed during two first years of SIDARUS execution), the limitations of retrieval capability of the MPD became clear. Even more strong limitations and retrieval errors are typical for all known algorithms [1, 2]. The MPD code was initially based mainly on the field data for the season of developed melting. Particularly, it was assumed [3] that melting results in formation of so-called 'white ice' (strongly scattering bright surface) and melt ponds (see Sec. 3.2).

We enucleate situations (see Sec. 2) where the developed MPD retrieval (and any other algorithm using information from satellite spectral sensors of type MODIS, MERIS) are not able to provide the reliable diagnostic of situation (first-year or 'blue' ice, water saturated ice). In these cases *a priori* input information is needed, but it is the subject of future studies.

Deployment of the MPD software in Arctic using historical MERIS data has shown that that such a version works reliably for multi-year-ice (mainly in North Arctic) in the period of developed melting (from second week of June up to second week of August) as it could be expected. To start with satellite monitoring of melting situation over the entire Arctic and throughout the light period it required in the first turn to get comprehensive and ample field measurements of optical properties of melting ice during the whole Arctic summer in various Arctic regions. We took the data, obtained in the Polarstern 2012 expedition and extensive optical measurements performed by L. Istomina. These data allowed us to check applicability of the developed optical models of the reflection by the sea ice and melt ponds (described in Deliverable D4.1) to the various melting situations.

In Sec. 3 we present the comparison of the developed optical models of the reflection by sea ice and melt ponds with measurements during Polarstern 2012 expedition for various situations, which showed good agreement of developed modeling and field truth even beyond classical developed melting situation.

Sec. 4 delivers the results of the study of effect of the *a priori* choice of the borders to parameters of ice and melt ponds on the retrieved values of the melt pond fraction and presents recommendations to the optimization of the choice of borders in different cases.

The increase of the possible scope of MPD software usage required including some borders to retrieved parameters in the MPD algorithm (optical thickness of white ice and pond underlying ice etc.). These borders were included in the new version of MPD software. Besides, the estimation of the error of the retrieval was included in the final versions MPD software.

During the third year of the SIDARUS execution two subsequent steps were performed for developing and improving the MPD software. Version MPD 1.20 and the final versions MPD 1.50 and 1.55 were developed,

delivered, and verified. Additions and changes in the MPD software are presented and described in Sec. 5. The detailed User Guide to the MPD software is included as *Attachment C*.

In what follows we will use the characteristics of the ice and melt pond, which were introduced in our previous SIDARUS Deliverables [6], these characteristics and their denotations are listed below in Table 1 (Sec. 3.2).

### 2.2 Undiagnosed situations

The first validation of the MPD using the filed data showed that some situations could not be recognized by the developed algorithm. These cases are 'blue ice' and 'wet ice'. The former is the first-year ice, quite transparent, without the scattering layer on the top. The color of such surface is usually dark-blue. The latter is the ice in the phase of strong melting, when the entire surface is water-saturated. This phase usually precedes the 'standard' situation, when water flows down, forming melt ponds and leaving the drained surface of white ice. The color of such surface is usually white-grey. Below the spectral reflectance of these surfaces is simulated and compared to the reflectance of a melt pond.

#### **2.2.1** Blue ice

For modeling the reflectance of blue ice we used the following model [4,5]. Solid ice contains no air bubbles but only brine inclusions, which are treated as optically soft particles [6]. The scattering coefficient is taken equal  $200 \text{ m}^{-1}$ , the effective inclusion radius is 1.3 µm (this value provides the average cosine of the phase function equal to 0.99). Then we calculated the bi-directional reflectance distribution function (BRDF) at the incident zenith angle  $60^{\circ}$  and observation zenith angle of  $0^{\circ}$  (at nadir) with the IRS software [6]. Then we found the melt pond characteristics, which gave the same BRDF spectrum (strictly speaking, the closest in the sense of least squares). The found characteristics of the melt pond were:  $tau\_pond = 0.0055$ ,  $sig\_ice = 1.3 \text{ m}^{-1}$ ,  $tau\_ice = 1.8$ . The both spectra are shown in Fig. 1.

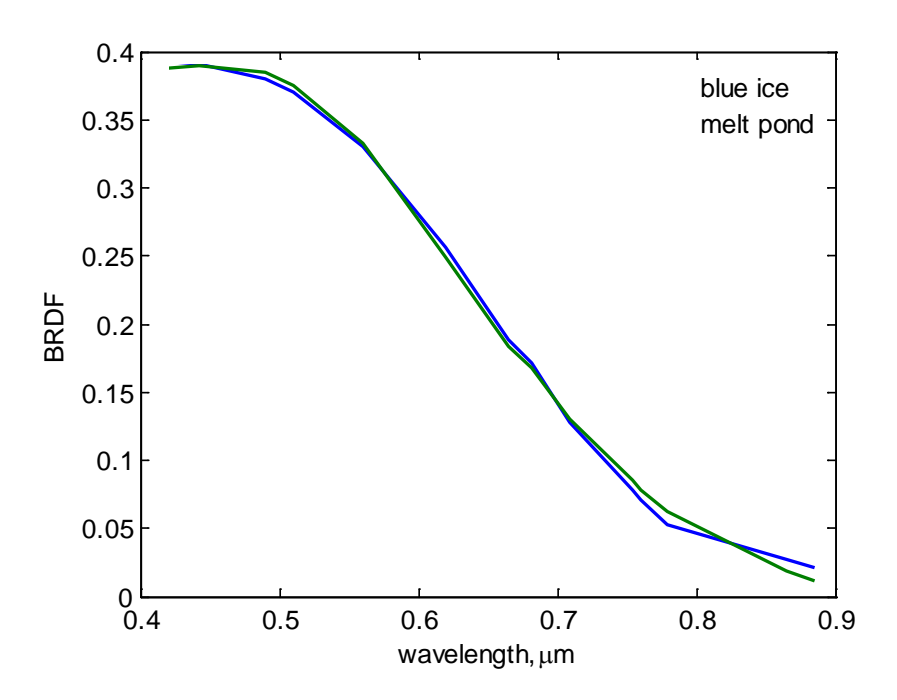


Fig. 1. BRDF of the blue ice and the melt pond at the incident zenith angle  $60^{\circ}$  and observation zenith angle of  $0^{\circ}$ 

As one can see, the presented spectra are very close. This means that the blue ice can always be interpreted from the space as a melt pond, if only optical reflection properties are used for the identification. In order to separate the blue ice from melt ponds the additional information, beside optical, should be included, e.g., it could be the temperature regime.

### **2.2.2** Wet ice

The second 'difficult' situation is wet, water-saturated, ice. As it is shown in Sec. 3, the reflection of this surface (as well as reflection of white ice) is simulated with good accuracy with the stochastic model [6]. But unlike real white ice [3], this wet ice has much less optical thickness and much greater effective grain size. In the presented here modeling we used the optical thickness of 3 and the grain size of 9000  $\mu$ m (and with no yellow substance).

As in the previous case we calculated the BRDF of such a layer at the incident zenith angle of  $60^{\circ}$  and the nadir observation and found the characteristics of the melt pond, which gave the closest BRDF spectrum. These characteristics turned out to equal:  $tau\_pond = 5.\times10^{-6}$ ;  $sig\_ice = 25. \text{ m}^{-1}$ ;  $tau\_ice = 1.3$ . The BRDF spectra are shown in Fig. 2.

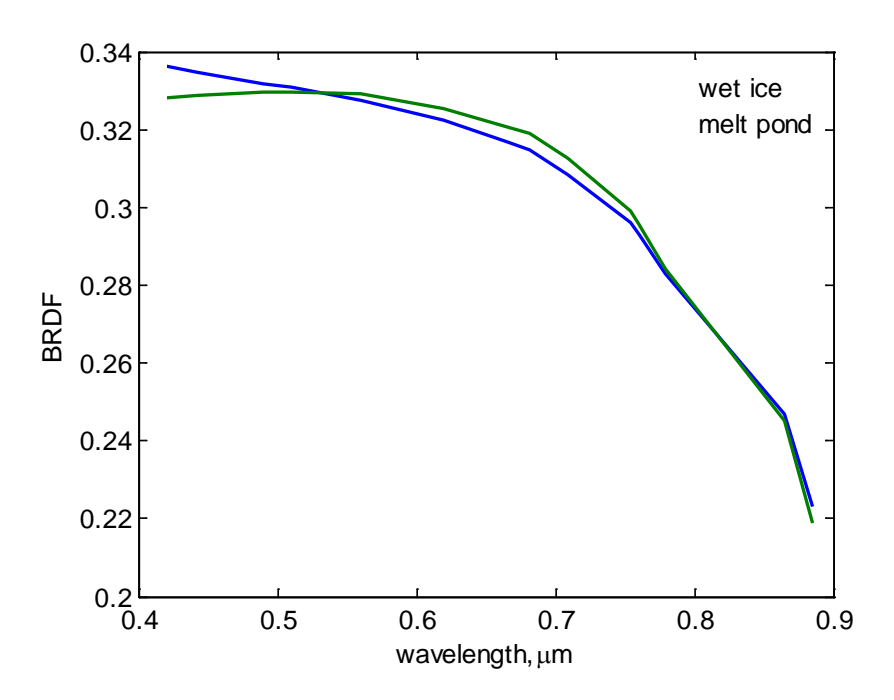


Fig. 2. BRDF of the wet ice and the melt pond at the incident zenith angle  $60^{\circ}$  and observation zenith angle of  $0^{\circ}$ 

The presented spectra are also very close. This can lead to an uncertainty in the melt pond fraction retrieval. Indeed, the approach of the MPD algorithm treats a melt pond as a layer of water on the underlying ice. From this point of view the surface, which is completely water covered, can be considered as one big melt pond, covering the whole surface. In the last version of MPD the value 1 for the melt pond fraction is used to identify this situation. However, in some cases the result can differ from 1, giving the other values for different *a priori* used characteristics (some aspects of this are discussed in Sec. 4.2). In general, the pond fraction retrieval for completely wet ice is unstable. Fortunately, this situation of strong melting usually continues for only a couple of days [3] and quickly leads to the 'standard' situation of developed melting with easily recognizable melt pond and drained highly scattering white ice.

The coincidence of the melt pond spectrum with that of 'blue ice' or 'wet ice' shows that there are no algorithms, which could solve this problem using the same spectral information. The possibility to include the additional information is a point of further researches.

### 2.3 Polarstern field data. Models vs. experiments

The first version of the developed MPD code was based mainly at scenario that includes white ice and melt ponds (developed melting) [3]. Optical and physical models of both white ice and melt ponds have been developed at the previous stages of SIDARUS execution. White ice in our notation is any type of ice, which optical properties are determined by a great number of air inclusions, so that its microphysics can be described with stochastic model of a mixture of ice and air. E.g., this model can certainly be applied to the drained scattering layer. Melt pond is considered as a layer of pure water with the ice bottom. These models have been described in detail in Deliverable D4.1 (also to be published in peer-reviewed journals). Now there are several questions to be answered, concerning these models.

- 1. How reliable these models are? I.e., how close the spectra they can describe with only few parameters, shown in Table 1, to the real measured spectra of white ice and melt ponds in different situations?
- 2. What is the scope of the applicability of these models? Can they be applied to the situations when the surface differs from the classical model [6] of white ice or melt pond?
- 3. What is the statistics of the ice/ponds parameters? What is the range of their changes in reality? The last question is very important for the regularization of the solution with the MPD software. When the problem (as in this case) is mathematically incorrect and needs regularization, it is very important to have some a priori information, in our case the range of variation of the sought-for parameters, to exclude the false solutions.

We have not found any database with reflectance spectra systematically measured for various melting ice situation. To get these data was one of the main goals of UB participation in the Polarstern expedition, where spectral reflectance of different types of Arctic ice and melt ponds were accurately measured. We took these measured spectra and simulated them with our models, i.e., fitted the spectra by adjustment of the parameters of the models (the results are shown and discussed below). Doing so, we see at once the answer to the first question (how many cases can be described with our models. And we used the retrieved parameters to make the statistics of their variations and to figure out the borders of their changes.

### 2.4 Angle of incidence

The measurements during Polarstern expedition were carried out from the end of August to the beginning of September. For the days of measurements and station coordinates the maximum solar elevation angles (at noon) were  $20^{\circ}$ ,  $20^{\circ}$ ,  $20^{\circ}$ ,  $17^{\circ}$ ,  $15^{\circ}$ , and  $10^{\circ}$ ; i.e., the measurements were carried out at the very low sun (zenith angle equals  $90^{\circ}$  minus elevation angle). The problem is that in case of overcast with the visible sun disk the incidence is partially diffuse, partially direct. So, the measured value is a superposition of the plane albedo (at direct incidence) and the spherical albedo (at diffuse incidence).

To account for this effect we used the following suggestion.

For bright surfaces (with albedo close to 1) the following approximate equation takes place:

$$1 - A(\cos \theta_0) = (1 - A)g(\theta_0), \tag{1}$$

where  $A(\cos\theta_0)$  is the plane albedo – albedo at direct incidence at zenith angle  $\theta_0$ , A is the spherical albedo – albedo at diffuse incidence,  $g(\theta_0) = \frac{3}{7} \big(1 + 2\cos\theta_0\big)$ .

Eq. (1) can be obtained from the asymptotic formulas for weekly absorbing scattering media [7]:

$$A(\cos \theta_0) = \frac{\sinh(\gamma \tau + 4q\gamma(1 - g(\theta_0)))}{\sinh(\gamma \tau + 4q\gamma)},$$

$$A = \frac{\sinh(\gamma \tau)}{\sinh(\gamma \tau + 4q\gamma)},$$
(2)

in the first order of  $\gamma$ . ( $\gamma$  is the attenuation coefficient at depth regime, it characterizes the absorption; value q characterizes the asymmetry of the phase function;  $\tau$  is the optical depth).

So, the plane albedo approximately equals to the spherical albedo at zenith angle of  $48^{\circ}$ . As we have a superposition of diffuse light (equal to plane albedo at  $\theta_0 = 48^{\circ}$ ) and direct light at incidence  $\theta_0 > 70^{\circ}$ , according to the mean value theorem, the resulting value is equal to the plane albedo at incidence angle  $\theta_0$  between  $48^{\circ}$  and  $70^{\circ}$ . Our simulations have shown the good agreement of the measured and modeled spectra at  $\theta_0$  of about  $57^{\circ}-58^{\circ}$ .

The similar situation concerns the melt ponds. Theoretically, reflectance of a melt pond at 1.2-1.4 $\mu$ m spectral region is completely defined by Fresnel reflection from the surface. However, as ponds always have limited size, in some cases specular reflection is not included in the reflected radiation, especially when the sun is low: the rays at very oblique incidence don't come to the receiver. It is important that these rays have very high reflectance. This may be the reason why the measured reflectance at 1.2-1.4 $\mu$ m is usually lower than Fresnel reflection for diffuse light. The effective angle of incidence, used previously, is the way to fit the modeled and measured spectra: the incidence angle is checked to make the measured reflectance at 1.2-1.4 $\mu$ m be equal to Fresnel specular reflectance from water surface.

### 2.5 Analysis of the field spectral measurements

In this Section we analyze the field data obtained during Polarstern expedition, simulate the reflectance spectra using the previously developed models [6], and analyze the parameters of ice and ponds, retrieved in this simulation.

For verification of the elaborated optical models of the surface reflection we choose and consider only the cases when the reflecting surface is homogeneous (as far as possible), i.e., it is either ice or melt pond.

The data are separated by the stations, where the measurements were carried out.

In general, the data processing consists of the following. We take the measured spectrum of the albedo of some surface (pond or ice) and find its characteristics according to developed physical model [6], which provide the best spectrum fitting (in the sense of least squares). The characteristics to be found are presented in Table 1.

Table 1. Characteristics of ponds and ice, used in the modeling. All characteristics are supposed to be given at wavelength 550 nm, except absorption of yellow pigments, which should be given at 390 nm.

Туре	Characteristic	Comments	
	tau_pond	Optical thickness of the water layer in the pond.	
Pond	sig_ice	Transport scattering coefficient of the underlying ice.	
	tau_ice	Optical thickness of the underlying ice.	
Ice	tau_white	Effective optical thickness of white scattering layer.	
	aeff	Effective grain size in white scattering layer (in μm).	

а_ур	Absorption of yellow pigments from seawater (in m <sup>-1</sup> ).

The characteristics, obtained in data processing are presented in appropriate tables in the text. The measured and retrieved spectra are both presented in figures in *Appendix A* (measured in blue, retrieved in green). The first column of the tables contains the value **Name** – it is the name of the measured spectrum in notation used in Polarstern database (first 6 signs in the **Name** indicates the date of measurement, e.g., '110812' means that the measurement was carried out on the 11<sup>th</sup> of August, 2012). This name is also written in the appropriate figure in *Appendix A*. The type of the surface and illumination conditions is indicated in the figures as well. The other columns of the tables contain the values of the retrieved characteristics, described in Table 1, for every measured spectrum. The decision either to include the case in the statistics or to discard is made by two reasons. First, the retrieved spectrum should fit well the measured one (see the figures). Second, the retrieved characteristics should have reasonable physical value.

### Station 1 (84°3.030'N 31°6.830'E)

Ponds.

Table 2. Ponds properties. Station 1

	Name	tau_pond	Estimated depth (m)
1	110812ROVtransect4e00000.asd	2.7654e-002	5.9493e-001
2	110812ROVtransect1112pe00000.asd	7.2855e-003	1.5674e-001
3	110812ROVtransect160pe00000.asd	5.2044e-005	1.1197e-003
4	110812ROVtransect23e24p00000.asd	1.1081e-002	2.3838e-001
5	110812ROVtransect78pe00000.asd	2.7184e-004	5.8482e-003
6	110812ROVtransect89pe00000.asd	2.8732e-005	6.1813e-004

All the spectra are retrieved with good accuracy. However, cases 3, 5, 6 (highlighted in red) give too small values of *tau\_pond*, and therefore of the pond depth, which is about millimeters (last one even less). In modeling this means that there is no actual pond, but only underlying ice. In reality this means, that quite a lot of white ice or

snow affect the reflection (it could be if white ice is in the filed-of-view of the sensor receiver or if the pond is frozen and covered with a little amount of snow). Typical footprint of white ice (snow) is seen as a small peak between  $1-1.2\mu m$ .

Conclusion: cases 1, 2, 4 can be included in the statistics; cases 3, 5, 6 should be discarded.

Ice.

Table 3. Ice properties. Station 1

	Name	tau_white	aeff (μm)	a_yp (m <sup>-1</sup> )
1	110812ROVtransect5e00000.asd	1.3824e+001	1.4875e+003	1.5083e-008
2	110812ROVtransect8e00000.asd	1.1828e+001	9.8034e+002	6.8365e-003
3	110812ROVtransect9e00000.asd	9.9643e+000	1.3128e+003	7.2934e-010
4	110812ROVtransect13e00000.asd	2.8367e+001	5.9588e+002	1.9260e+000
5	110812ROVtransect14e00000.asd	1.2319e+001	9.8022e+002	6.1637e-001
6	110812ROVtransect17e00000.asd	7.5098e+000	2.5020e+003	4.4036e-024
7	110812ROVtransect18e00000.asd	1.1686e+001	1.4268e+003	6.1487e-016
8	110812ROVtransect19e00000.asd	2.2104e+001	9.7524e+002	9.6976e-003
9	110812ROVtransect21e00000.asd	1.3167e+001	1.1440e+003	8.0221e-004
10	110812ROVtransect22e00000.asd	1.5015e+001	1.2044e+003	3.9333e-005
11	110812ROVtransect23e00000.asd	1.5751e+001	1.2445e+003	1.6245e-004
12	110812ROVtransect24e00000.asd	2.0741e+003	6.4641e+002	6.8768e-001
13	110812ROVtransect25e200000.asd	1.7817e+001	1.1491e+003	1.2377e-002
14	110812ROVtransect26e00000.asd	1.1936e+001	1.3814e+003	2.2269e-003

Cases 1, 6, 7 (highlighted in red) show bad spectra retrieval. We cannot explain such an increase of reflectance in the shortwave range. Good spectrum retrieval is seen in cases 2, 3, 8, 9, 10, 11, 13, 14. Cases 4, 5, 12 demonstrate excellent fitting.

All optical thicknesses are in reasonable range (minimal is 7.5). Case 12 outranges: *tau\_white* is much greater (2e+3), *aeff* is much less (646µm). We can suggest from this that this surface is snow-covered.

Interesting is the fact that the best cases show the highest values of yellow pigments absorption, whereas the worst cases show extremely low pigments amount (except case 3).

Conclusion: cases 1, 6, 7 should be discarded; all other cases can be included in the statistics.

### Station 2 (83°59.190'N, 78°6.200'E)

#### Ponds.

Table 4. Ponds properties. Station 2

Name	Tau_pond	Sig_ice (m <sup>-1</sup> )	Tau_ice
150812pond1e00000.asd	1.0099e-004	1.0743e+000	1.0951e+000
150812pond2e00000.asd	7.6765e-005	1.3744e+000	1.1405e+000
160812bluepond1e00000.asd	1.7386e-004	9.2859e-001	3.7121e+000
160812bluepond1morebubble00000.asd	1.1286e-004	1.1676e+000	5.3941e+000
160812bluepond1nobubble00000.asd	1.8353e-004	9.6736e-001	3.8955e+000
160812pond2e00000.asd	7.9188e-005	2.1855e+000	2.4707e+000
160812rovponde00000.asd	1.0975e-004	1.1003e+000	8.7437e-001

Despite all the ponds were frozen, all the spectra are represented satisfactorily. Also the retrieved characteristics have reasonable physical values.

Conclusion: all cases can be included in the statistics.

Ice.

Table 5. Ice properties. Station 2

	Name	tau_white	aeff (µm)	a_yp (m <sup>-1</sup> )
1	150812ROV11icee00000.asd	1.2386e+001	3.0684e+003	2.1621e-001
2	150812ROV12icee00000.asd	1.4548e+001	3.0446e+003	7.0854e-002
3	150812ROV13icee00000.asd	1.6280e+001	2.7174e+003	4.9617e-001
4	150812ROV14icee00000.asd	1.6104e+001	3.0404e+003	1.3028e-001
5	150812ROV15icee00000.asd	1.6288e+001	2.9167e+003	1.9456e-001
6	150812ROV16icere00000.asd	2.7298e+001	2.8414e+003	1.1296e-001
7	150812ROV18icee00000.asd	2.1150e+001	2.7661e+003	1.9417e-001
8	150812ROV19icepe00000.asd	1.6735e+001	2.9214e+003	2.0122e-001
9	150812ROV1icee00000.asd	1.8639e+001	2.8402e+003	1.0822e-001
10	150812ROV20icee00000.asd	1.5393e+001	3.0640e+003	2.9797e-001
11	150812ROV21icee00000.asd	9.9872e+000	3.4035e+003	1.7522e-001
12	150812ROV22icee00000.asd	7.8128e+000	3.9397e+003	6.4418e-003
13	150812ROV23icee00000.asd	1.7711e+001	3.0672e+003	2.0308e-001
14	150812ROV24icee00000.asd	8.9617e+000	3.1296e+003	2.9736e-001
15	150812ROV2icee00000.asd	1.7377e+001	3.1040e+003	2.3932e-003
16	150812ROV4icee00000.asd	1.5100e+001	3.1379e+003	3.8563e-003
17	150812ROV6wicee00000.asd	1.4276e+001	3.0828e+003	2.9488e-001
18	150812ROV8icee00000.asd	1.5539e+001	2.7559e+003	3.9971e-001
19	150812ROV9icee00000.asd	1.2427e+001	3.5291e+003	5.6879e-002

The data is very stable. The spectra fit very well. The discrepancy between the measured and retrieved spectra in the range 1.2-1.4  $\mu$ m can be explained by the fact that the asymptotic formulas, used in the retrieval, overestimate the albedo for low values ( < 0.3 ).

Conclusion: all cases can be included in the statistics.

### Station 3 (82°40.240'N, 109°35.370'E)

Ponds. August 20.

Table 6. Ponds properties. Station 3. August 20

	Name	tau_pond	Estimated depth (m)
1	200812ROV0pe00000.asd	3.9360e-004	8.4646e-003
2	200812ROV13futpe00000.asd	5.2955e-005	1.1388e-003
3	200812ROV1415psmalle00000.asd	6.2315e-005	1.3401e-003
4	200812ROV1pe00000.asd	1.8133e-004	3.8996e-003
5	200812ROV6afterpe00000.asd	1.8327e-004	3.9412e-003
6	200812ROV6pe00000.asd	1.7906e-004	3.8507e-003

All the cases, except 2 and 3, show good spectra fitting. However, the retrieved pond depth is too small (about millimeters). Also, in all the plots the footprint of white ice (or snow) is clearly seen as a peak between 1-1.2 $\mu$ m for all cases.

Conclusion: no cases can be included in the statistics.

Ponds. August 21.

Table 7. Ponds properties. Station 3. August 21

Name	Tau_pond	Sig_ice (m <sup>-1</sup> )	Tau_ice
210012muralaFa00000 and	6.1197e-003	6.7808e-001	4.4996e-001
210812puralg5e00000.asd	6.11976-003	6.78086-001	4.49966-001
210812purbp1e00000.asd	1.1753e-003	1.7862e+000	3.7350e+000
210812purbp2e00000.asd	1.3965e-004	2.8669e+000	3.2359e+000
210812purbp3e00000.asd	4.2708e-003	7.4053e-001	2.1726e+000
210812purwhitep4e00000.asd	1.8848e-004	2.6096e+000	2.6382e+000

Despite all the ponds were frozen, all the spectra are represented satisfactorily. Also the retrieved characteristics have reasonable physical values.

Conclusion: all cases can be included in the statistics.

Ice.

Table 8. Ice properties. Station 3

	Name	tau_white	aeff (µm)	a_yp (m <sup>-1</sup> )
1	200812ROV11icee00000.asd	8.7503e+000	3.1484e+003	1.1975e-002
2	200812ROV12icee00000.asd	5.4769e+000	3.7755e+003	1.7953e-002
3	200812ROV14icee00000.asd	7.5045e+000	3.5438e+003	1.9557e-001
4	200812ROV15icee00000.asd	4.5886e+000	4.5849e+003	2.7360e-003
5	200812ROV16icee00000.asd	1.0400e+001	4.9788e+003	4.5198e-003
6	200812ROV18icee00000.asd	8.2859e+000	4.4594e+003	2.2342e-002
7	200812ROV20icee00000.asd	3.4284e+000	6.6954e+003	6.0770e-003
8	200812ROV21icee00000.asd	2.1633e+000	1.0419e+004	6.9152e-003
9	200812ROV24icee00000.asd	7.3340e+000	3.8161e+003	4.7250e-002
10	200812ROV22icee00000.asd	3.1864e+000	6.0912e+003	4.0164e-007
11	200812ROV25icee00000.asd	8.1989e+000	3.6564e+003	7.8298e-002
12	200812ROV26icee00000.asd	8.6825e+000	4.0095e+003	1.0606e-003
13	200812ROV3icee00000.asd	7.3607e+000	3.6681e+003	7.1722e-003
14	200812ROV5icee00000.asd	5.4098e+000	4.6983e+003	2.6130e-004
15	200812ROV7icee00000.asd	1.1554e+001	3.1267e+003	1.6792e-001
16	200812ROV8cracke00000.asd	2.2849e+000	1.2413e+004	4.4186e-002
17	200812ROV9icee00000.asd	6.0630e+000	3.6014e+003	1.2011e-003

At this station strong surface melting was observed. Most of ice samples are melting wet ice. However, there are cases with high reflectance, which can be treated as white ice (cases 1-6, 9, 11-15, 17). Cases 7, 8, 9, 10, 16 (highlighted in dark blue) are dark, water saturated ice. These cases should be excluded from the statistical processing. However, these cases are important, because they demonstrate the scope of the applicability of the developed models. Fig. 3 shows the photograph of the melt ice in case 7.



Fig. 3. Photo of the melt ice in case 7

Although the stochastic model was developed to describe the reflectance of white dry ice, it reproduces the spectrum of wet melting ice as well, i.e., outside the scope of its initial applicability. The features in these cases (describing melt ice) are low optical thickness ( $tau\_white < 5$ ) and very large ice grains (aeff > 6 mm). These features will be used hereinafter in modeling reflectance of wet ice.

### Station 4a (82°52.950'N, 130°7.770'E)

Ponds.

Table 9. Ponds properties. Station 4a

	Name	tau_pond	Estimated depth (m)
1	260812Larm2pond1e00000.asd	2.2156e-002	4.7647e-001
2	260812Larm2pond2e00000.asd	1.6515e-002	3.5517e-001

Both pond spectra have a little footprint of ice (peak at 1-1.2  $\mu$ m). However, 1<sup>st</sup> pond has the underlying ice depth of less than millimeter (extremely low optical depth with extremely high scattering coefficient) and should be discarded. The 2<sup>nd</sup> case can be included into statistics.

Ice.

Table 10. Ice properties. Station 4a

	Name	tau_white	aeff (µm)	a_yp (m <sup>-1</sup> )
1	260812Larm1icee00000.asd	1.1511e+001	2.7599e+003	6.6650e-002
2	260812Larm4ice2e00000.asd	1.2062e+001	2.9925e+003	4.9403e-002

Measured and simulated spectra fit very well. Thicknesses and grain sizes are in the typical range for white ice, pigments concentration is very small.

Conclusion: both cases can be included in the statistics.

#### Station 4b (82°53.690'N, 129°46.580'E)

#### Ponds.

Table 11. Ponds properties. Station 4b

	Name	tau_pond	Estimated depth (m)
1	260812purbp1e00000.asd	1.6562e-002	3.5618e-001
2	260812purbp2de00000.asd	1.9411e-002	4.1744e-001
3	260812purdpw3e00000.asd	1.3159e-002	2.8299e-001

In cases 1 and 2 spectra fitting is well. In case 3 the coincidence is moderate. Also in case the underlying ice depth is less than millimeter.

Conclusion: cases 1 and 2 can be included in the statistics; case 3 should be discarded.

#### Ice.

Table 12. Ice properties. Station 4b

	Name	tau_white	aeff (µm)	a_yp (m <sup>-1</sup> )
1	260812purice1e00000.asd	1.6268e+001	3.2475e+003	4.4992e-003
2	260812purice2e00000.asd	5.9162e+000	2.7048e+003	3.9934e-002

Both spectra fit very well. The retrieved parameters are in the typical range.

Conclusion: both cases can be included in the statistics.

#### Station 5 (81°55.530'N, 131°7.720'E)

No ponds.

Ice.

Table 13. Ice properties. Station 5

	Name	tau_white	aeff (µm)	a_yp (m <sup>-1</sup> )
1	050912ROVice0e00000.asd	7.6669e+001	1.8992e+002	1.0971e+001
2	050912ROVice11e00000.asd	1.5528e+001	3.1005e+002	1.4075e+001
3	050912ROVice12i00000.asd	4.5067e+010	1.9760e+002	1.4817e+001
4	050912ROVice13e00000.asd	1.7503e+001	2.6377e+002	7.5274e-005
5	050912ROVice14e00000.asd	5.3819e+001	2.1180e+002	6.2669e+001
6	050912ROVice15e00000.asd	2.7733e+001	2.3243e+002	1.0449e+000
7	050912ROVice16e00000.asd	9.3489e+000	6.8807e+002	5.9362e-001
8	050912ROVice18e00000.asd	2.3120e+001	2.9731e+002	9.9097e-001

9	050912ROVice1e00000.asd	2.4446e+002	1.3063e+002	1.6460e+000
10	050912ROVice21e00000.asd	7.2004e+000	7.0238e+002	3.7139e-010
11	050912ROVice22e00000.asd	1.9274e+004	1.2732e+002	8.7230e+000
12	050912ROVice23e00000.asd	1.2699e+001	7.1260e+002	5.5606e+000
13	050912ROVice24e00000.asd	4.7018e+001	1.7596e+002	1.1827e+001
14	050912ROVice26e00000.asd	4.9016e+000	1.9249e+003	1.4016e+000
15	050912ROVice28e00000.asd	4.2320e+001	2.2617e+002	8.1613e+000
16	050912ROVice3e00000.asd	3.2544e+001	1.8991e+002	1.4211e+000
17	050912ROVice5e00000.asd	5.4934e+002	9.5922e+001	7.0181e+000
18	050912ROVice6e00000.asd	7.3988e+002	9.1760e+001	8.9145e+000
19	050912ROVice7e00000.asd	4.0029e+001	2.0303e+002	7.1894e-001
20	050912ROVice9e00000.asd	4.7268e+002	1.0673e+002	2.3315e+000
21	050912ROVpond20e00000.asd	5.5597e+000	1.1230e+003	5.5797e-002

Sky is practically clear, sun angle is 75°. Cases 2, 3, and 5 show reflectance greater than 1. This is treated as a systematical error. These cases are discarded.

Surprising are high values of pigments absorption, even for the cases with very good spectrum retrieval (1, 6, 7, 12, 14, 15, 18).

Cases 7, 10, 12, 14, 21 (highlighted in blue) show characteristics, typical for white ice. All other cases have high optical depth and very low grain size, which is typical for snow.

### Station 6 (85°6.110'N, 122°14.720'E)

No ponds.

Ice.

Table 14. Ice properties. Station 6

	Name	tau_white	aeff (µm)	a_yp (m <sup>-1</sup> )
1	090912ROVice0e00000.asd	3.3724e+001	9.9694e+002	2.7185e-001
2	090912ROVice11e00000.asd	3.4121e+001	1.1456e+003	2.0877e-001
3	090912ROVice12e00000.asd	1.5442e+001	1.3916e+003	4.5679e-001
4	090912ROVice15e00000.asd	2.8441e+001	1.1886e+003	1.8317e-001
5	090912ROVice16e00000.asd	4.5890e+001	8.7055e+002	1.0264e-001
6	090912ROVice18e00000.asd	2.8594e+001	1.1130e+003	2.1652e-001
7	090912ROVice1e00000.asd	2.5849e+001	1.3086e+003	5.4094e-001
8	090912ROVice20e00000.asd	4.0690e+001	9.7047e+002	2.1563e-001
9	090912ROVice21e00000.asd	4.0441e+001	9.7316e+002	1.1794e-001
10	090912ROVice22e00000.asd	1.9768e+001	1.6582e+003	3.3055e-003
11	090912ROVice23e00000.asd	5.2709e+001	8.7911e+002	3.3828e-003
12	090912ROVice24e00000.asd	9.2299e+008	4.8825e+002	1.4011e-001
13	090912ROVice25e00000.asd	1.0931e+002	7.6282e+002	1.3799e-001
14	090912ROVice26e00000.asd	5.6975e+001	8.9207e+002	6.3521e-002
15	090912ROVice3e00000.asd	1.9111e+001	1.5233e+003	3.1437e-003
16	090912ROVice5e00000.asd	2.7540e+001	1.1395e+003	6.2590e-001
17	090912ROVice6e00000.asd	3.0740e+001	1.0909e+003	4.2607e-001
18	090912ROVice9i00000.asd	1.8860e+004	5.0054e+002	1.1325e-001
19	090912ROVpond67e00000.asd	8.6850e+000	9.3733e+003	7.9945e-007
20	090912ROVpondedge7e00000.asd	1.4887e+001	1.9288e+003	5.5934e-005

All values are reasonable, except cases 12 and 18 (red), where albedo is greater than 1. These case should be discarded. The other cases can be included in the statistics.

Case 19 shows the optical thickness of a snow layer, which covers the frozen pond.

# 2.6 Borders to variations of melting ice parameters for the iteration procedure in the MPD software

In the MPD code 7 parameters are determined in the iteration procedure: 3 parameters for ice, 3 parameters for ponds (see Table 1), and pond fraction. Because there is more than one mathematical solutions of the retrieval problem, it is necessary to perform some regularization. This procedure can be carried through the right choose the borders for the changes of the most influential parameters of the iteration process. The analysis presented here allows us to justify the real range of changes of ice/pond characteristics and to include the borders for their changes into the MPD algorithm.

#### 2.6.1 Selection of the borders from experimental data

Here we consider the statistics of the parameters, presented in tables in the previous section.

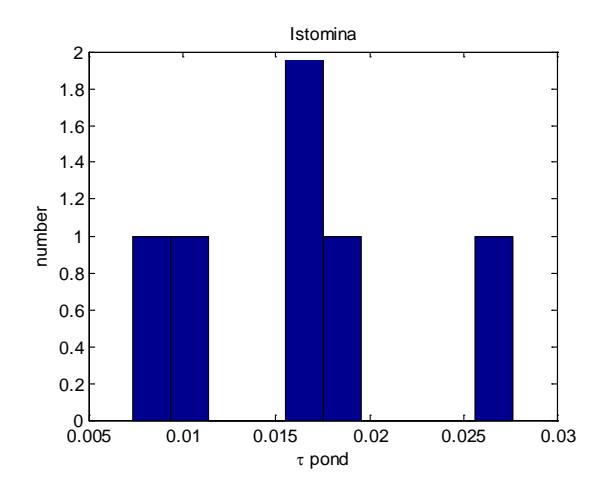
It is seen from tables for ice properties that the minimal value  $tau\_white = 5$  can be used to discriminate wet ice from white dry ice. So, we recommend this value as a low border for  $tau\_white$  in the 'standard' situation, when the surface is supposed to consist of white ice and ponds.

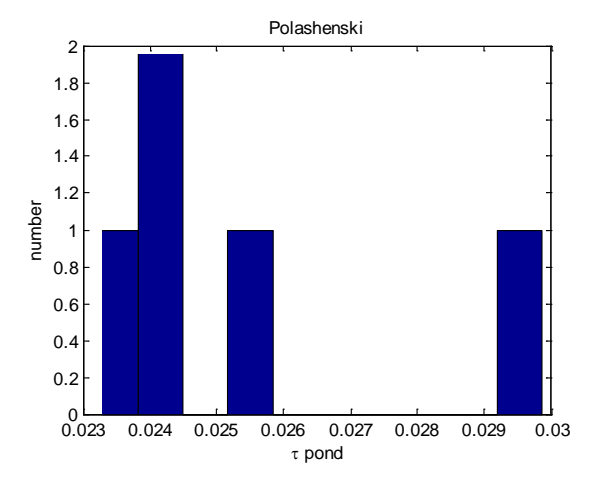
The maximum value of *tau\_white* should not be limited, because the optical thickness can be very large if the surface is snow-covered.

We recommend the minimum value of  $aeff = 30 \, \mu m$  – this is the case of extremely fresh snow. The maximum value, as it follow from the tables, is about 10000  $\mu m$ .

What concerns yellow pigment absorption, there are no restriction (except  $a_yp > 0$ ).

To define the borders for melt pond characteristics, we present the histograms (Fig. 4) with the pond parameters, retrieved from the data, measured by L. Istomina during the Polarstern expedition and by C. Polashenski at Barrow, Alaska.





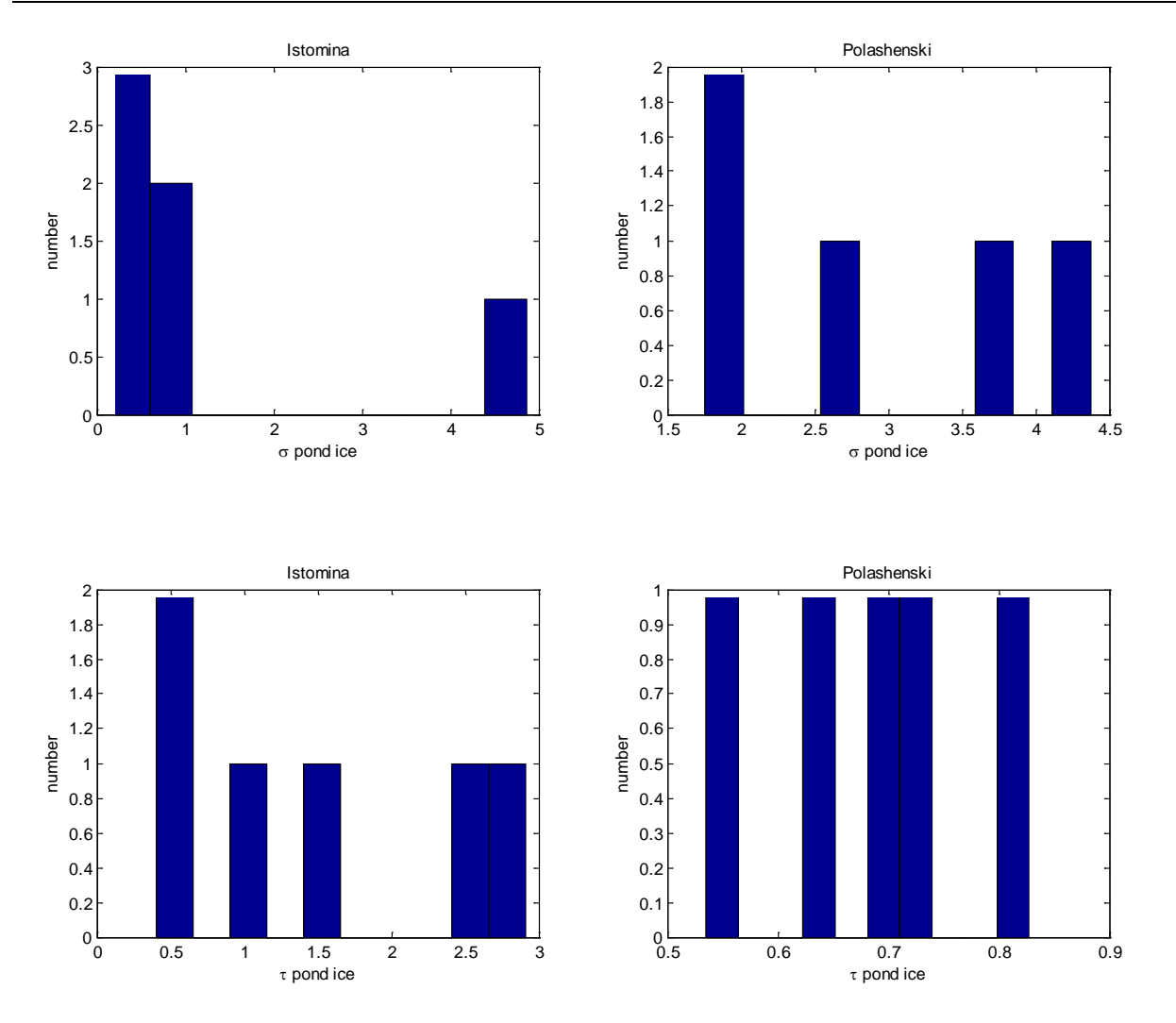


Fig. 4. Histograms of melt pond characteristics, retrieved from the data measured by Istomina in the Polarstern expedition (left) and by Polashenski at Barrow, Alaska (right)

Also, in Table 15 we present the statistical values (minimal, maximal, and mean) of melt pond optical thickness for ponds, observed at Polarstern Stations 1 and 2 (processed together) and Station 3.

Table 15. Pond optical thickness statistics

Tau_pond	Stations 1, 2	Station 3

Min	7.2855e-003	7.6765e-005
Max	2.7653e-002	6.1197e-003
Mean	1.6418e-002	1.0609e-003

Based on the presented statistics, we recommend the following borders for the melt pond characteristics.

The minimum value of tau\_pond = 0.0005. The maximum value for tau\_pond is not specified.

Value sig\_ice has a range from 0.1 m<sup>-1</sup> to 5 m<sup>-1</sup>.

Value *tau\_ice* has a range from 0.4 to 6.

These border values are recommended as the default values. They can be changed by the user, if any *a priori* information is present.

#### 2.6.2 Sensitivity of the retrieved pond fraction to the chosen borders

Once we choose the bordrs to parameters changes, we should analyze the sensitivity of the result to the chosen borders. *Appendix B* presents the retrieval for different types of ice and ponds with different borders. Three curves are in every plot: blue, green, and red for border value shifted down, recommended in the last version, and shifted up, respectively. (Note that the curves are drawn in exactly this order: blue, green, red. If one of them is not visible, it means that the curves coincide and the next one covers the previous one.) The results of the modeling are quite predictable. The most sensitive value is the minimal white ice optical thickness *tau\_white*. The next - min and max *tau\_ice* (optical thickness of ice which is the bottom of a melt pond). Generally, the greater the optical thickness the higher reflectance.

Case "bright ice - dark pond": if we increase tau\_white\_min or decrease tau\_ice\_max (i.e., move these borders closer to real values), we get a little bit better retrieval, because we move these borders closer to their true values. Other parameters don't make a notable change.

Case "bright ice - very light pond": very bad situation only for low value of tau\_ice\_max, where we cannot describe the light pond with such low tau\_ice (max 1).

Case "std ice - very light pond": the case of low *aeff\_max*=1000 differs. This border means in fact that we consider snow, instead of white ice, and cannot describe the spectral difference (in blue and in near IR). This difference is compensated by a melt pond. Again, *tau\_ice\_max* =1 is too low to describe the very light pond.

Case "std ice - dark pond": very sensitive to *tau\_white\_min*. For large values the pond fraction is strongly overestimated (however the recommended value gives a quite good result).

Low value of *aeff\_max* =1000 again gives the overestimated pond fraction. The retrieval for *tau\_ice\_min*=1.5 is not stable (min value is too high for a dark pond).

Case "Melting ice - dark pond": here we took white ice with tau=3.5. Close values were good to describe spectra of melt ice (water saturated but with white spots if ice – see cases 3, 4, 9, 10, 12, 18 from Station 3). Reasonable results gives only  $tau\_white\_min=1$ , others overestimates pond fraction strongly. Value  $aeff\_max=1000$  again overestimates the pond fraction.

Other values have little influence, except too high *tau\_ice\_min*, where the algorithm is very unstable (cannot distinguish between light pond and dark water saturated ice).

#### Resumé from this analysis is:

- 1. The retrieved fraction is very sensitive to border value when the true value is outside the borders.
- 2. High tau\_white\_min is good for bright surfaces and low for dark ice (water saturated).

In general, the borders for characteristics of melt ponds are taken quite reasonable. If not to take the extreme borders (too high min or low max), the sensitivity of the pond fraction retrieval to the chosen values of borders is low.

But tau\_white and aeff have great ranges in reality. We would recommend giving the user the possibility to change them. If one knows exactly that ice is melting and water-saturated, he can put high aeff\_min and low tau\_white\_min. If it is the opposite case and one is sure there is just dry snow, he can put low aeff\_max and high tau\_white\_min. The use of standard values is recommended if there is no additional information or the entire Arctic area is to process.

#### **2.7** New in version **1.50**

The Final version of the MPD software, Here we show shortly, what is new in the MPD, version 1.50:

- 1. Pixels, flagged as TOO\_BRIGHT, are not discarded now. They are considered as pixels with no melt ponds (S=0) and processed as snow or bright ice surfaces. Albedo is retrieved.
- 2. Starting values for iteration process are changed. Now the starting value of *tau\_white\_ice* depends on the measured signal in the 3<sup>rd</sup> MERIS channel.
- 3. The most parameters have the border values: they cannot be greater than MAX value or less than MIN value. The standard bodr values are:

tau\_white\_MIN = 5
aeff\_MIN = 30
aeff\_MAX = 10000
tau\_pond\_MIN = 0.0005
sig\_ice\_MIN = 0.1
sig\_ice\_MAX = 5
tau\_ice\_MIN = 0.4
tau\_ice\_MAX = 6

4. Output file has a field *Precision*, defined for every pixel as the root mean square of difference between measured and retrieved signals:

$$prec = \sqrt{\frac{1}{m} \sum_{i} (R_{meas}^{i} - R_{ret}^{i})^{2}}.$$

This value is a good estimation for the albedo retrieval error (absolute):

$$A_{true} = A_{ret} \pm prec$$
.

Also it can be used to estimate the *relative* error of pond fraction retrieval (except the case S=0):

$$\frac{\Delta S}{S} = \sqrt{\frac{m}{n}} \frac{prec}{lev},$$

where m is the number of channels used, n is the number of parameters to retrieve, lev is the level of regularization of the pseudo-inverse matrix. In the last version:

$$m = 8$$
,  $n = 7$ ,  $lev = 0.0075$ ,

That is the *relative* error of pond fraction retrieval can be estimated as  $\frac{\Delta S}{S} = prec * 143$ .

#### 2.8 Conclusion

Main results obtained for the third year of the SIDARUS execution are:

- The developed optical models of sea ice and melt pond reflection were successfully verified with existent experimental data and measurements for various realizations of Arctic summer ice. The experimental spectra of ice and melt ponds used are taken from data banks of The Cold Regions Research and Engineering Laboratory (CRREL, USA) and from Polarstern expedition 2012 measurements (UB), performed in the framework of the SIDARUS project.
- At the base of performed analysis of experimental data the borders for possible values of the main parameters, which are iterated in the process of the MPD retrieval, are established. The including of these

borders in the retrieval code implements (at least partially) regularization of the solved problem. It was shown that if not to take the extreme borders (too high min or low max of values), the sensitivity of the pond fraction retrieval to the chosen values of borders is low.

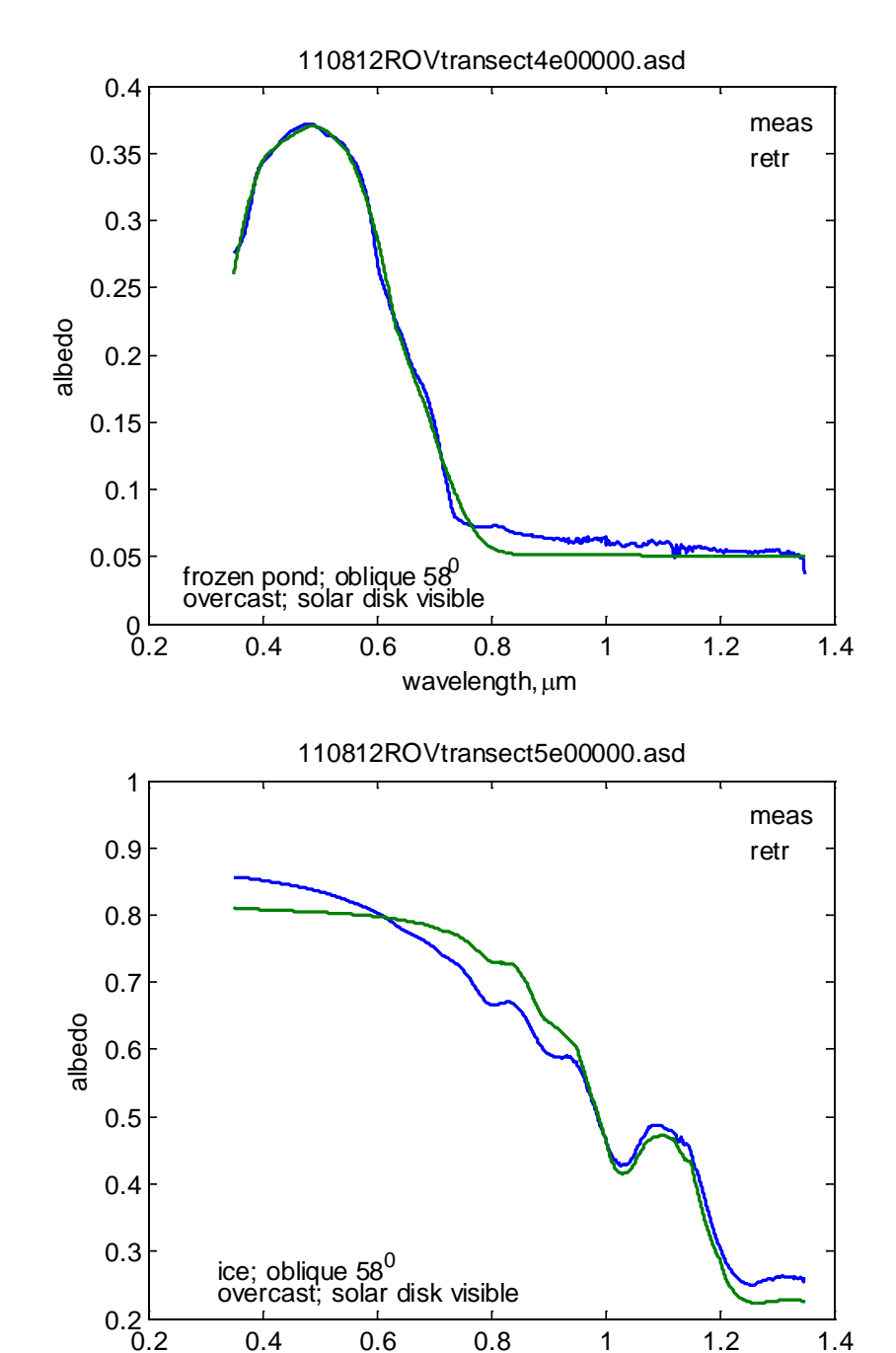
- It was shown that there are cases when the discrimination of melt pond and sea ice if only spectral data in Visible and near IR is available is essentially impossible. For instance, the blue ice may be interpreted from the space as a melt pond; in the case of water saturated ice it is impossible to separate the melt pond fraction.
- During year 2013 improving of the MPD software has been continued. Consequently three updated versions of the MPD (MPD 1.20, 1.50, 1.55) were developed, tested and transferred to UB SIDARUS group. These versions were implemented in the MERIS processing chain by UB team and used for the satellite data processing. The final versions of the MPD software (MPD 1.55) includes borders for the main parameters of iterative process and allows a user to retrieve melt pond fraction and spectral albedo of the ice surface even in cases of melting ice and freezing melt ponds. Version MPD 1.55 additionally allows a user to change borders in the case when any additional information on retrieved scenario is available. A few other improvements included in the new MPD versions are described in presented Manuals in detail. The one more new feature should be mentioned. That is the Map of the precision of modeled TOA radiances included in the output which gives a good estimation for the albedo retrieval error.

## References

- 1. M.A. Tschudi, J.A. Maslanik and D.K. Perovich, "Derivation of melt pond coverage on Arctic sea ice using MODIS observations," Remote Sens. Environ., 112(5), 2605–2614 (2008).
- 2. A. Rösel, L. Kaleschke, and G. Birnbaum, "Melt ponds on Arctic sea ice determined from MODIS satellite data using an artificial neural network," The Cryosphere, 6, 431–446 (2012).
- 3. D.K. Perovich, T.C. Grenfell, B. Light, and P.V. Hobbs, "Seasonal evolution of the albedo of multiyear Arctic sea ice," J. Geophys. Res. 107, C10, 8044 (2002).
- 4. B. Light, H. Eicken, G.A. Maykut, and T.C. Grenfell, "The effect of included particulates on the spectral albedo of sea ice," J. Geophys. Res. 103, C12, 27,739-27,752 (1998).
- 5. B. Light, "Theoretical and observational techniques for estimating light scattering in first-year Arctic sea ice," in Light Scattering Reviews 5. Single Light Scattering and Radiative Transfer (A. Kokhanovsky ed., Springer, 2010), p. 331-391.
- 6. SIDARUS Deliverable D4.1 (2011).
- 7. E. P. Zege, Ivanov, A. P., Katsev, I. L. (1991). Image transfer through a scattering medium. Heidelberg: Springer-Verlag.

# Appendix A

# Station 1



1.2

1.4

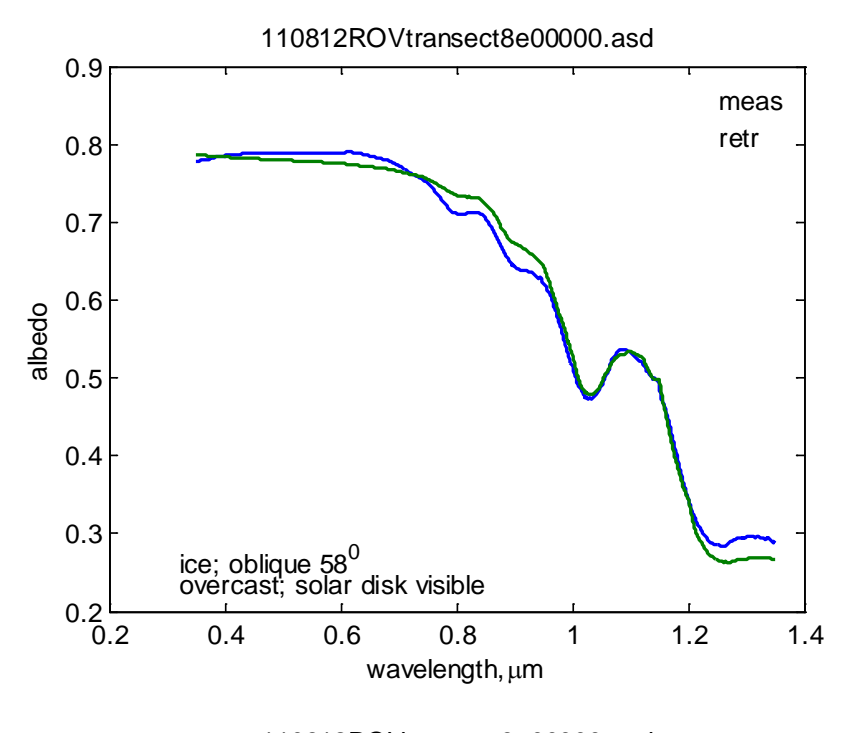
1

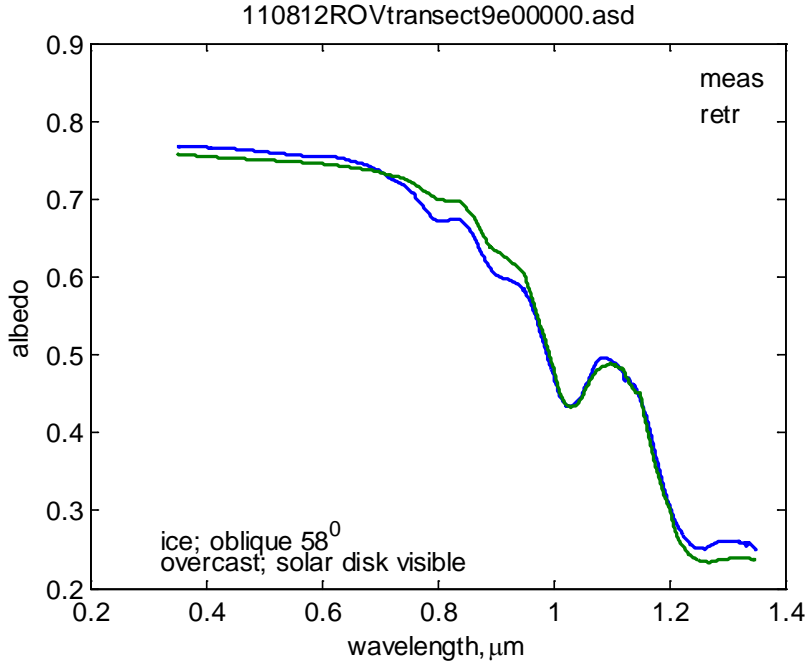
0.4

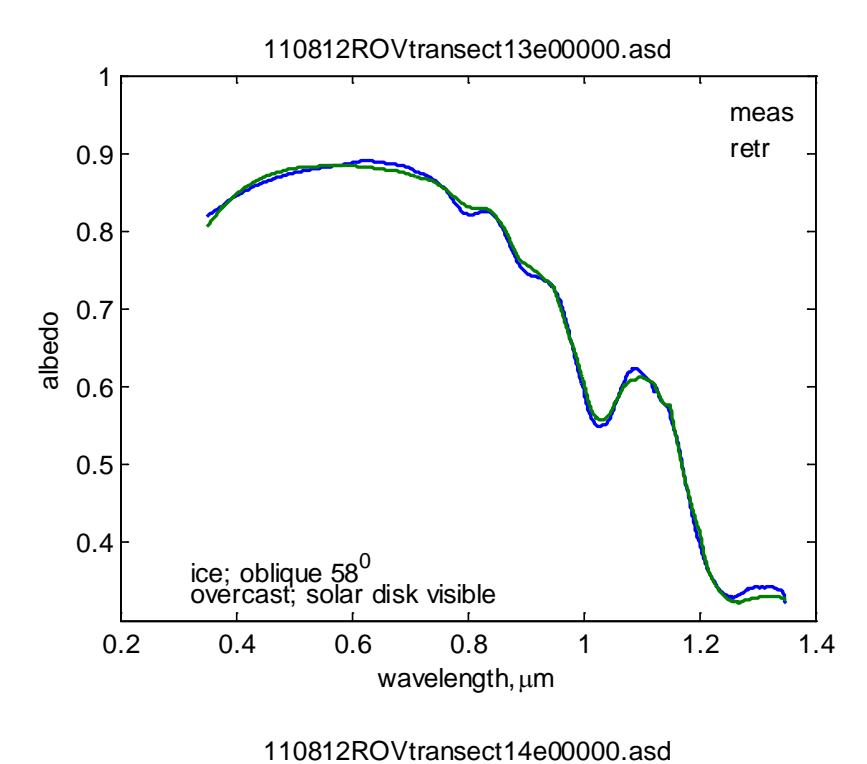
0.6

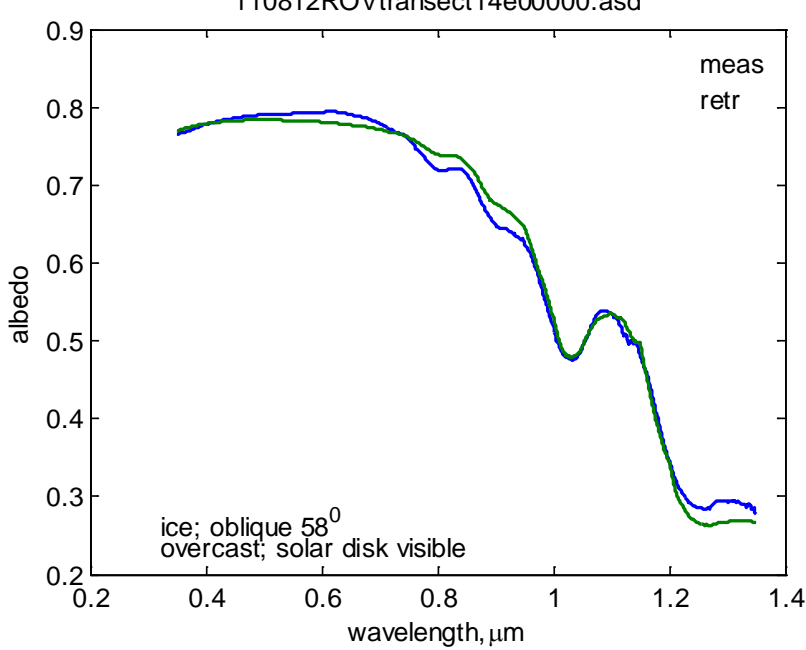
8.0

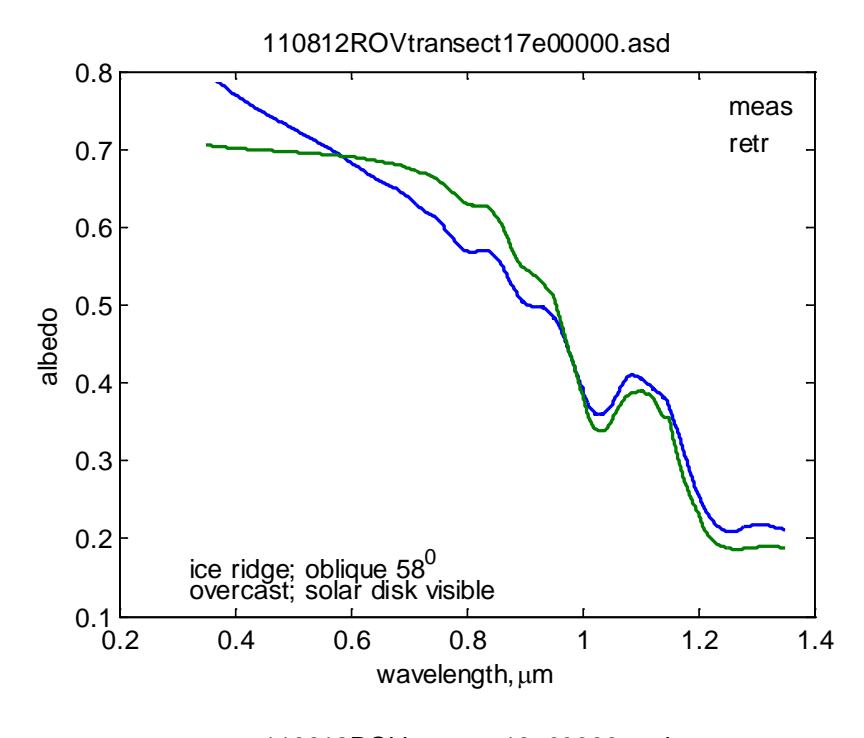
wavelength, µm

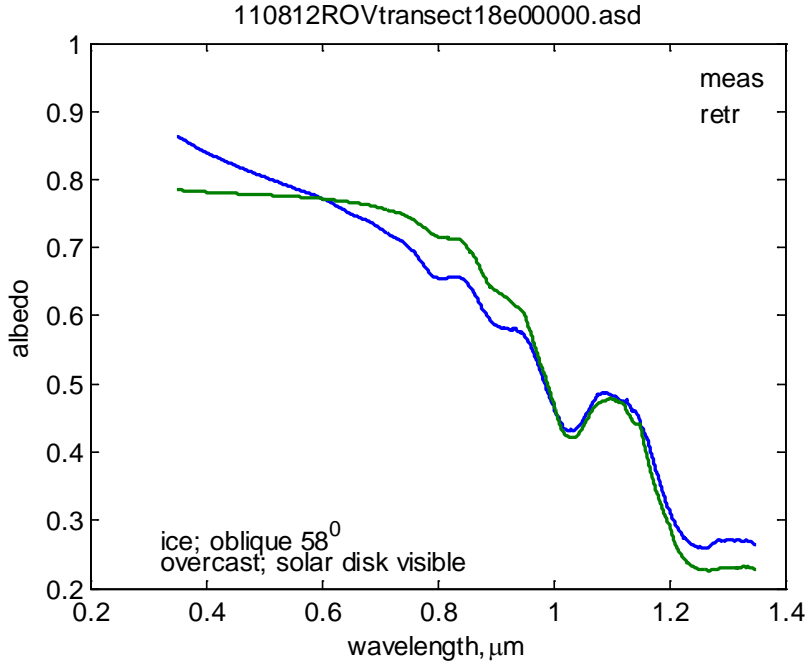


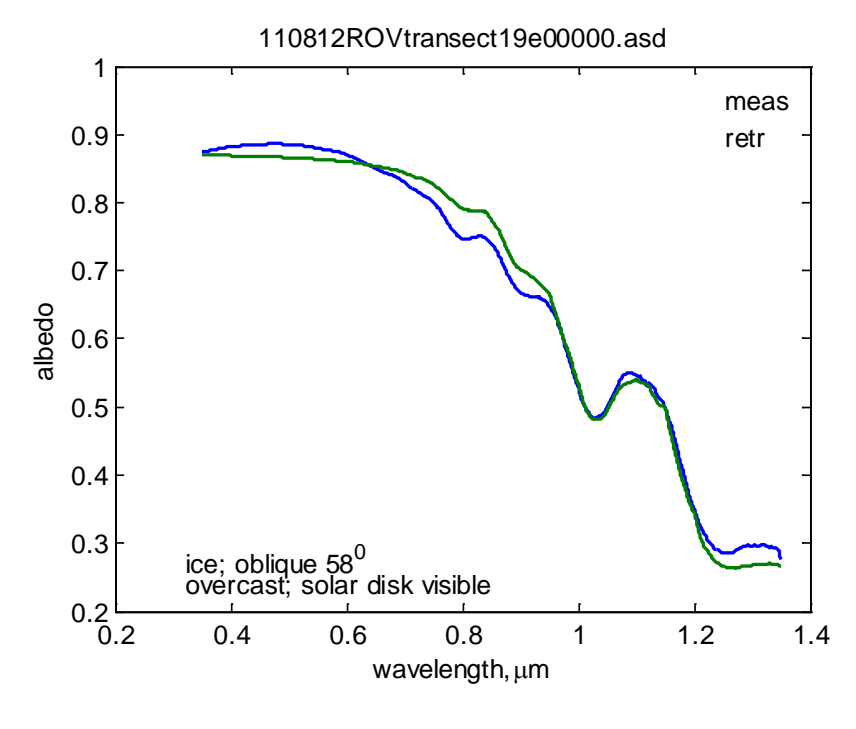


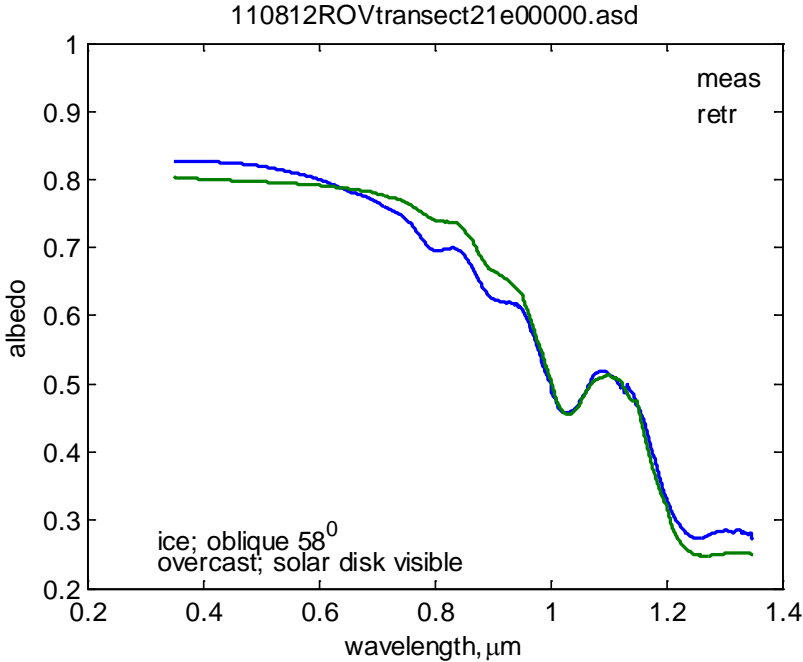


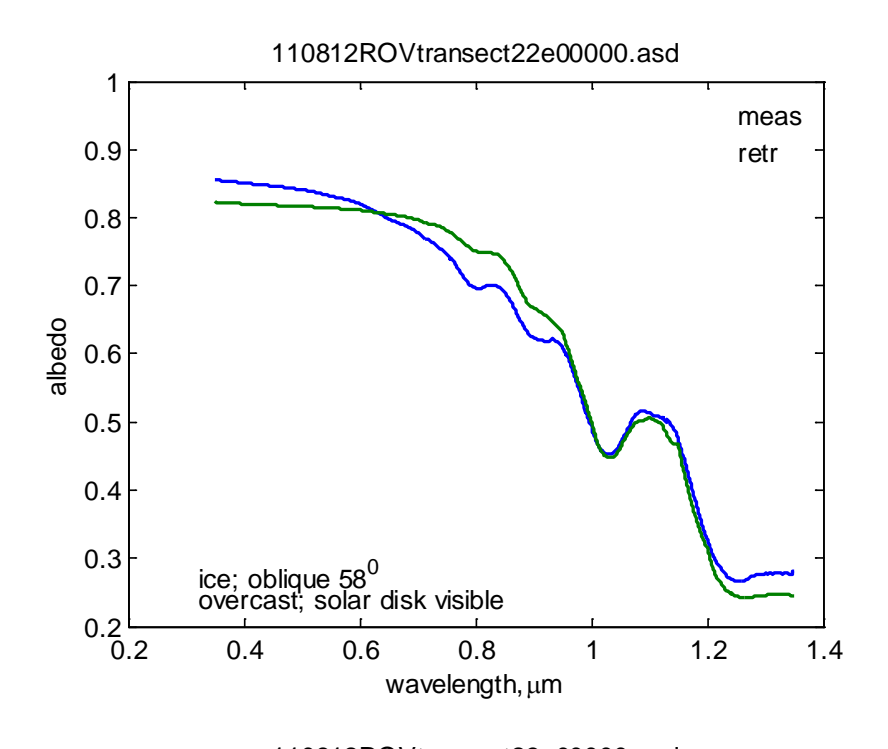


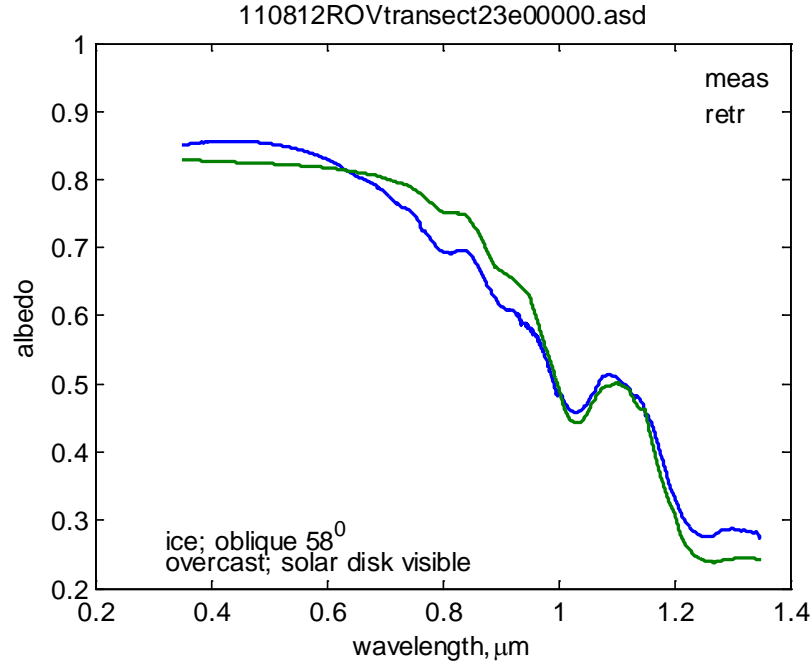


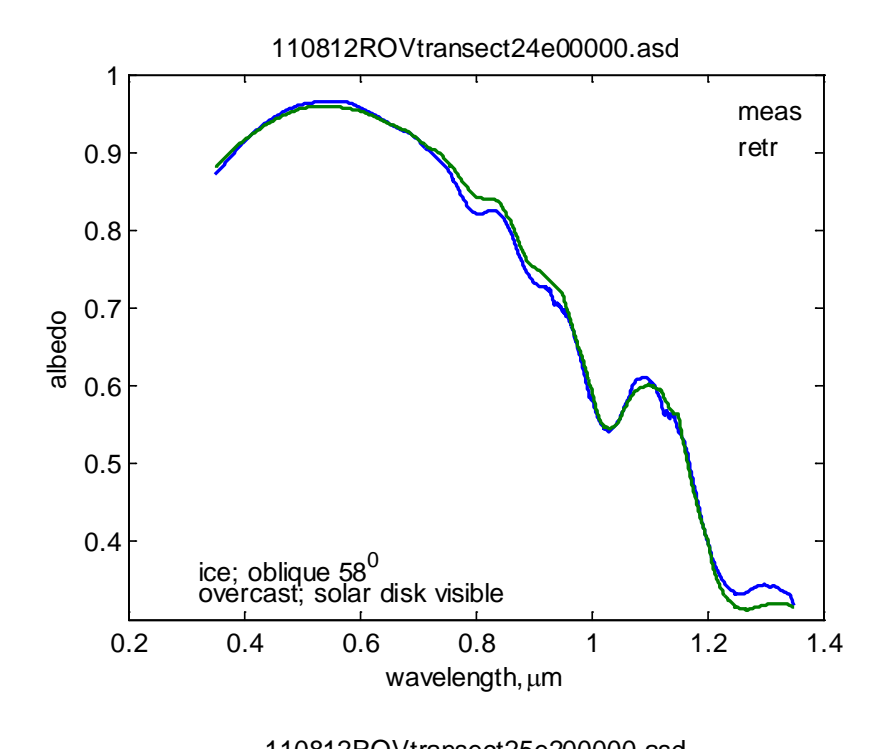


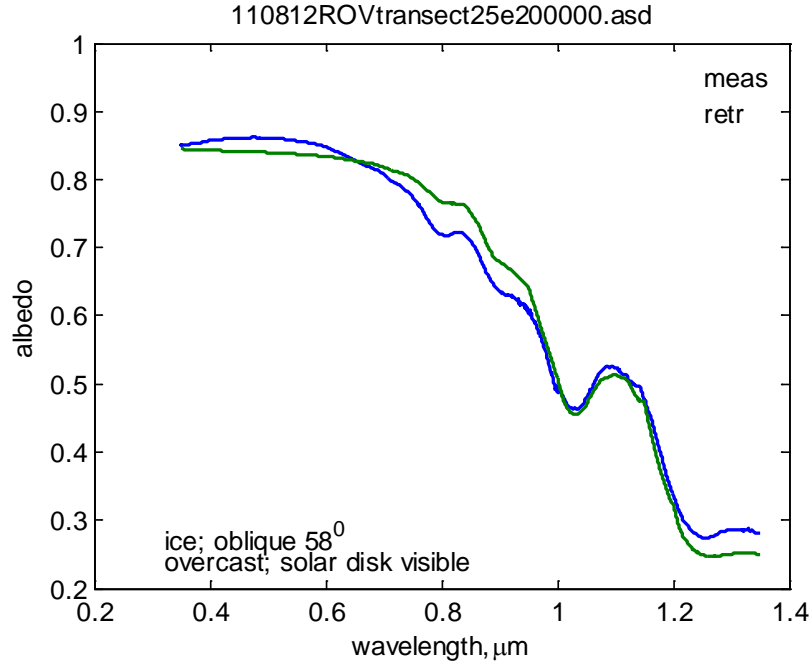


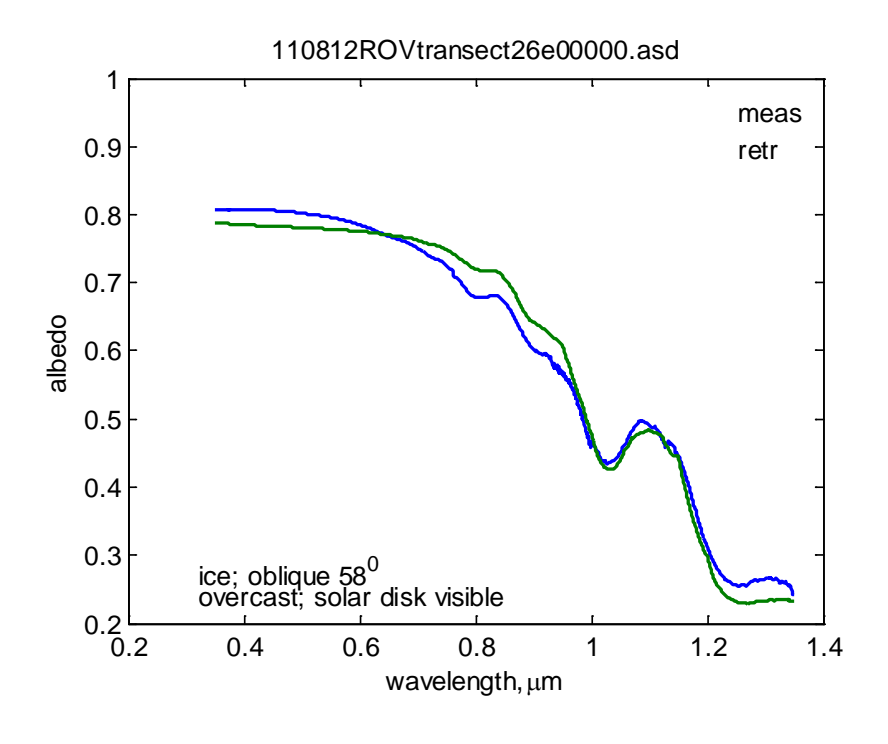


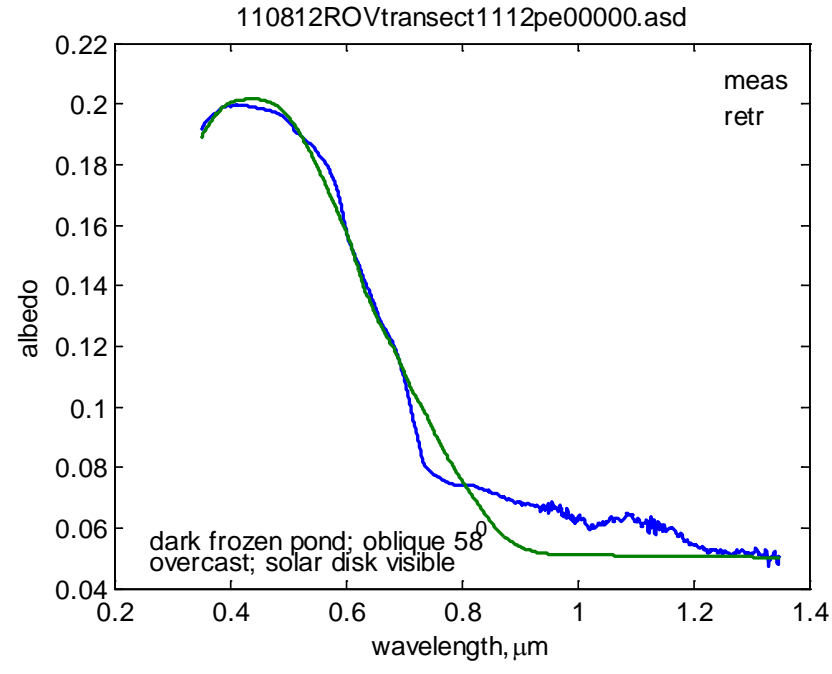


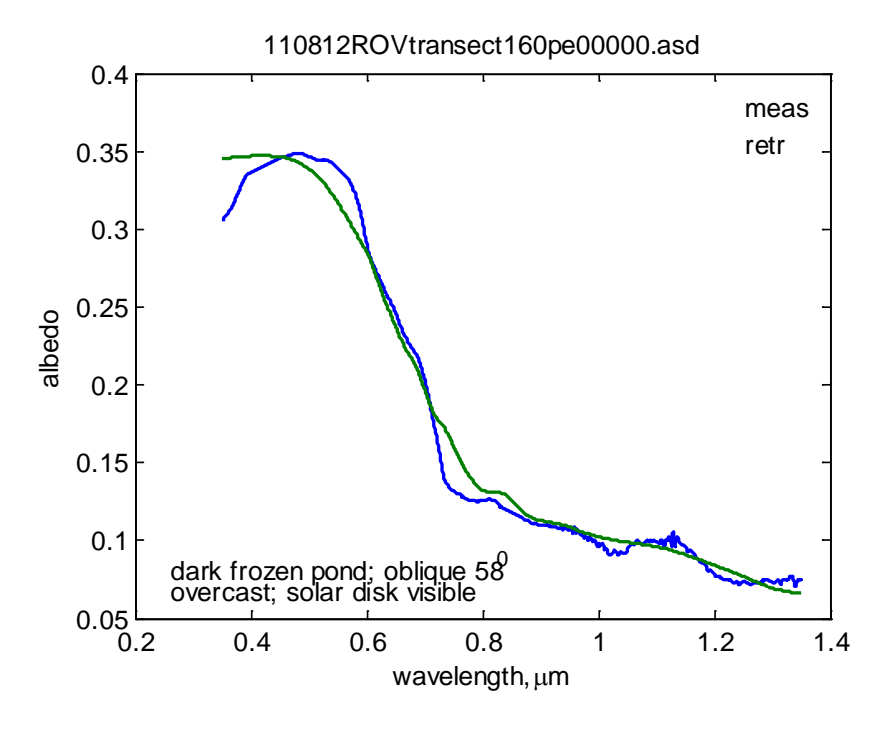


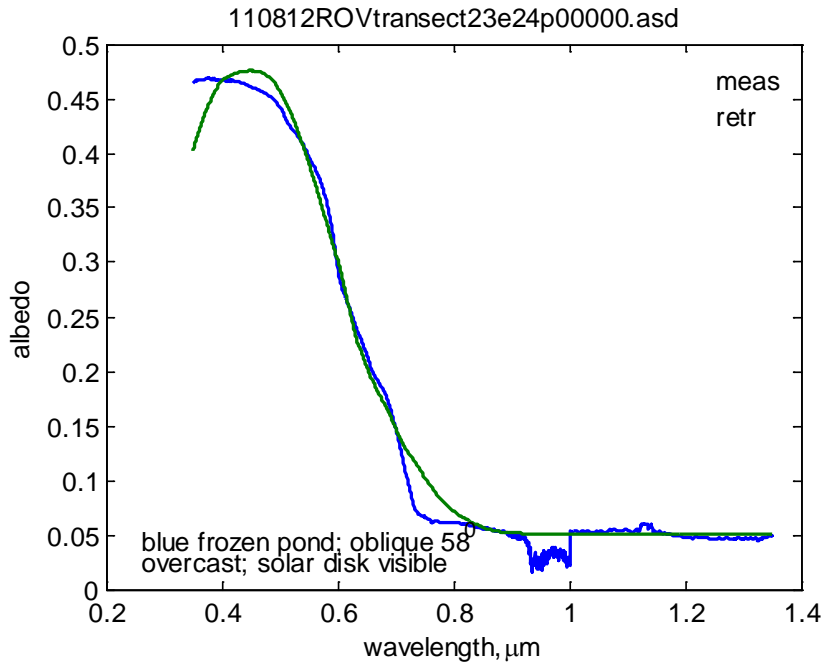


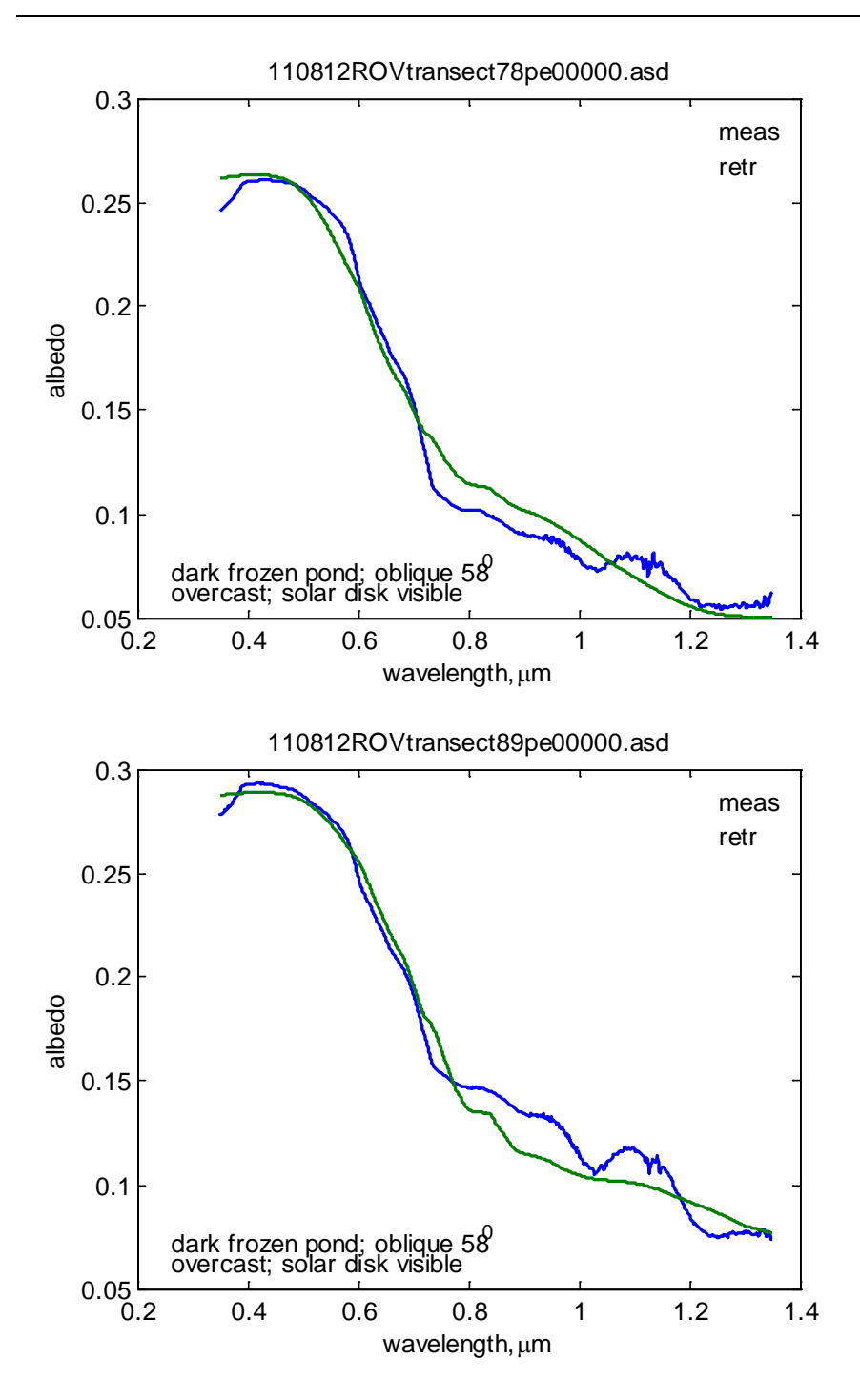




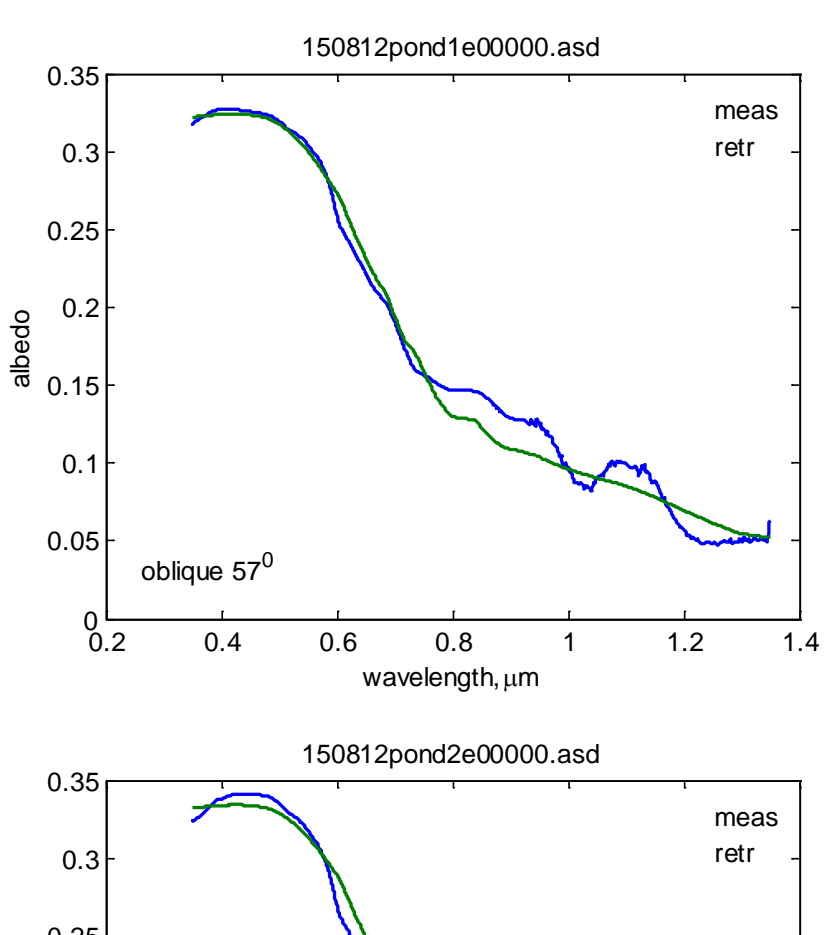


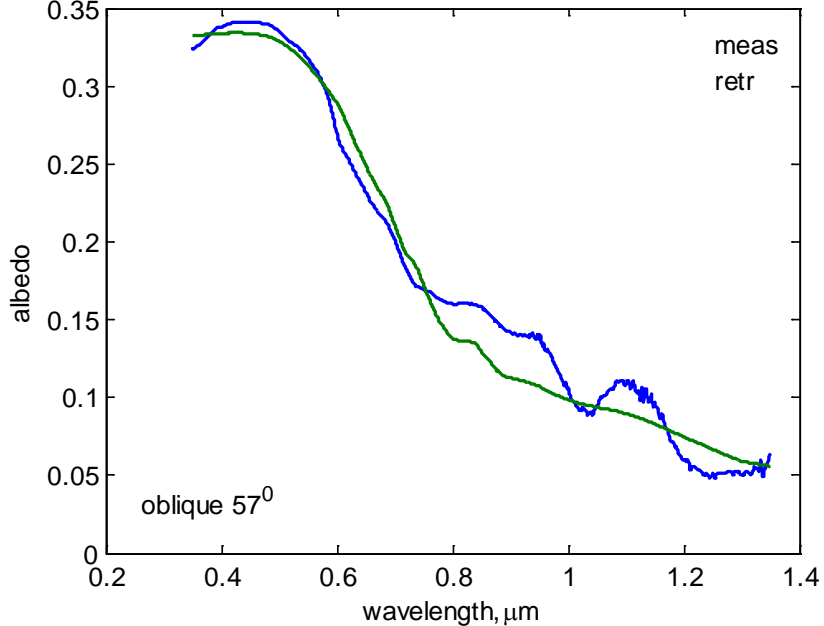


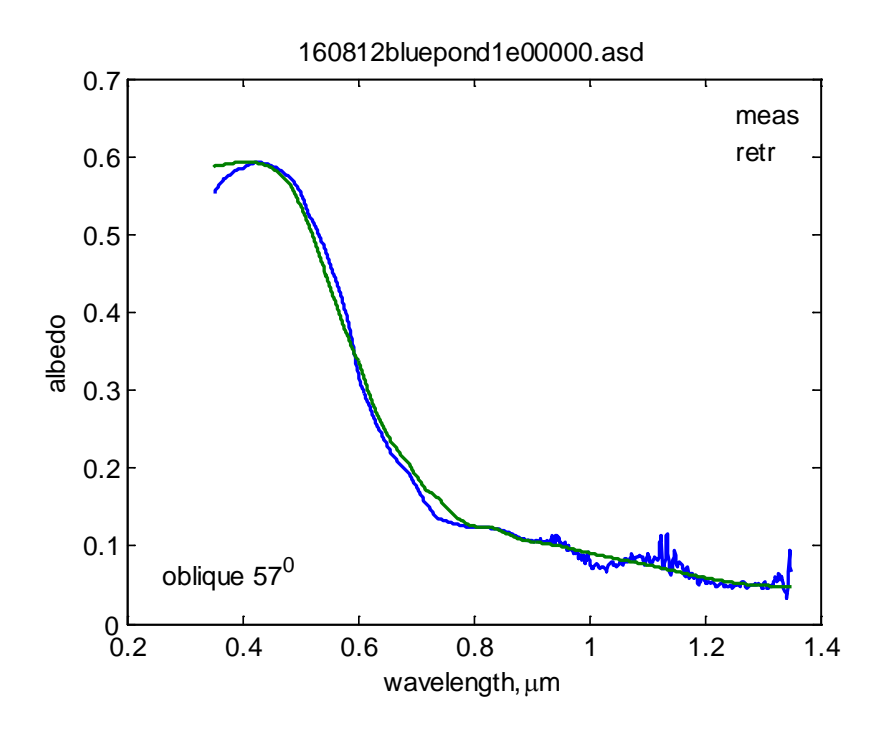


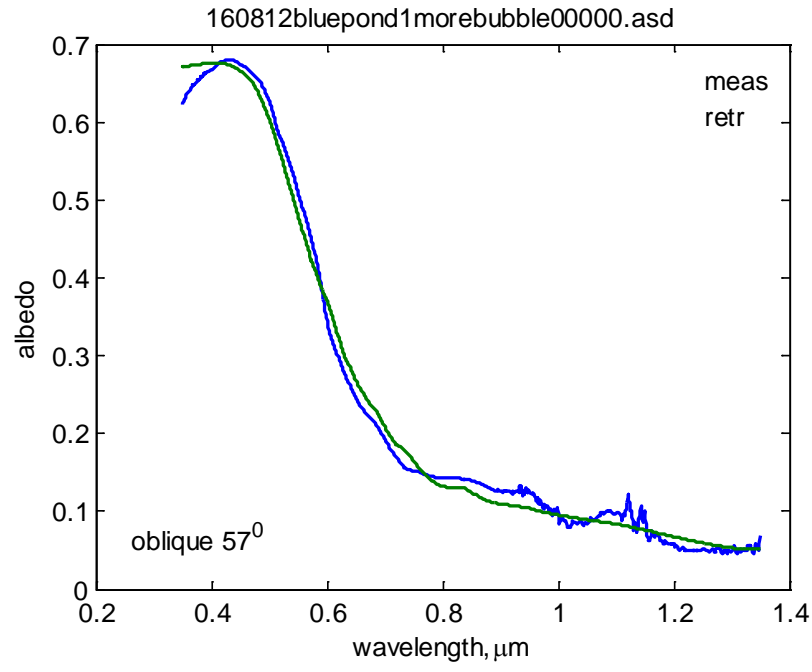


Station 2



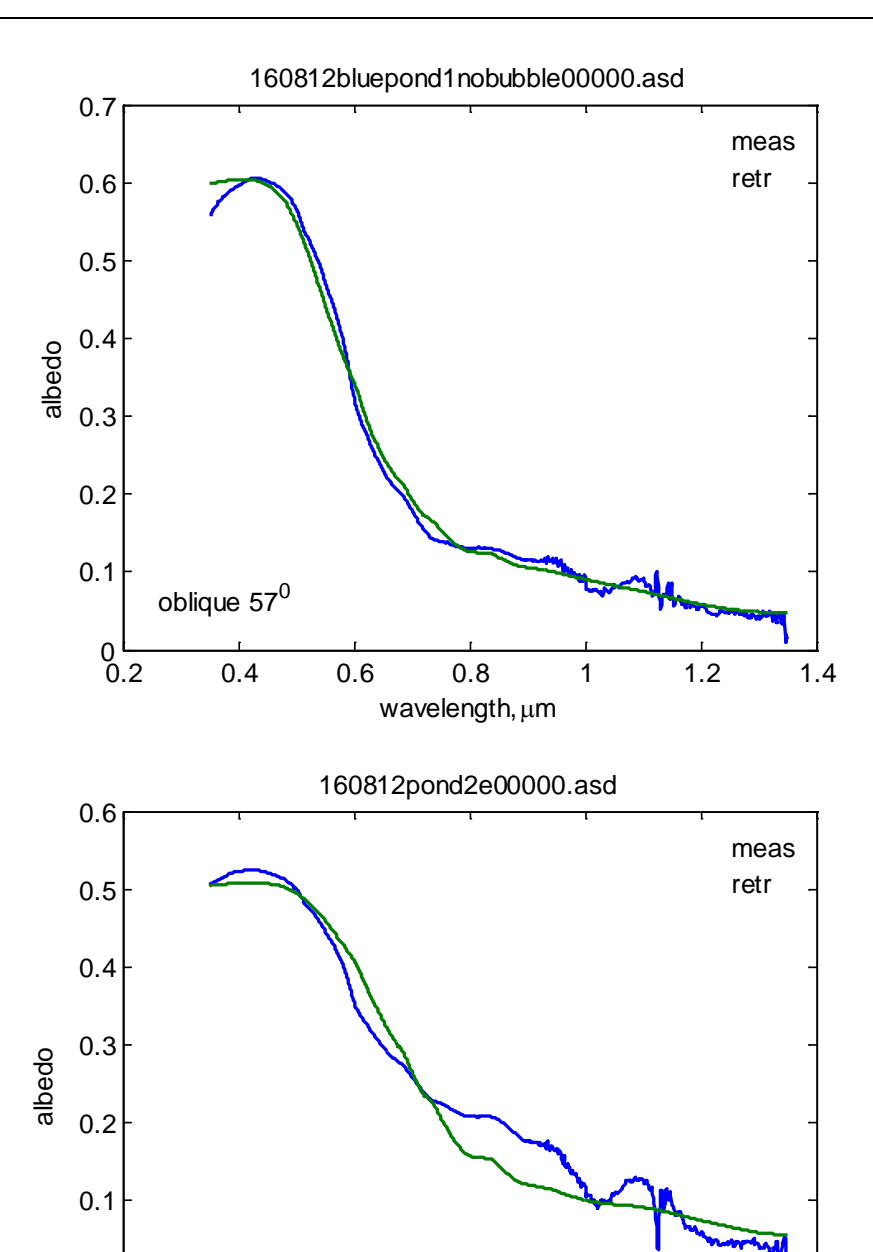






1.2

1.4



0

-0.1<u></u> 0.2 oblique 57<sup>0</sup>

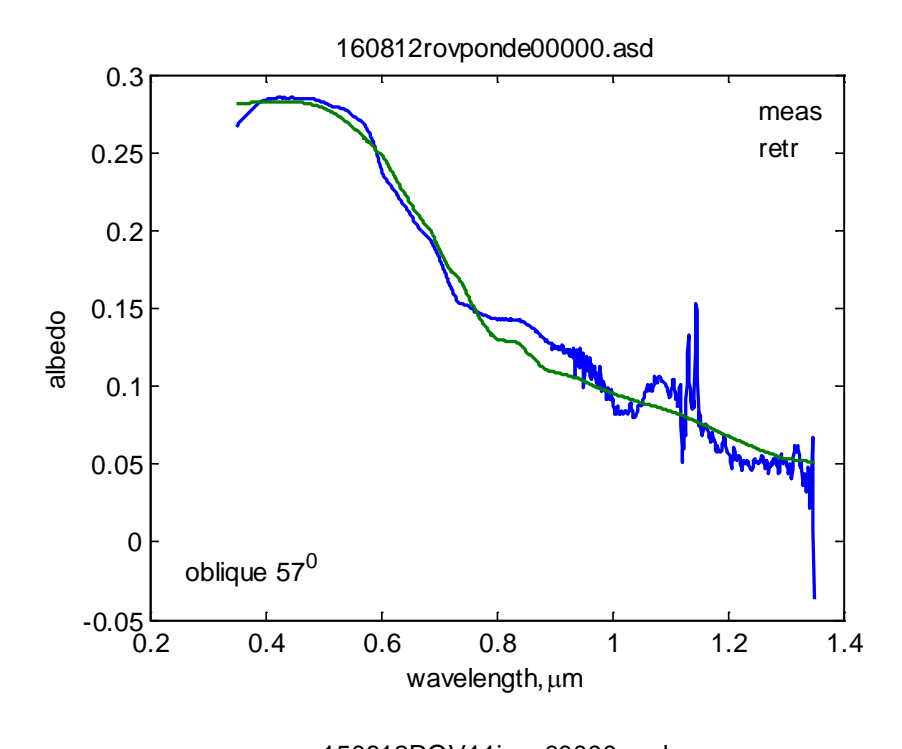
0.4

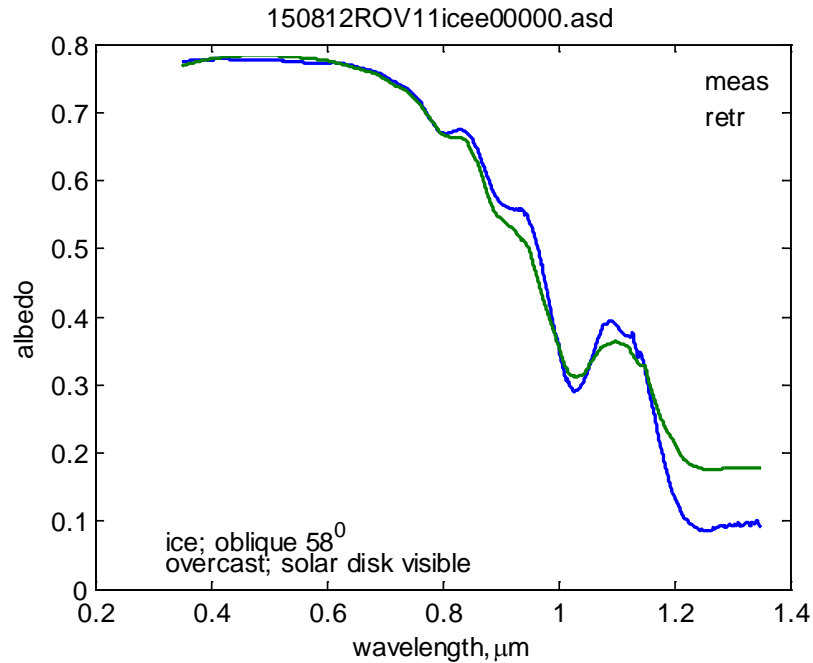
0.6

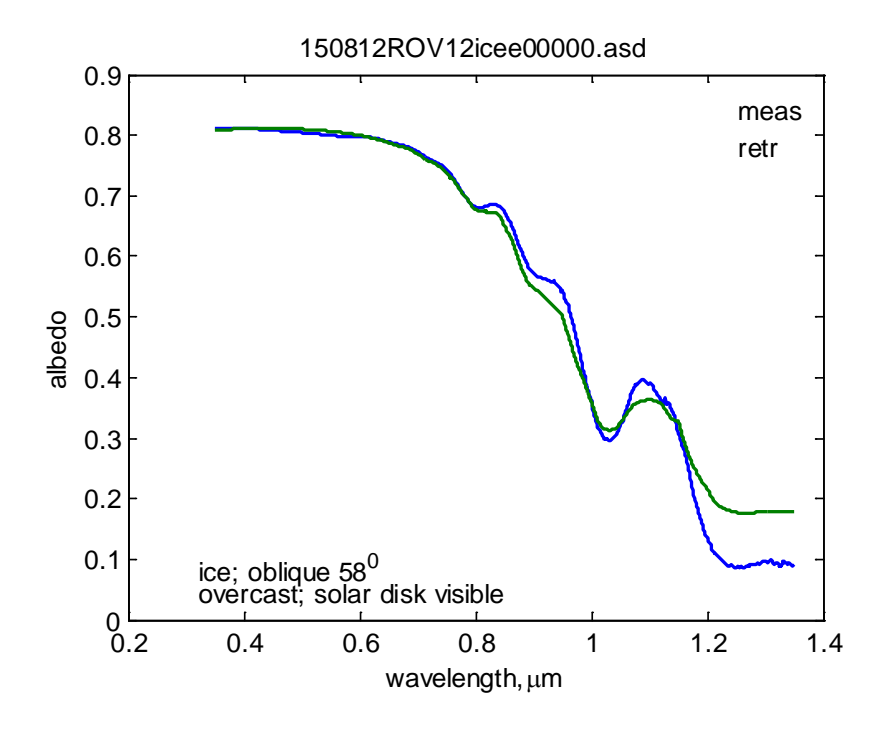
0.8

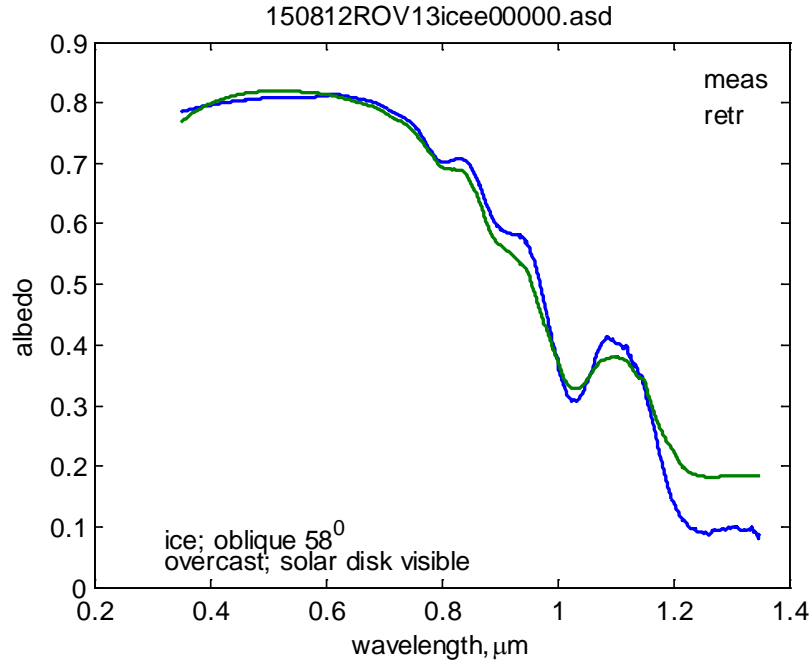
 $wavelength, \mu\text{m}$ 

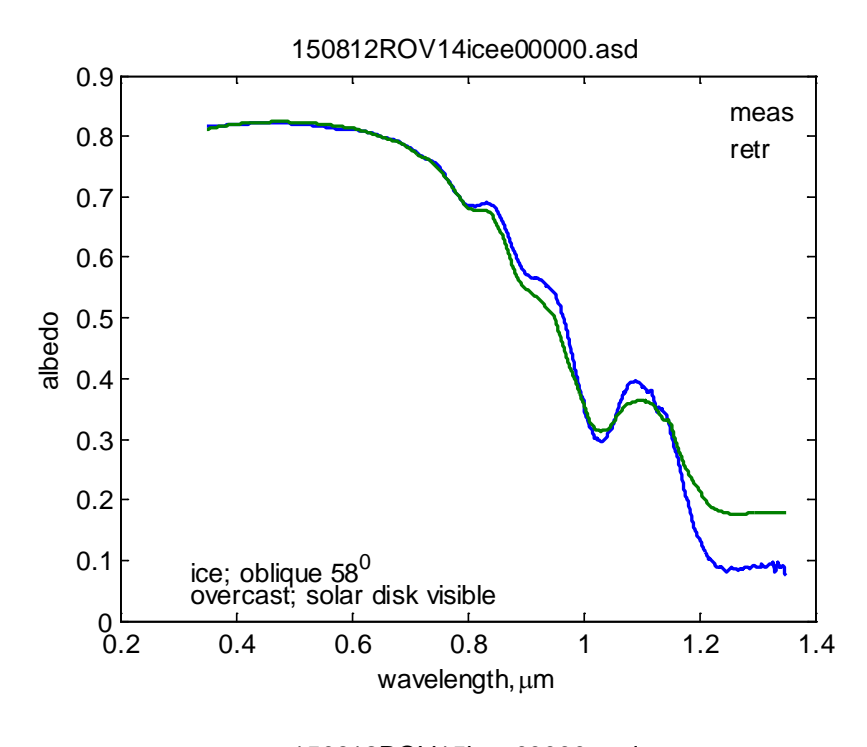
1

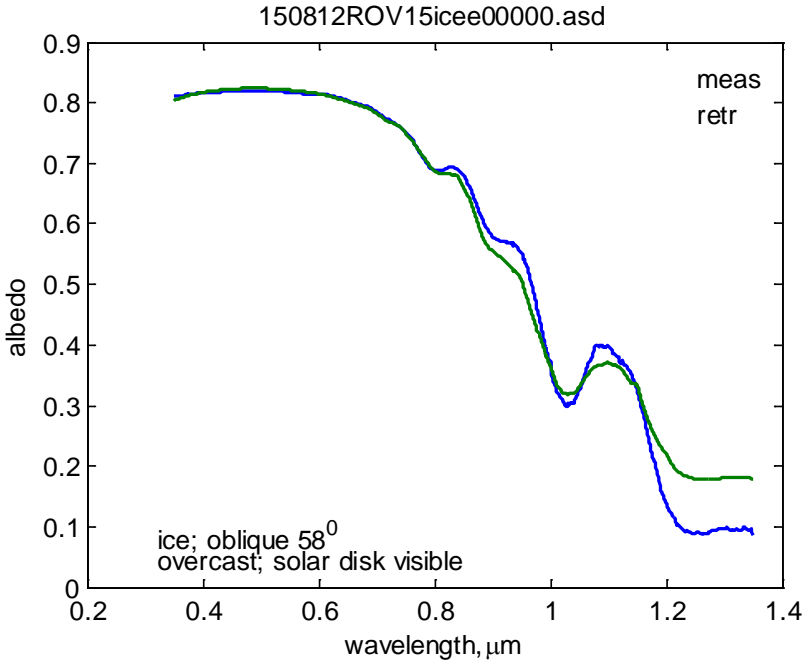


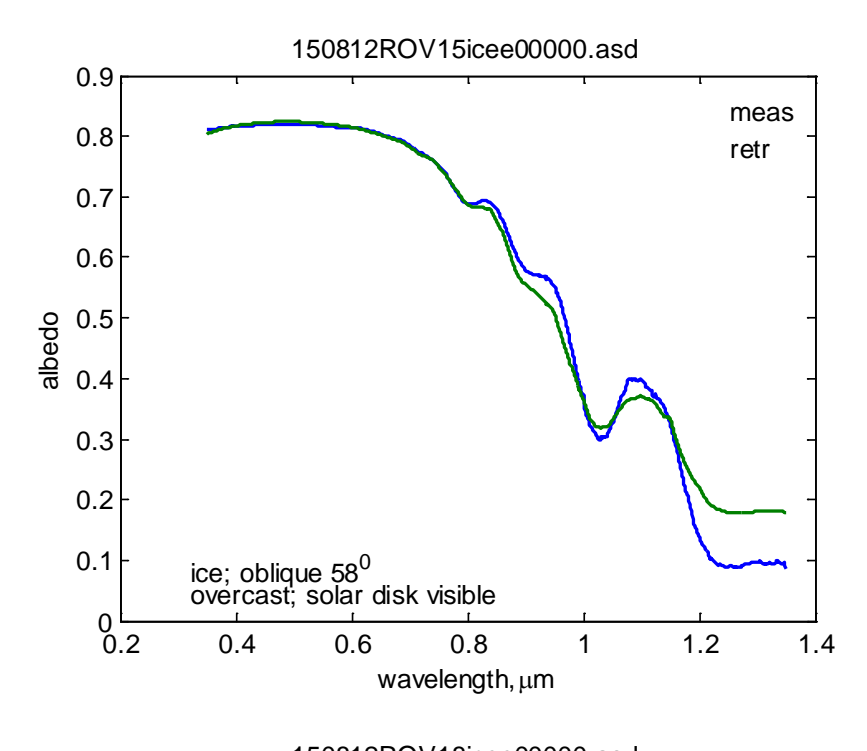


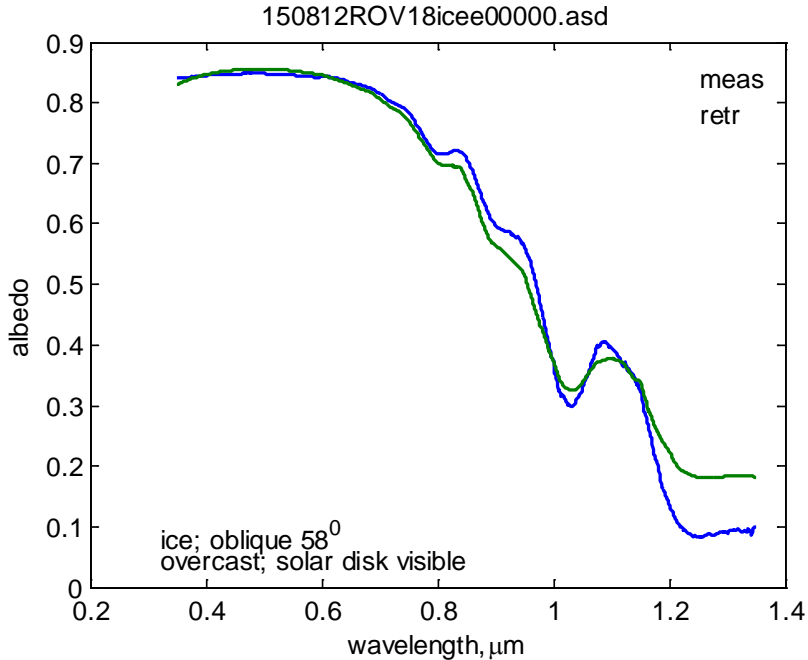


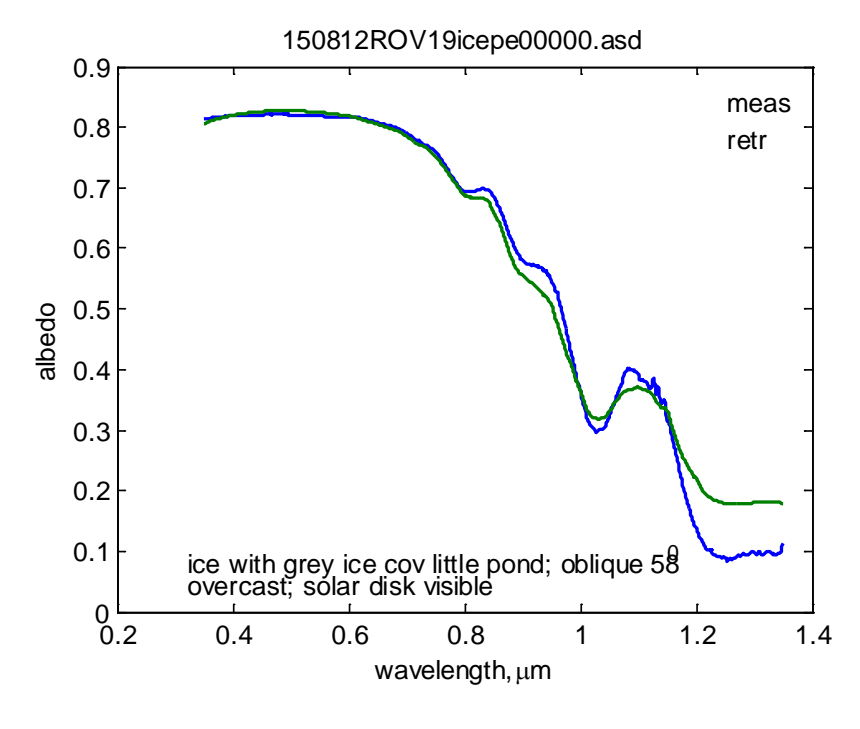


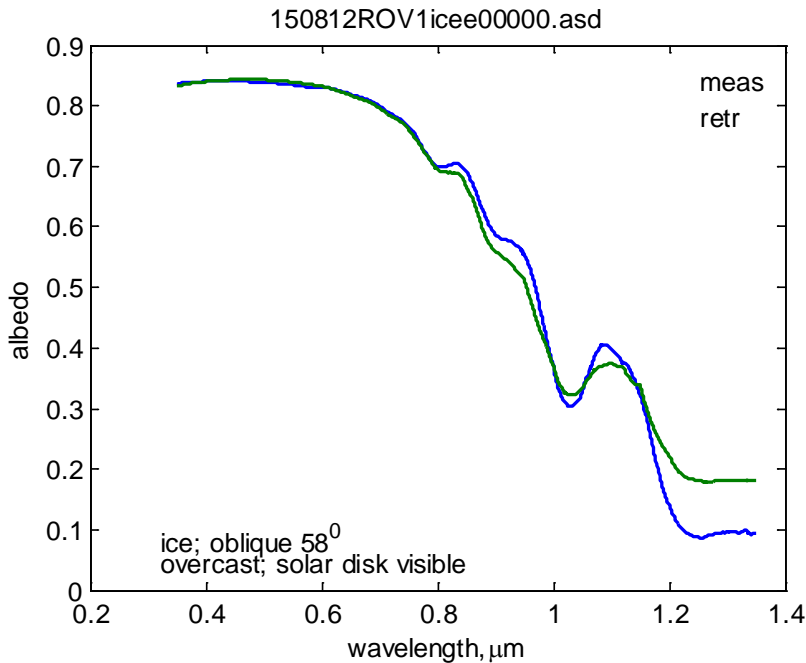


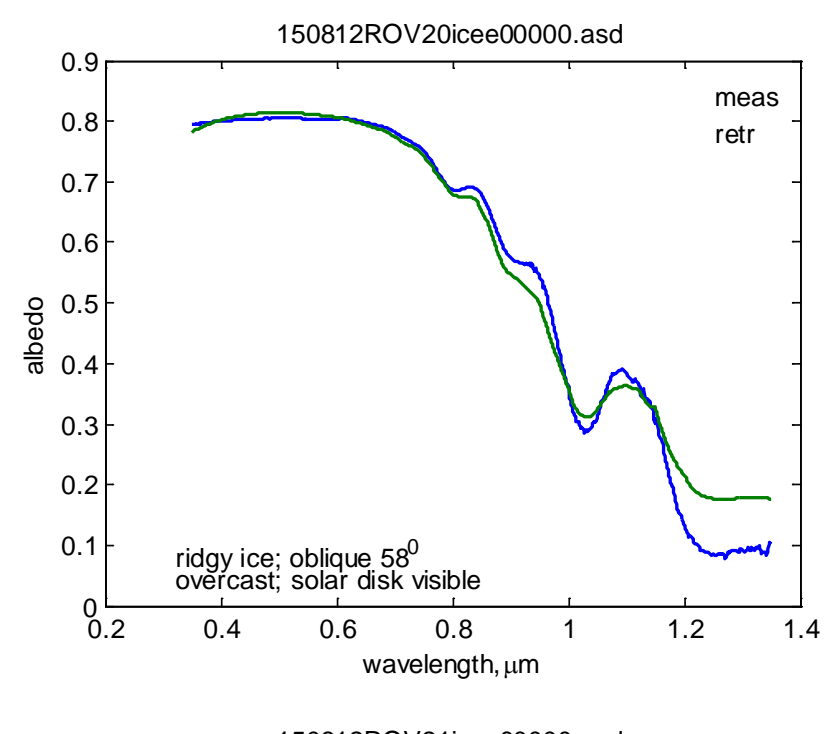


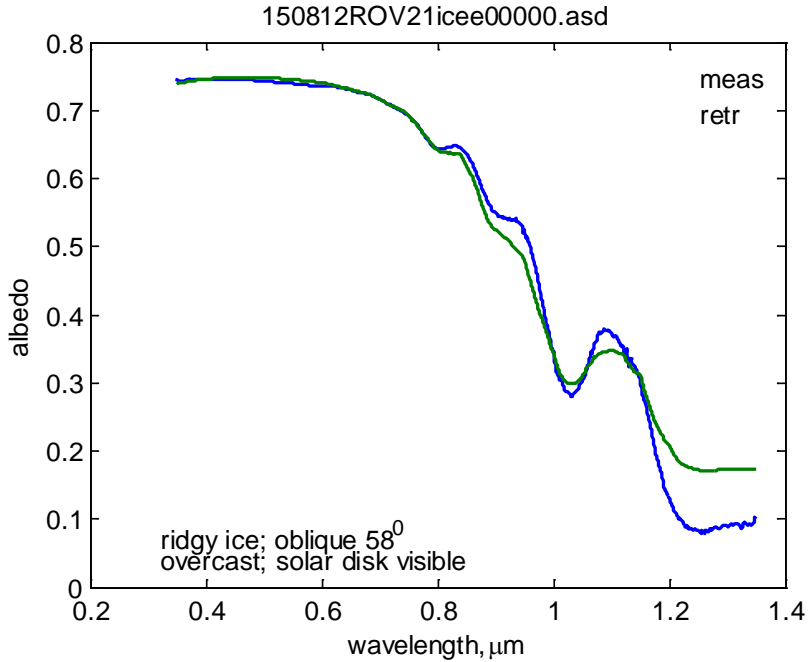


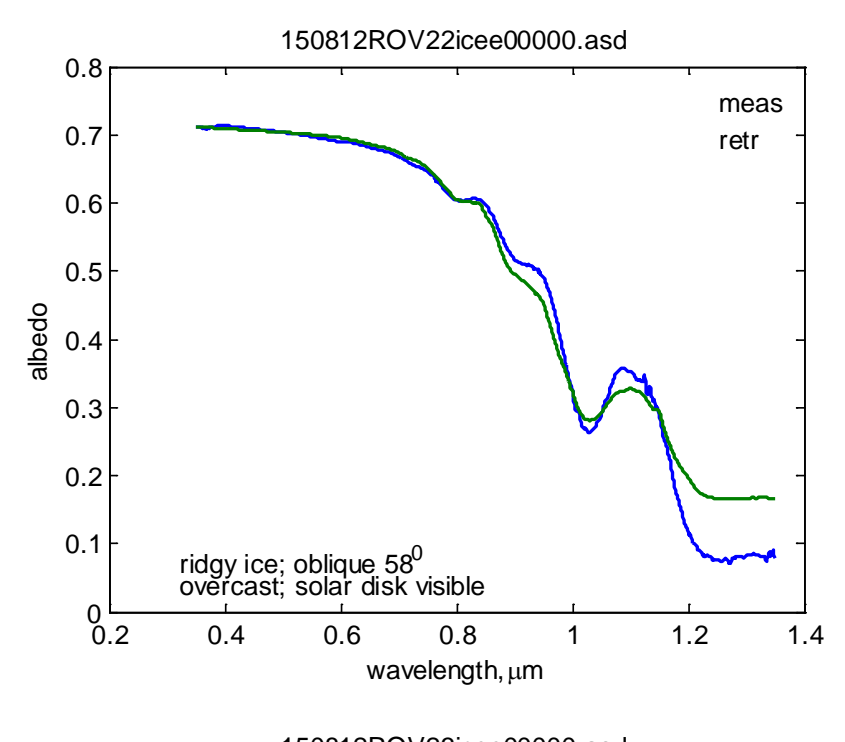


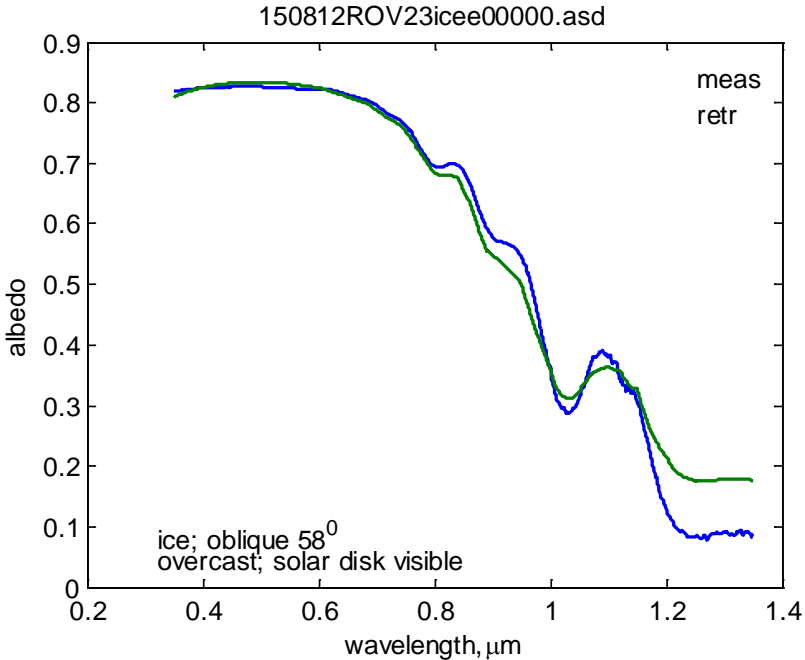


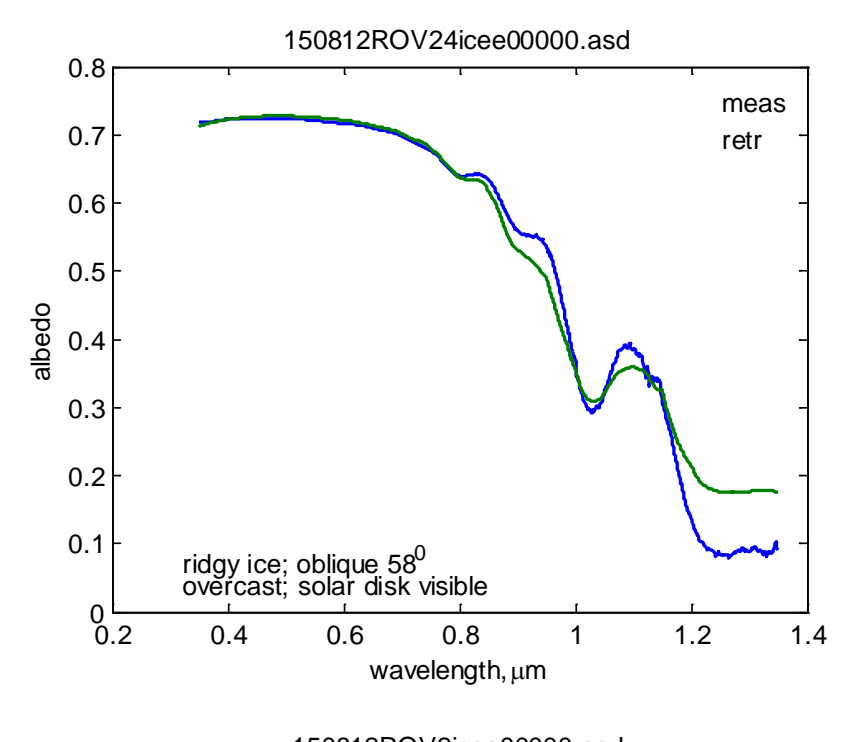


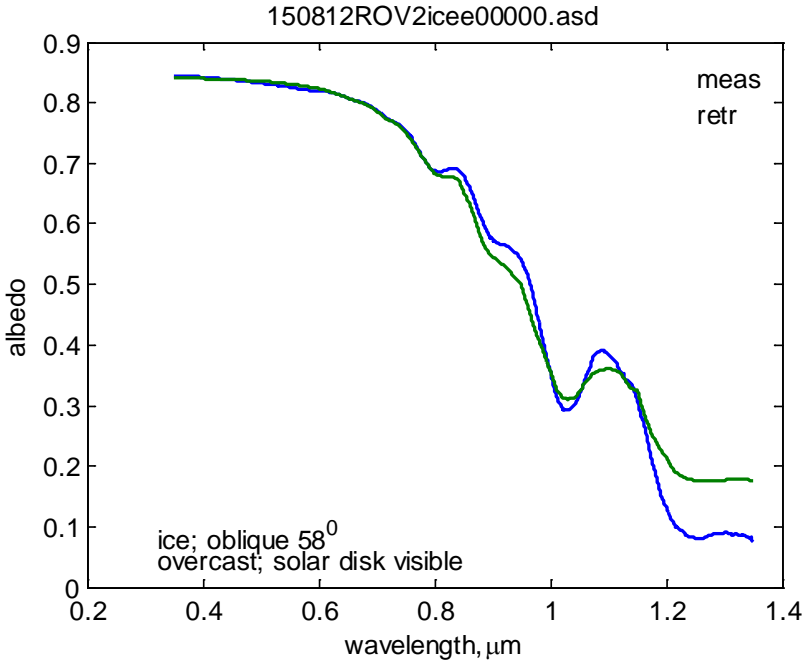


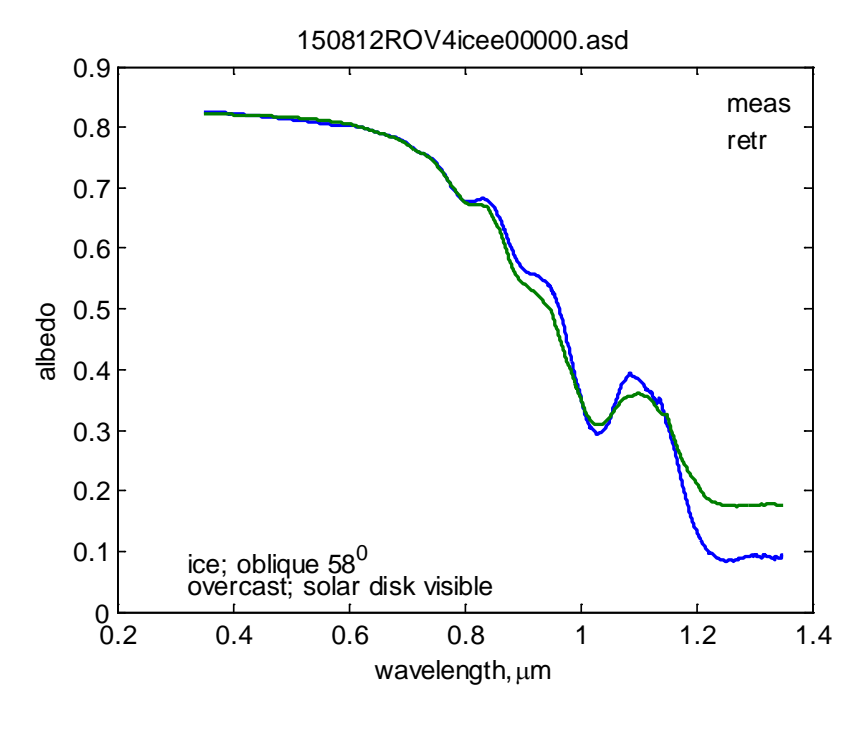


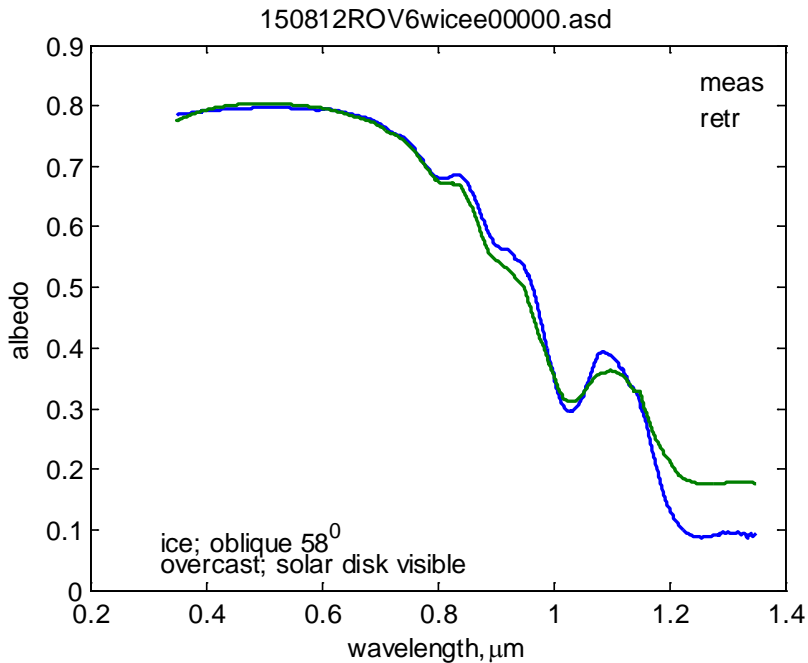


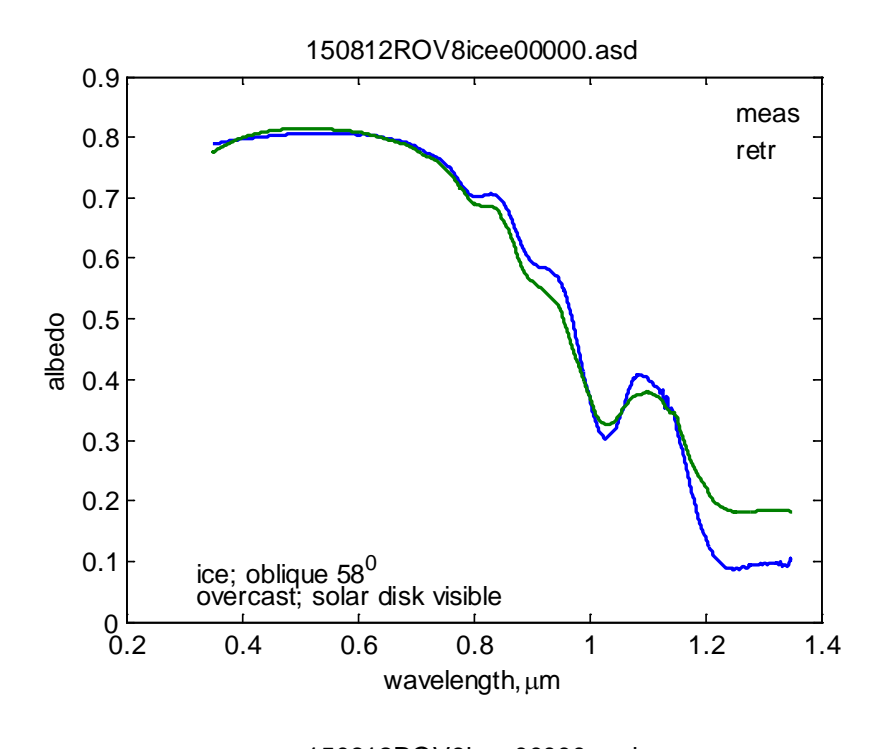


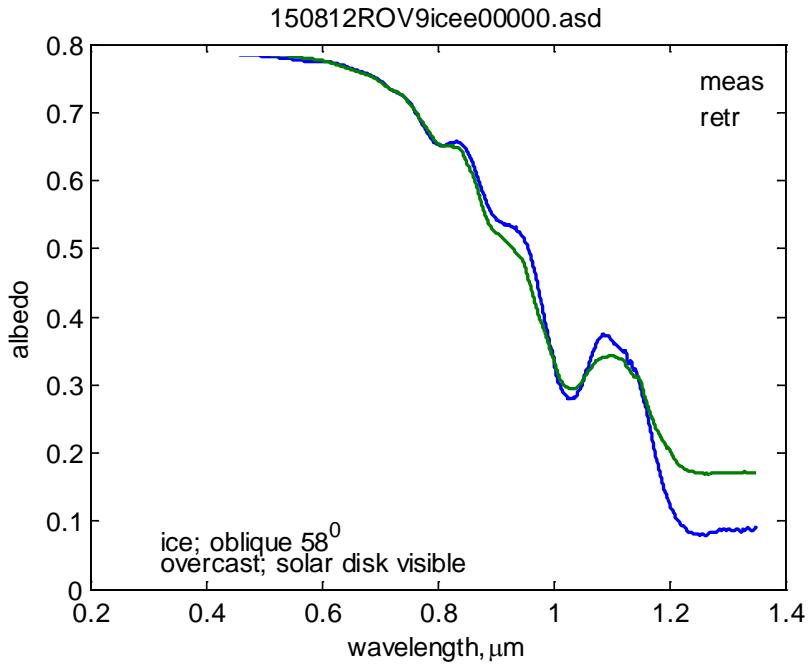




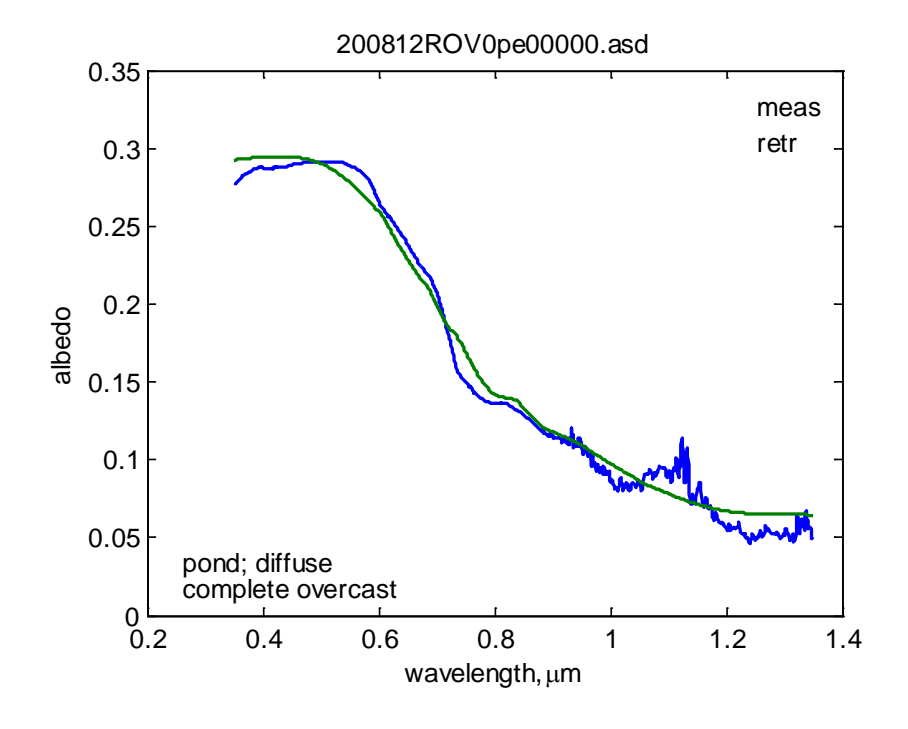


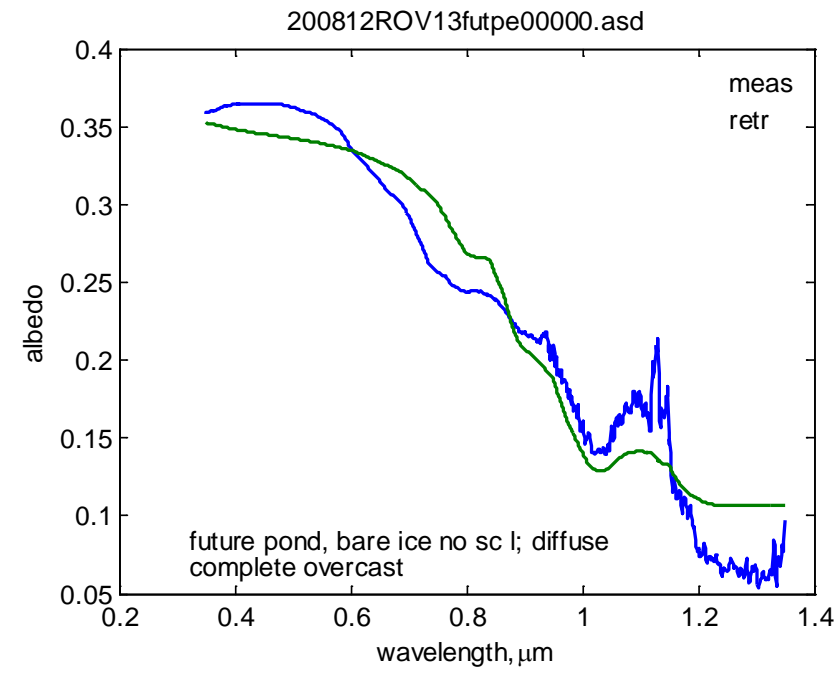


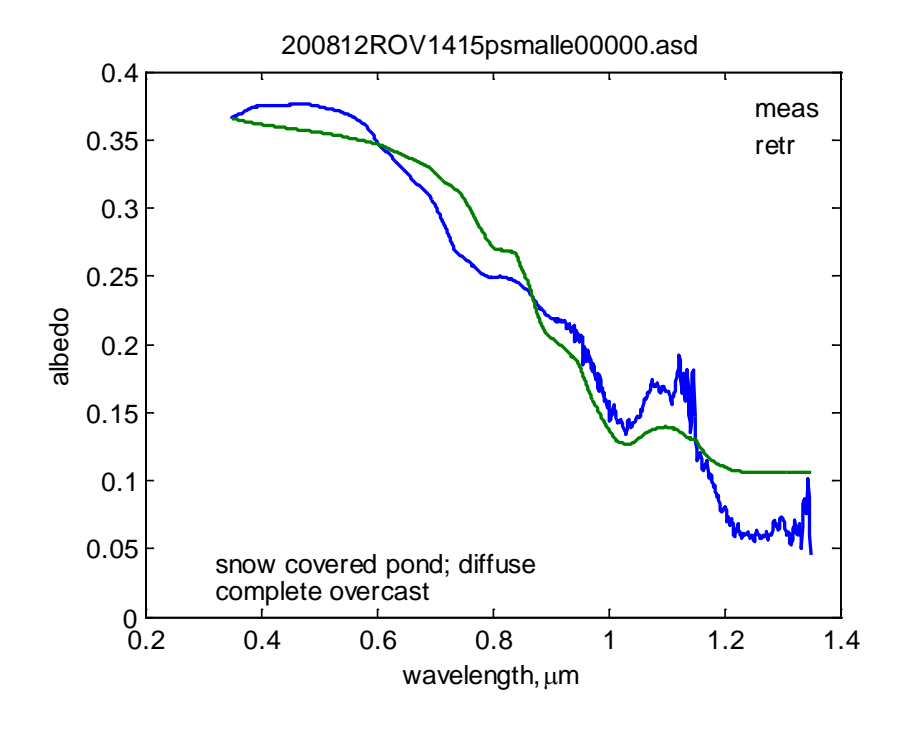


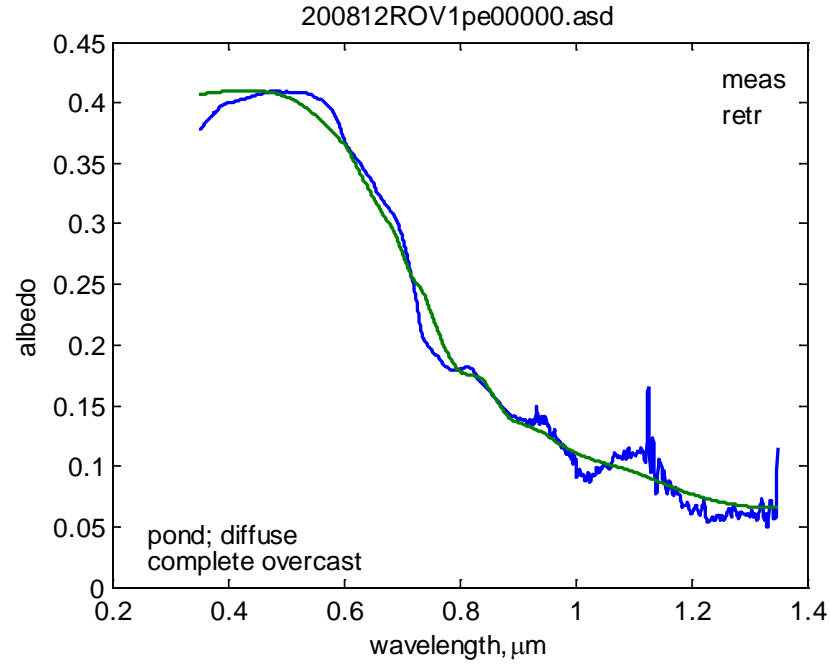


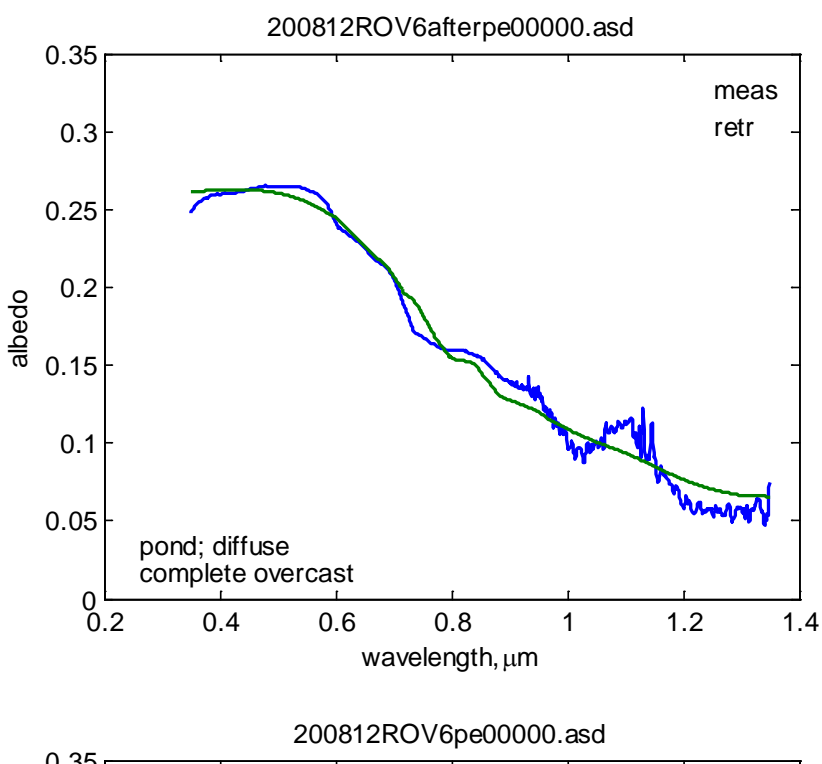
# Station 3

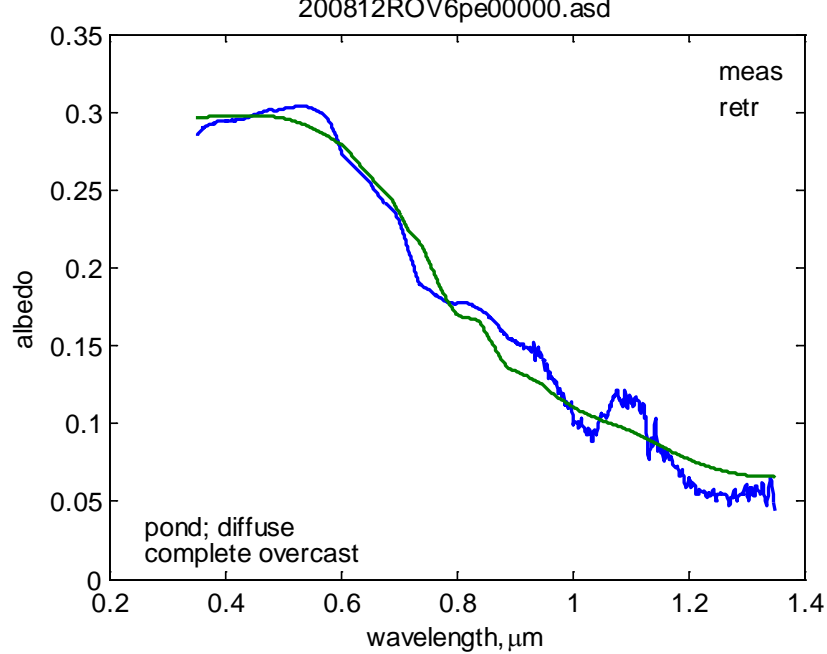


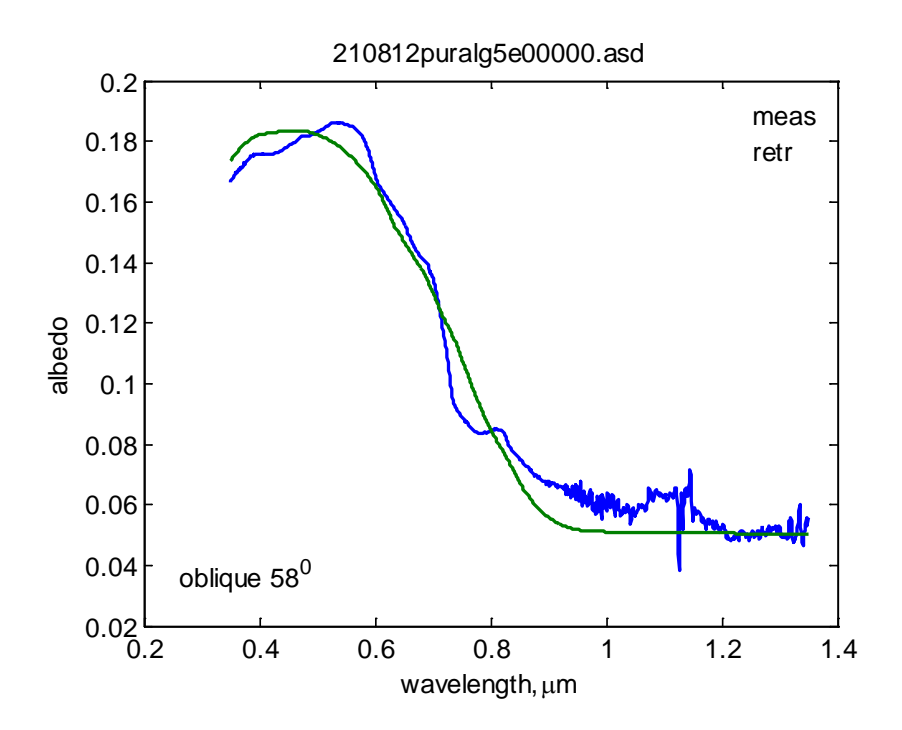


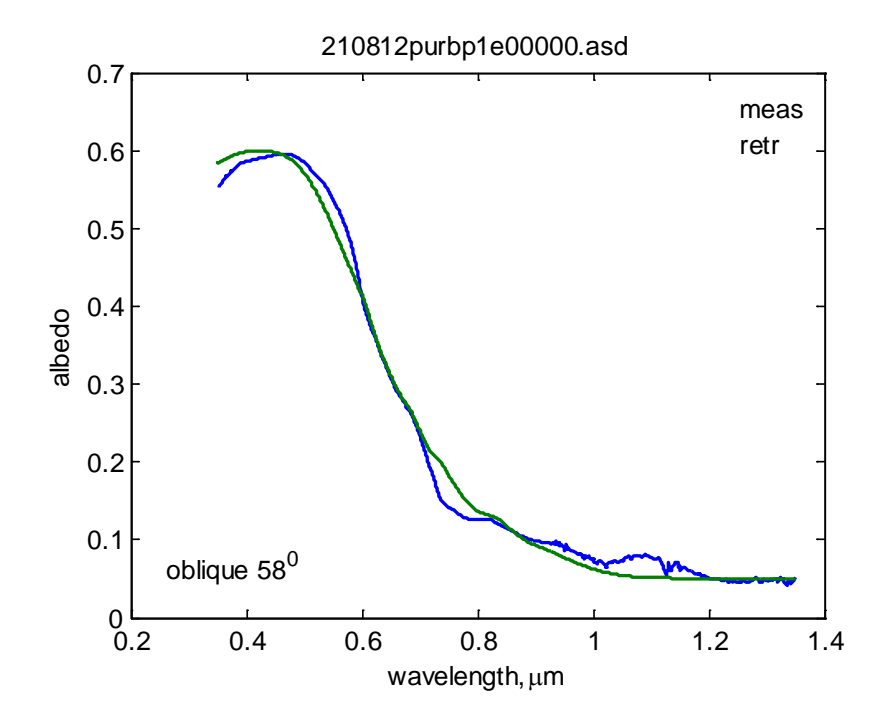


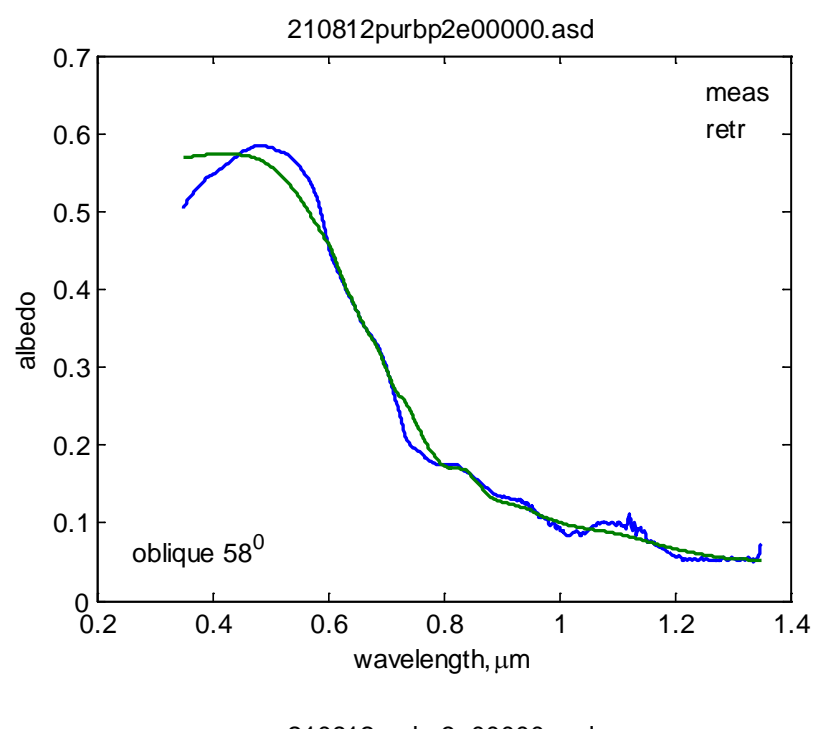


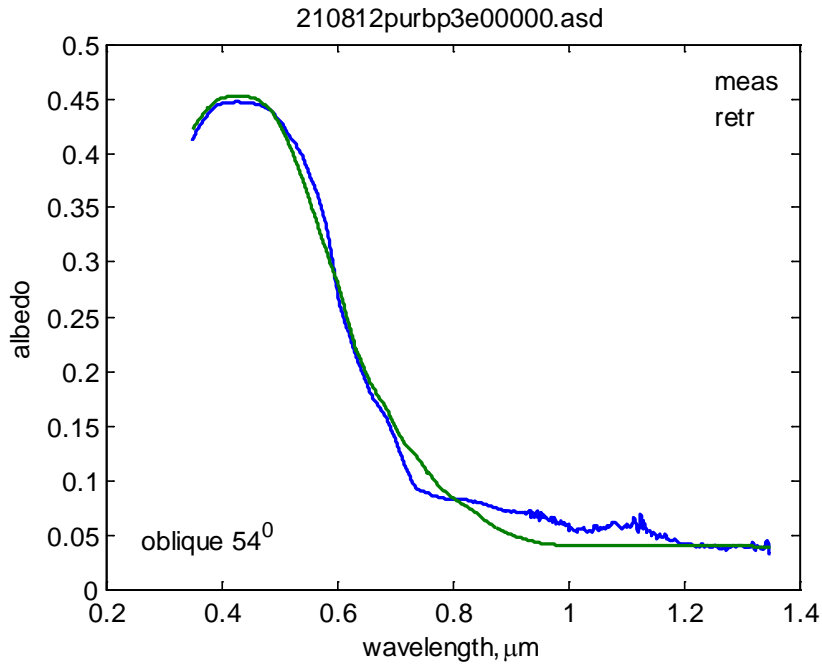


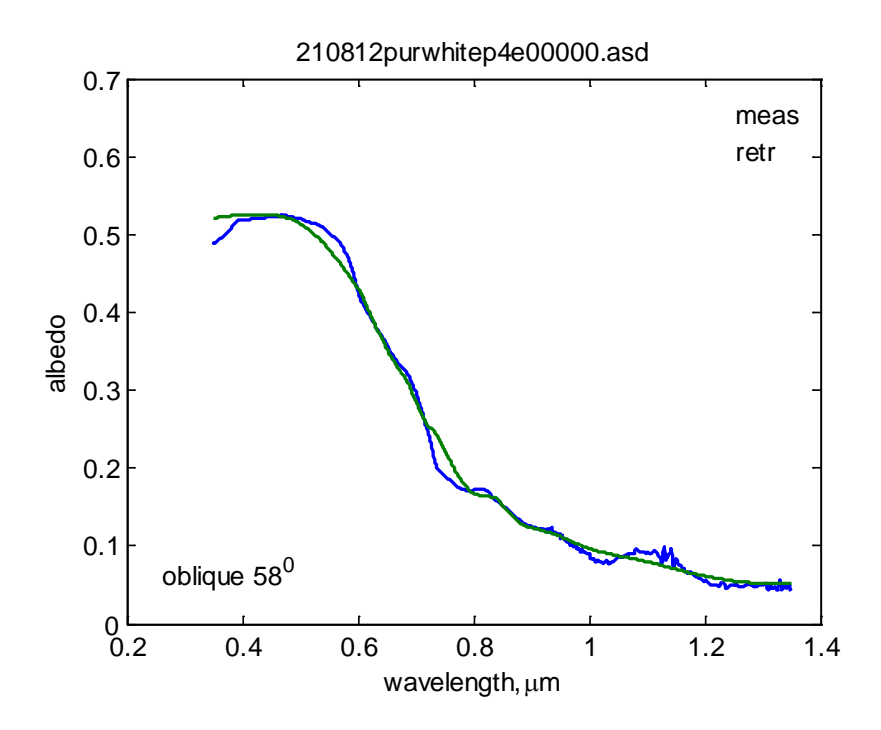


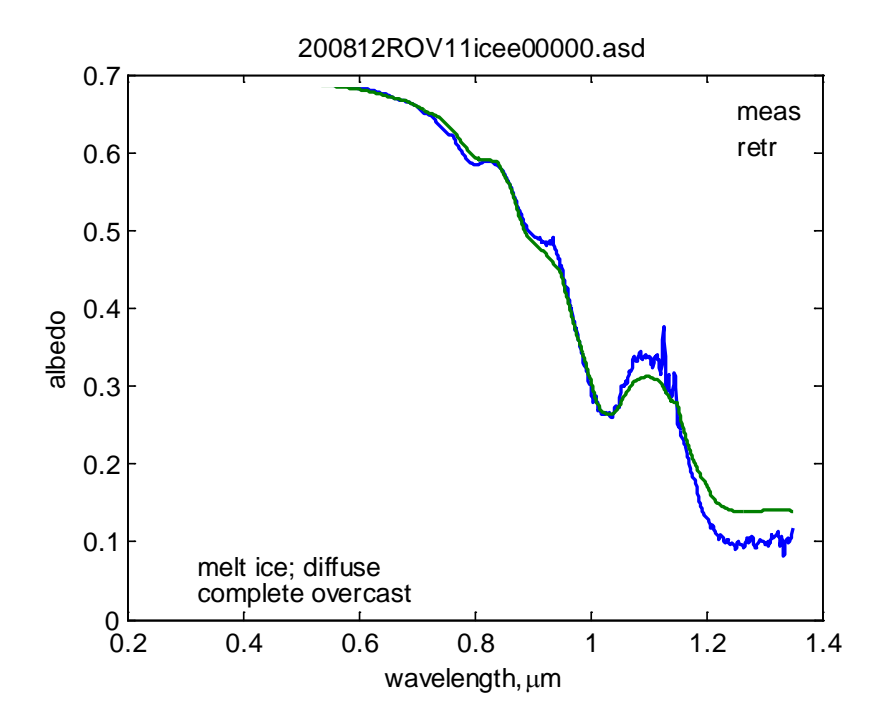


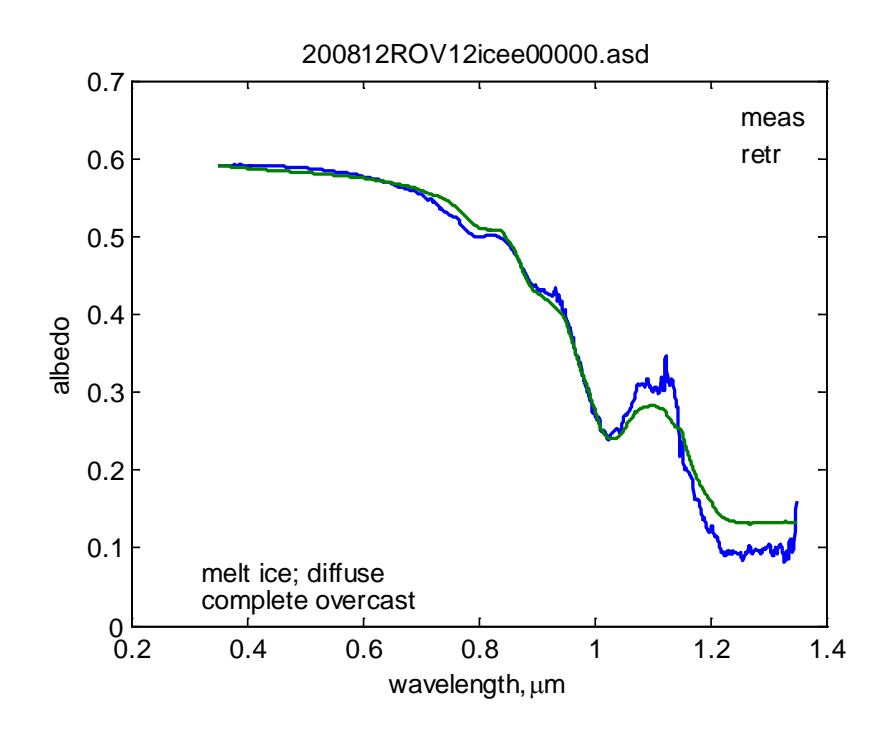


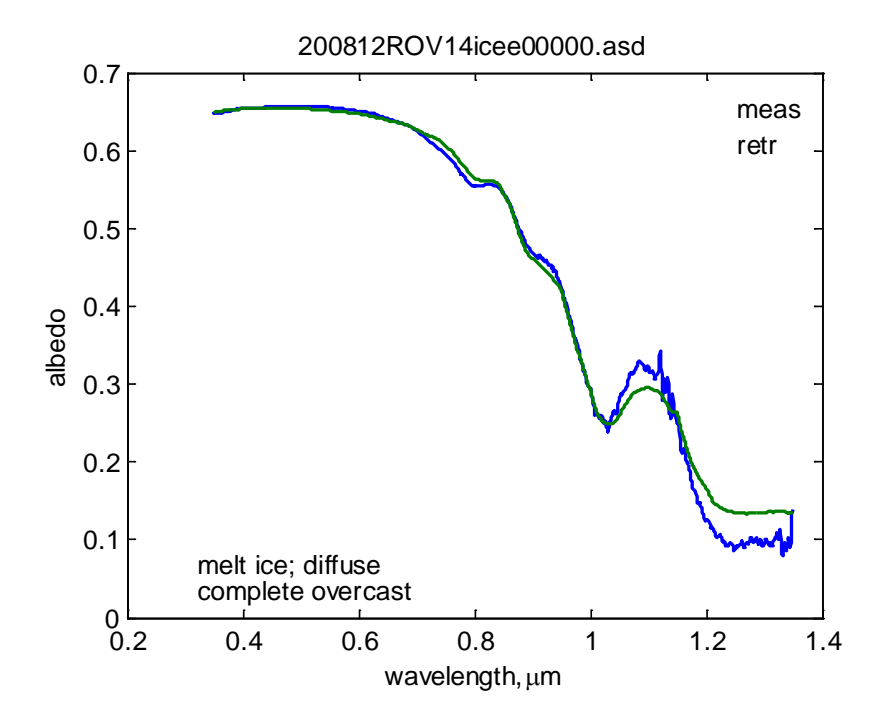


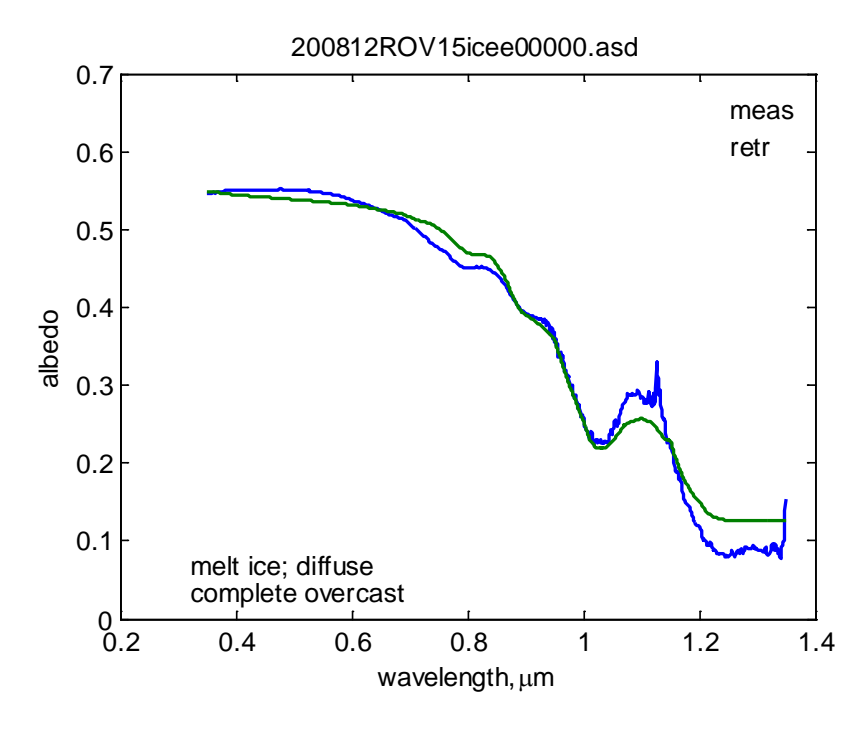


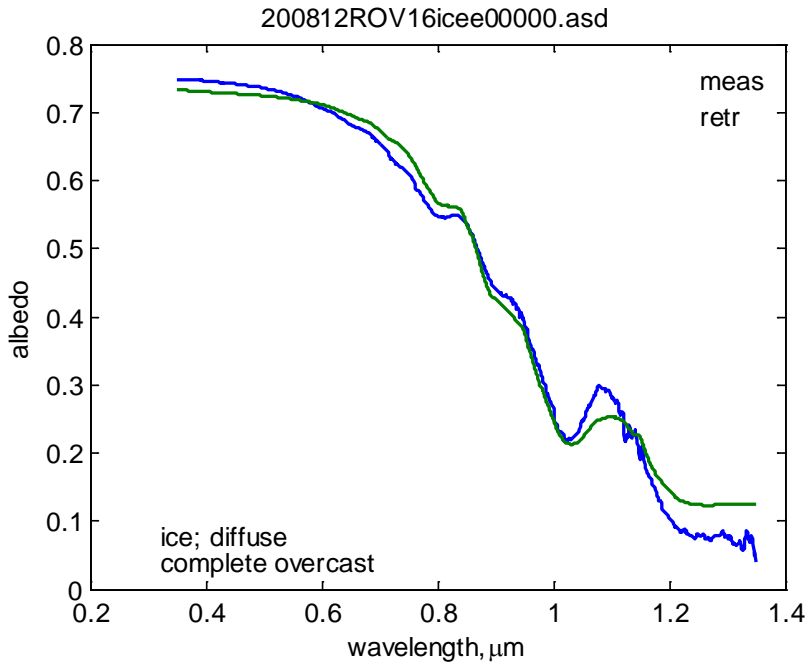


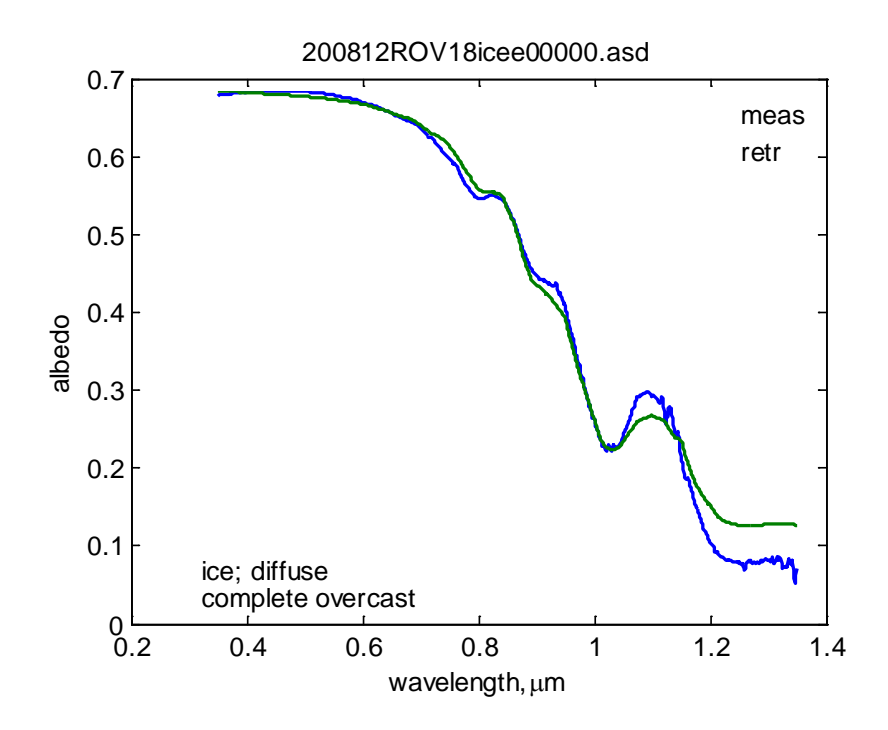


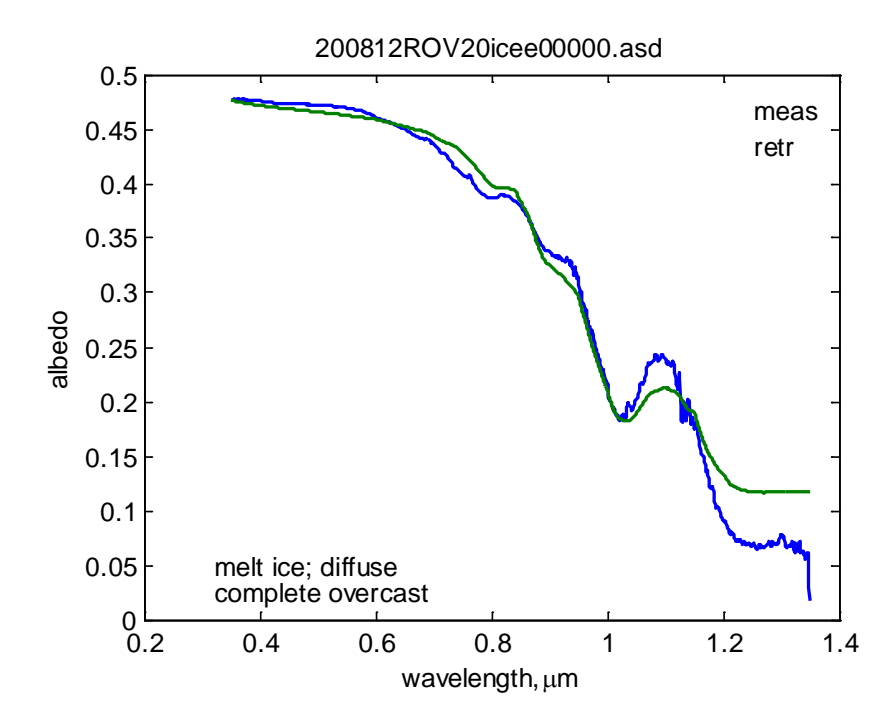


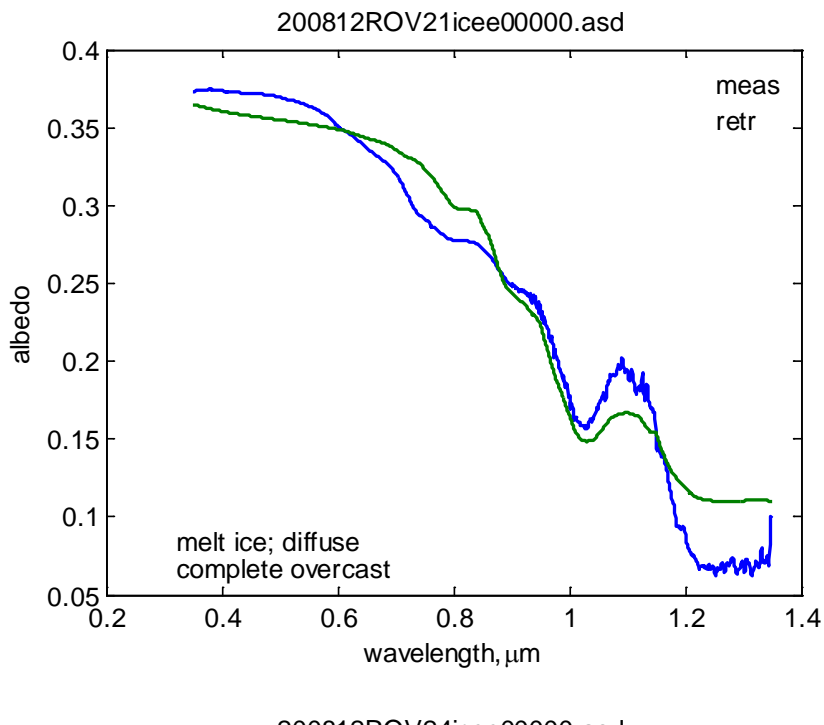


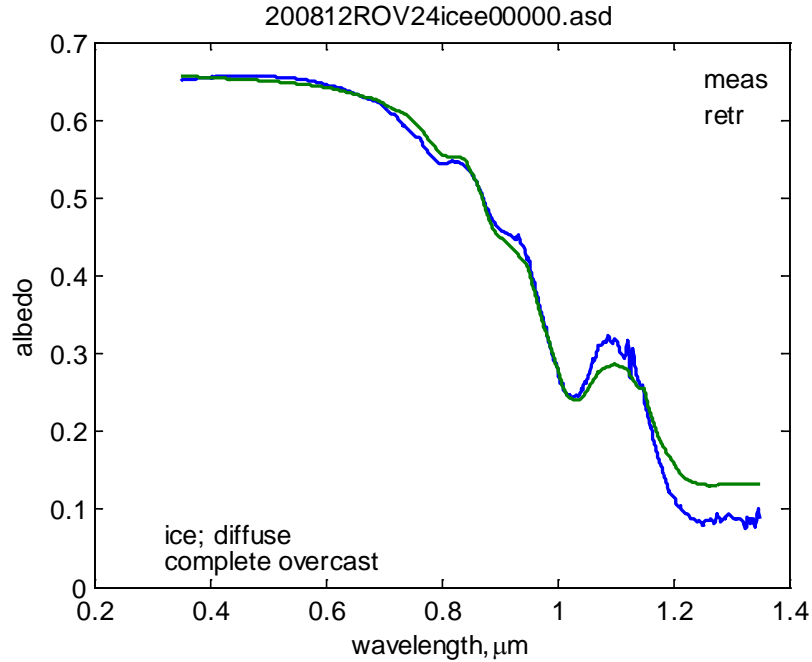


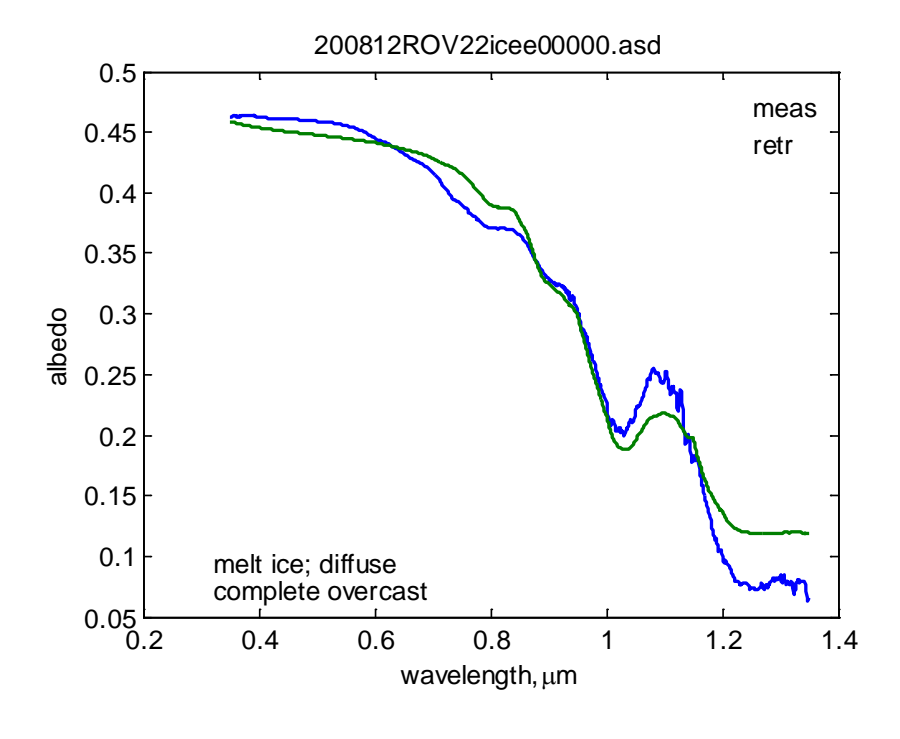


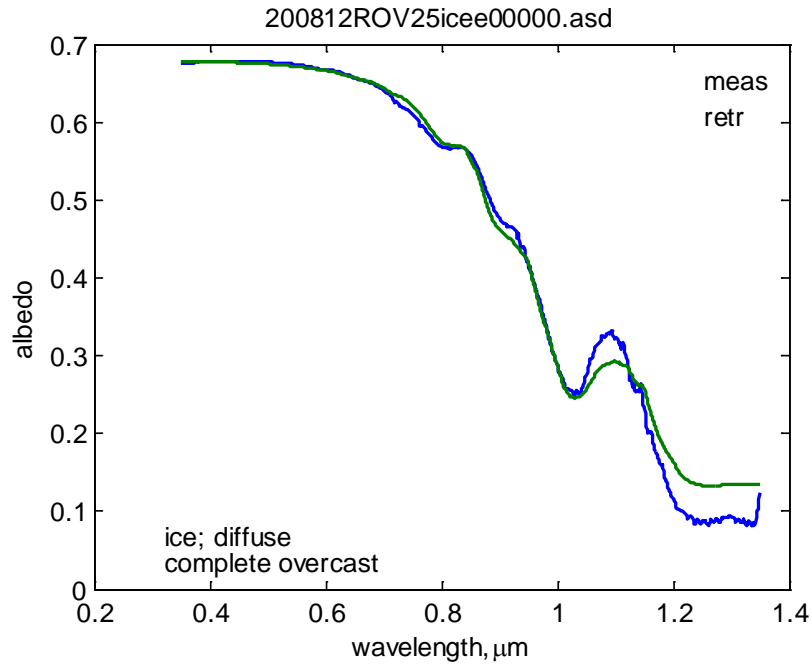


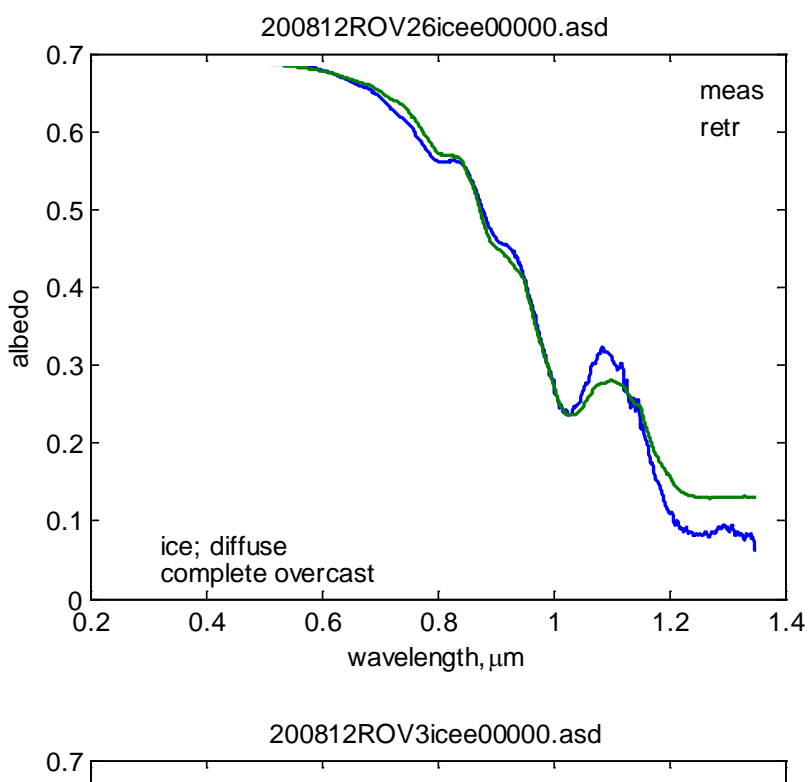


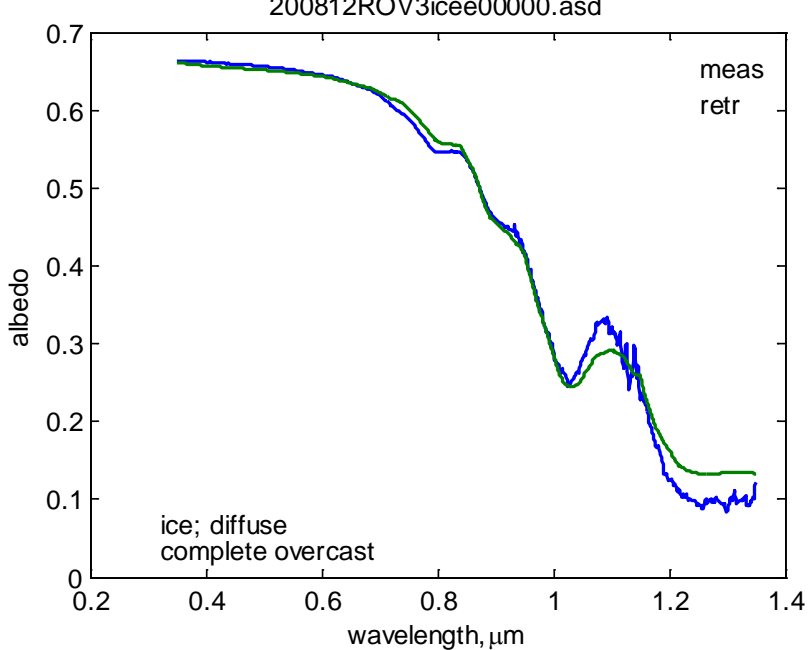


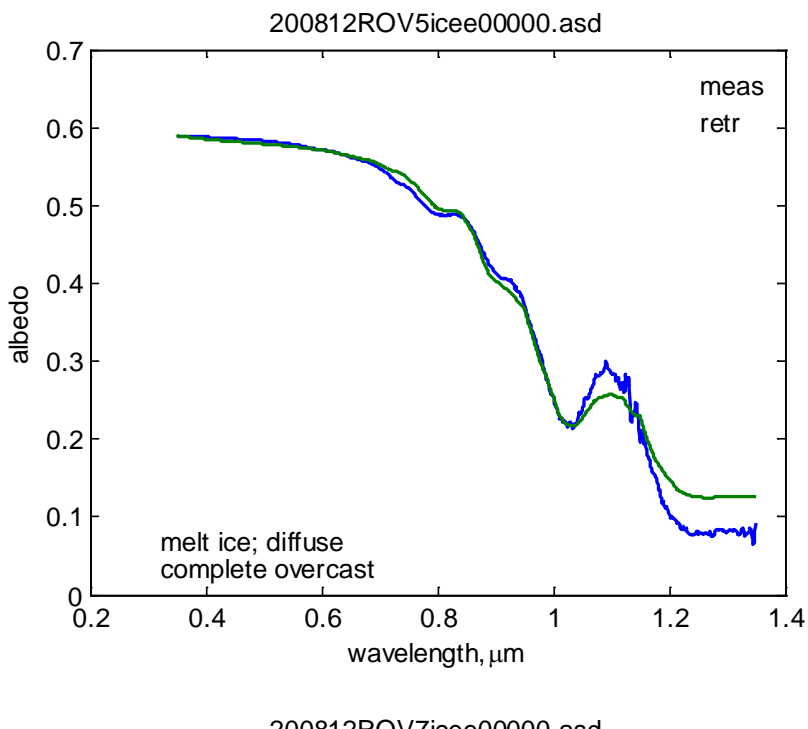


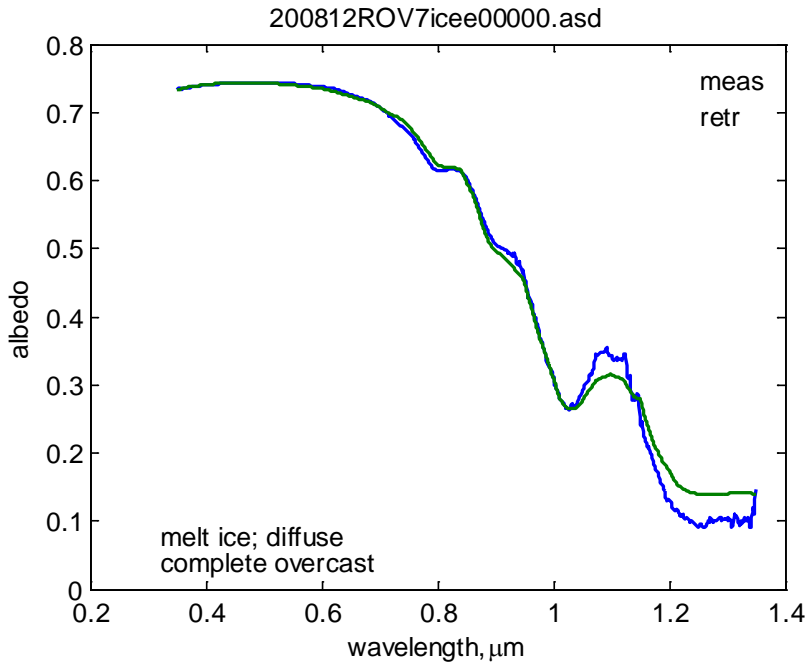


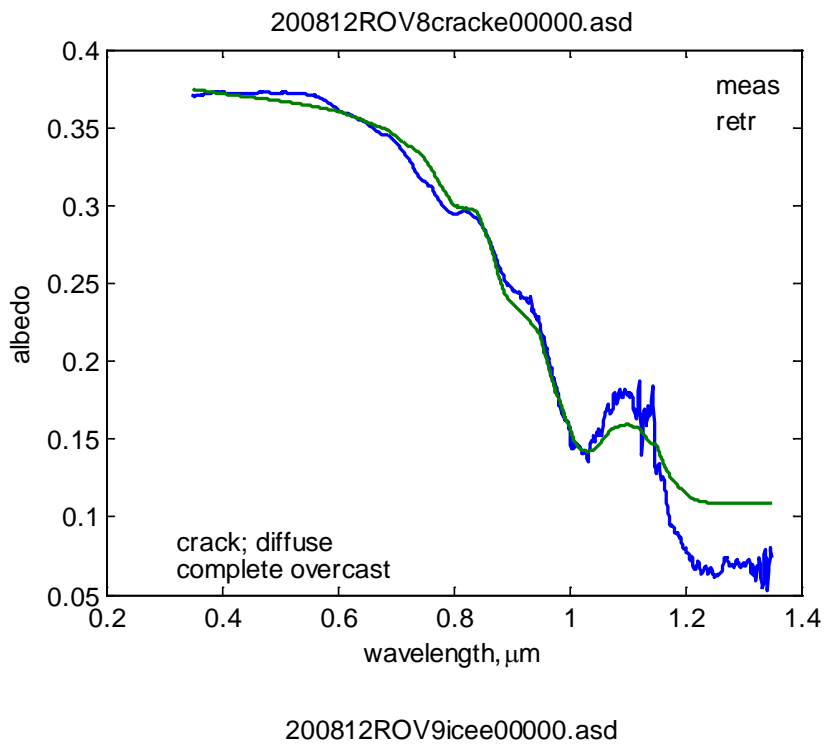


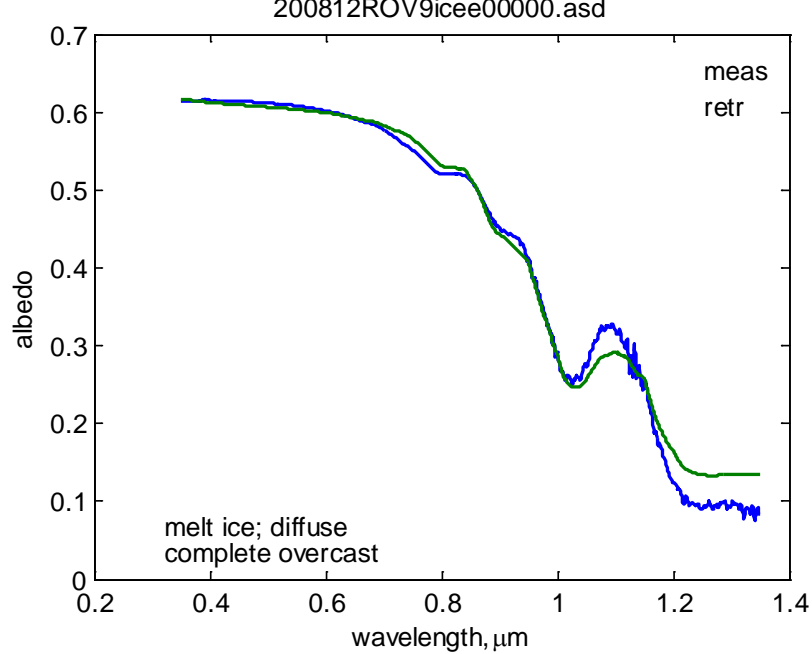




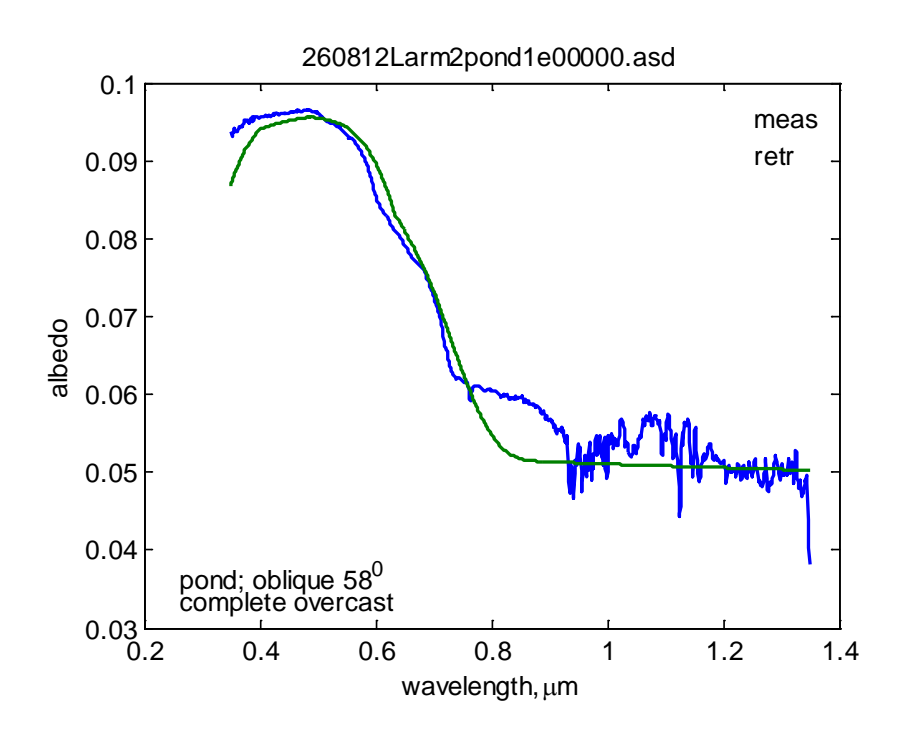


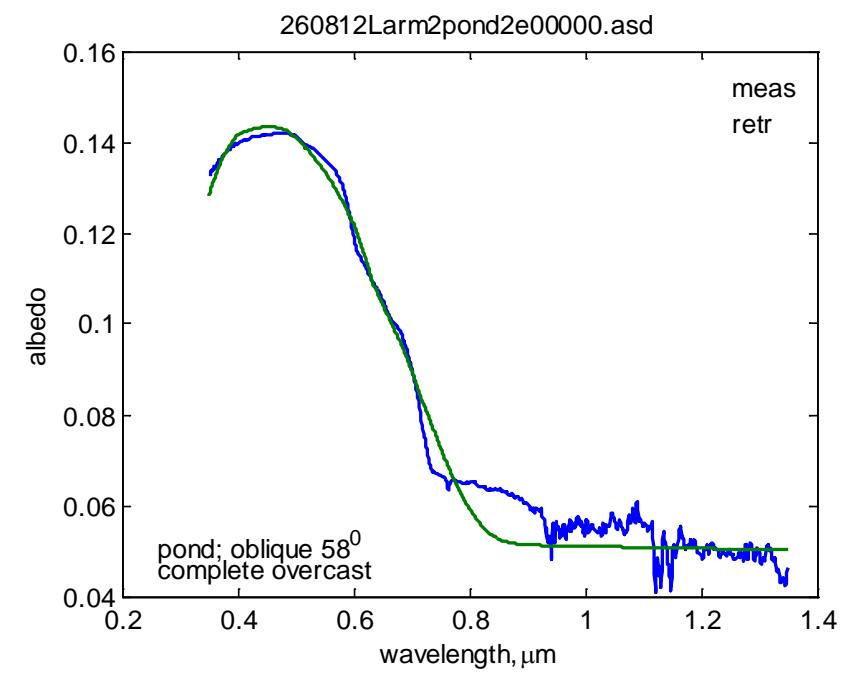


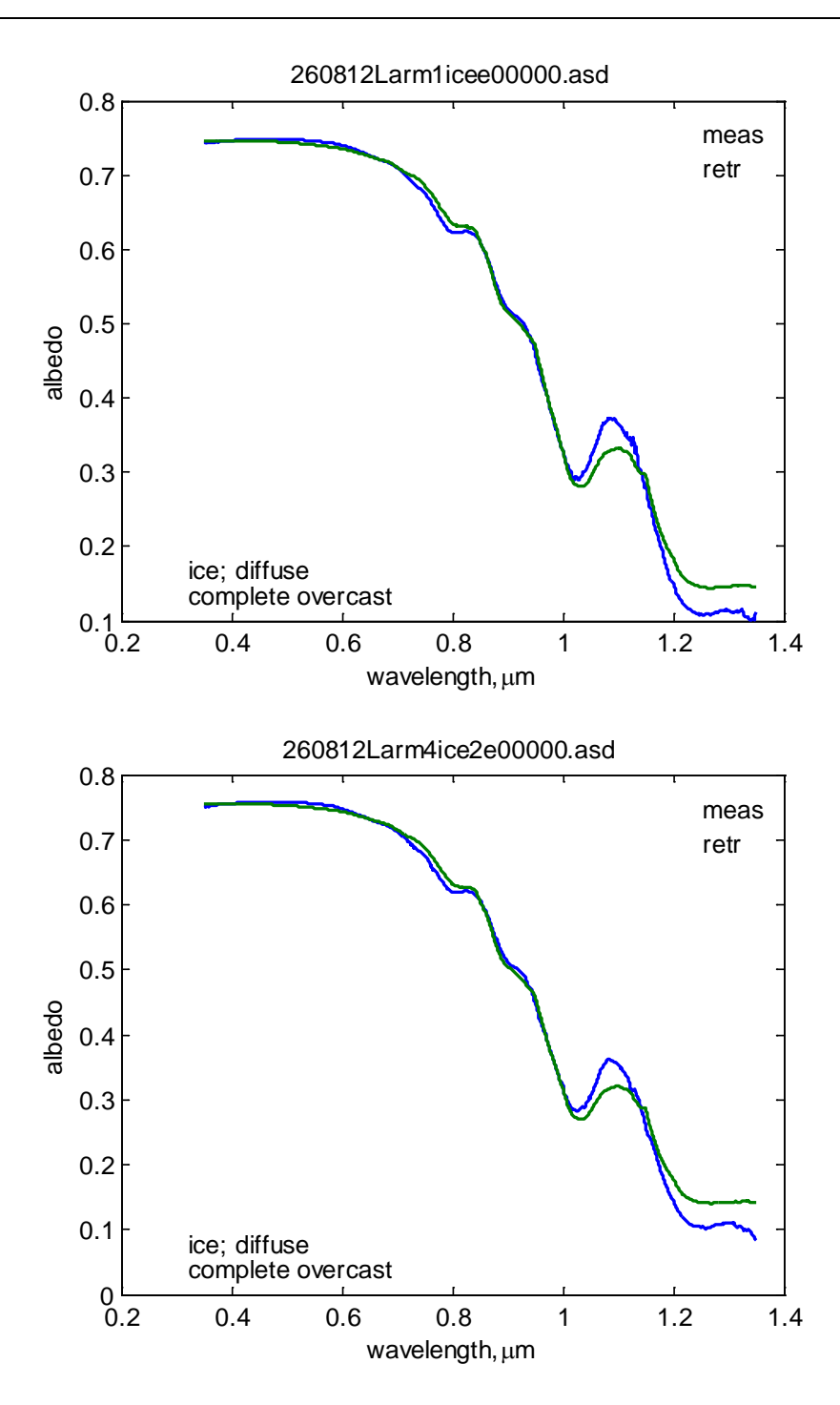




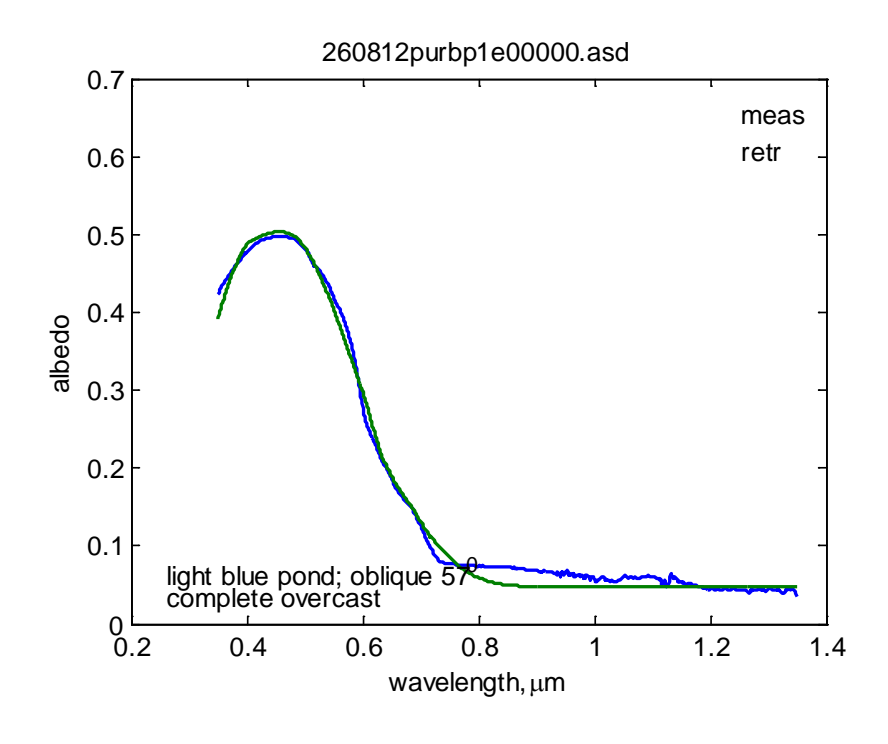
## Station 4a

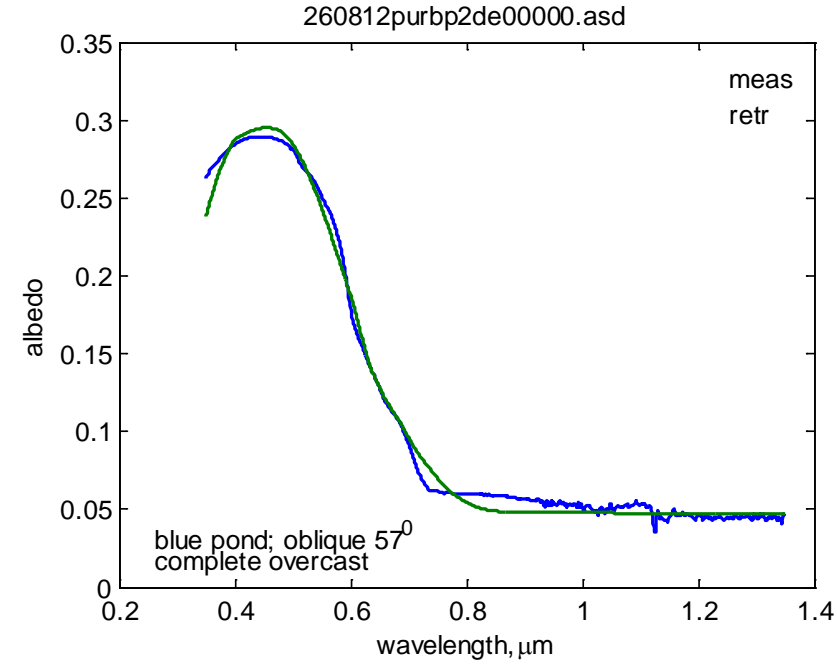


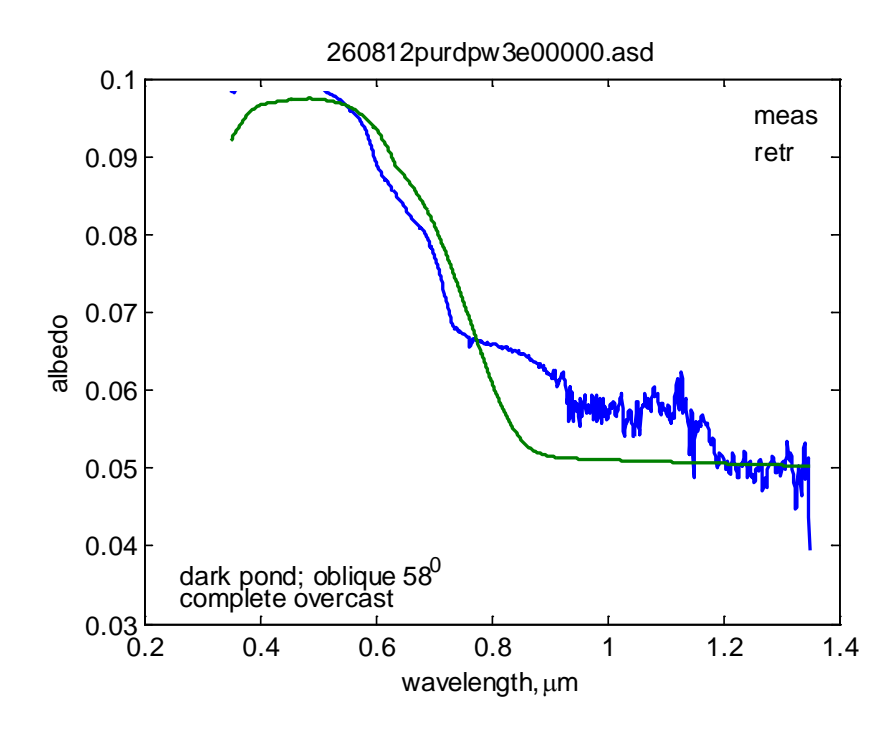


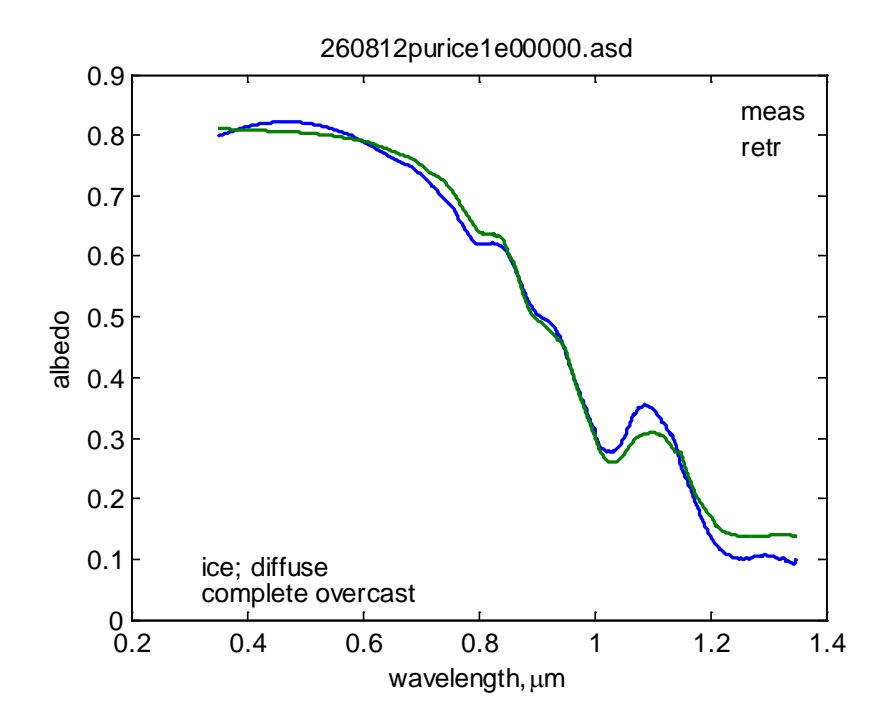


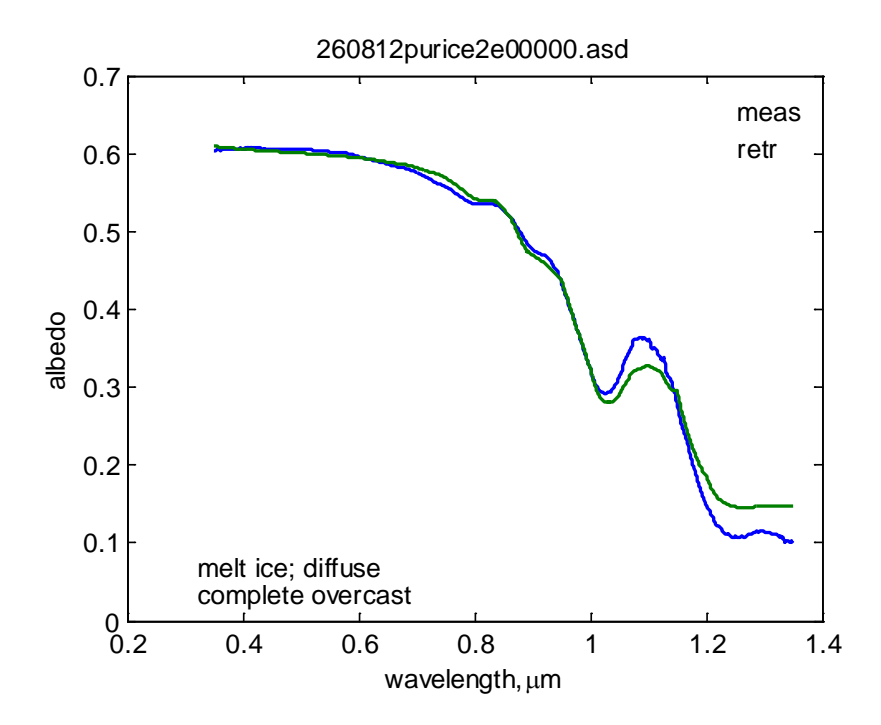
**Station 4b** 



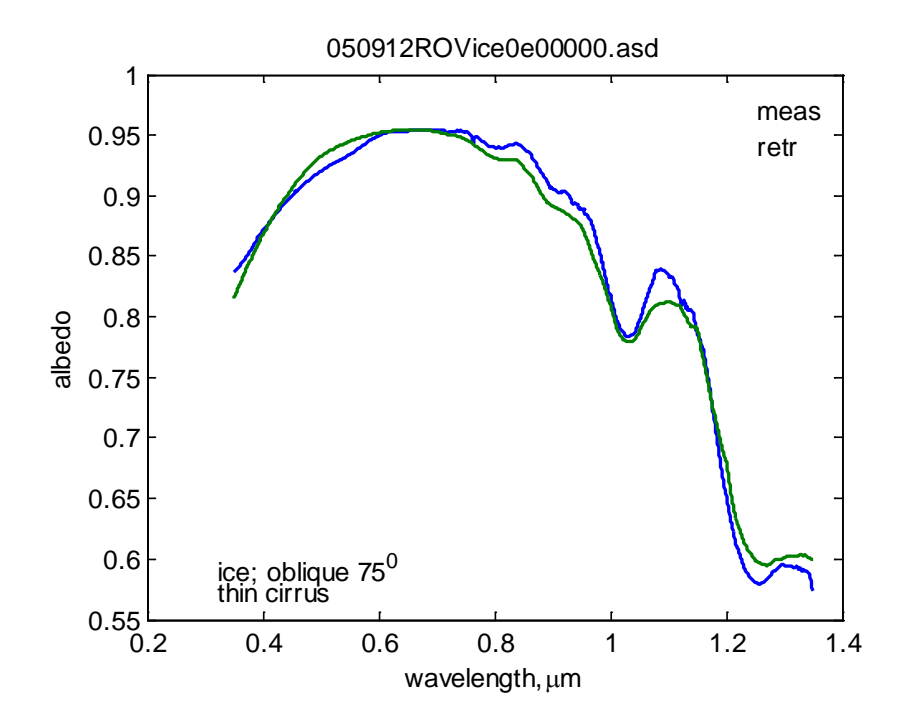


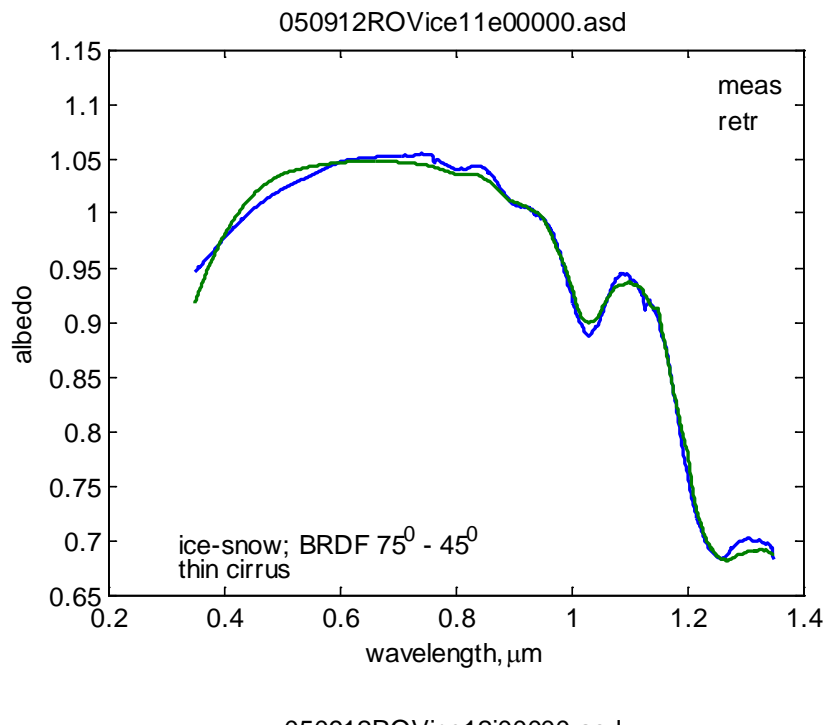


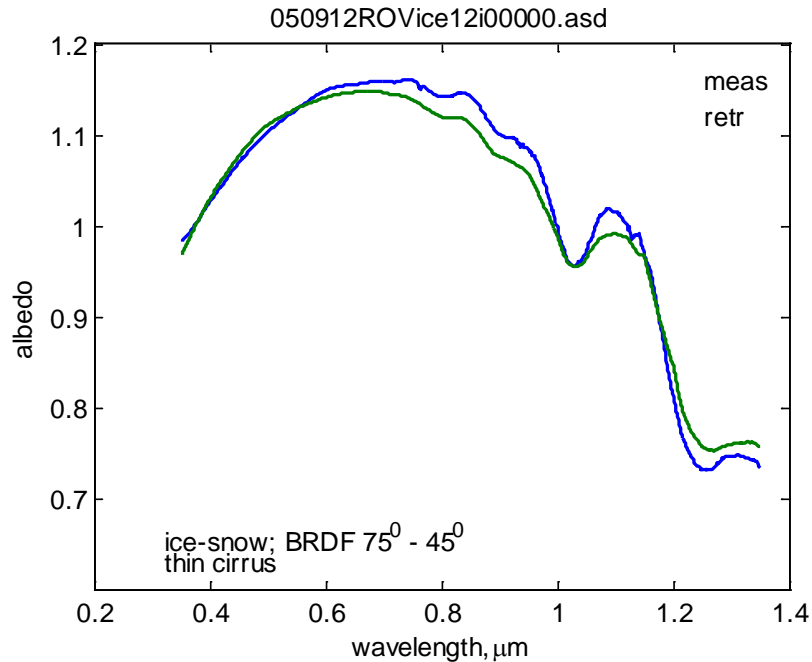


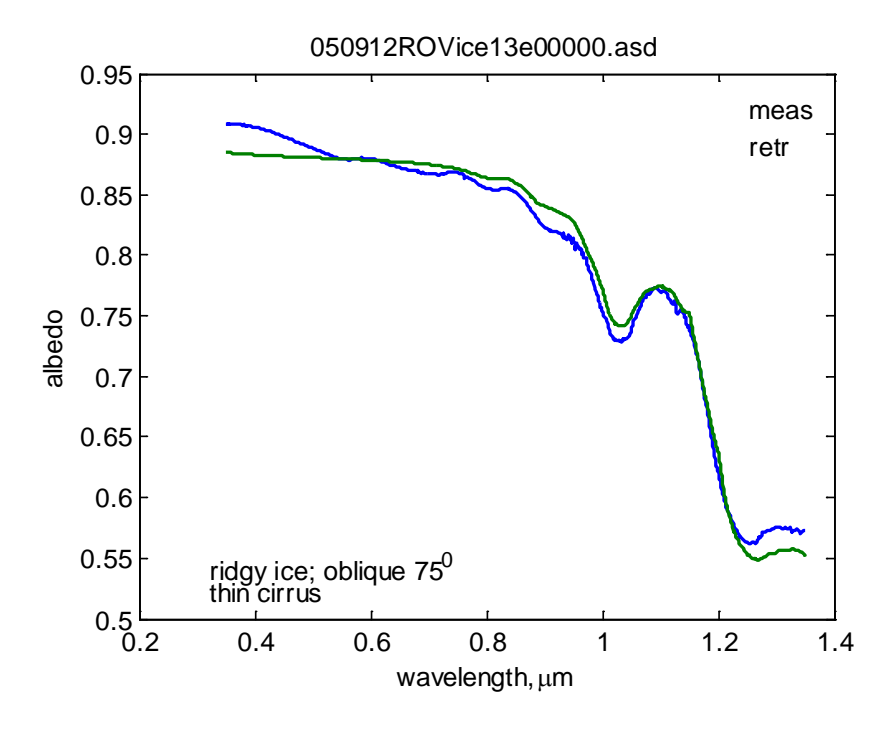


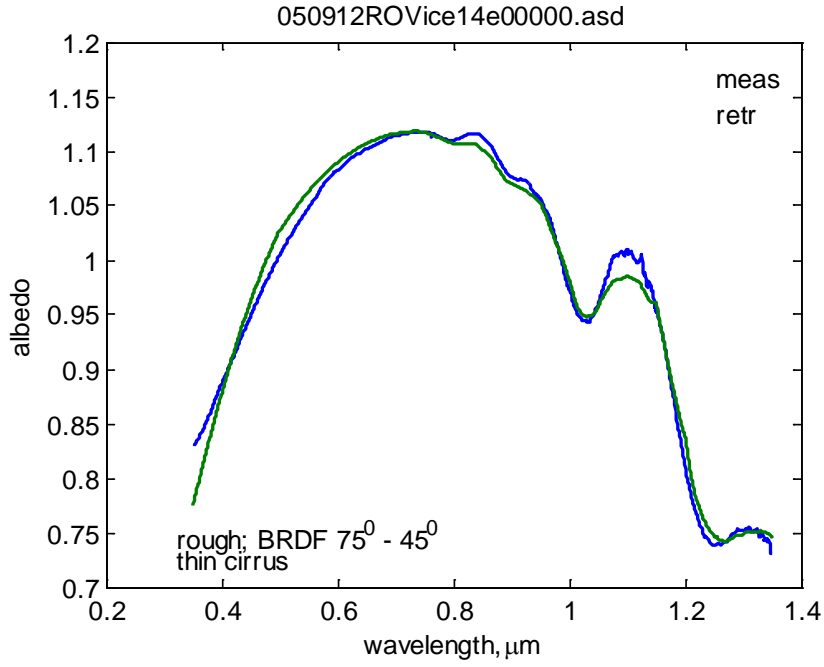
## Station 5

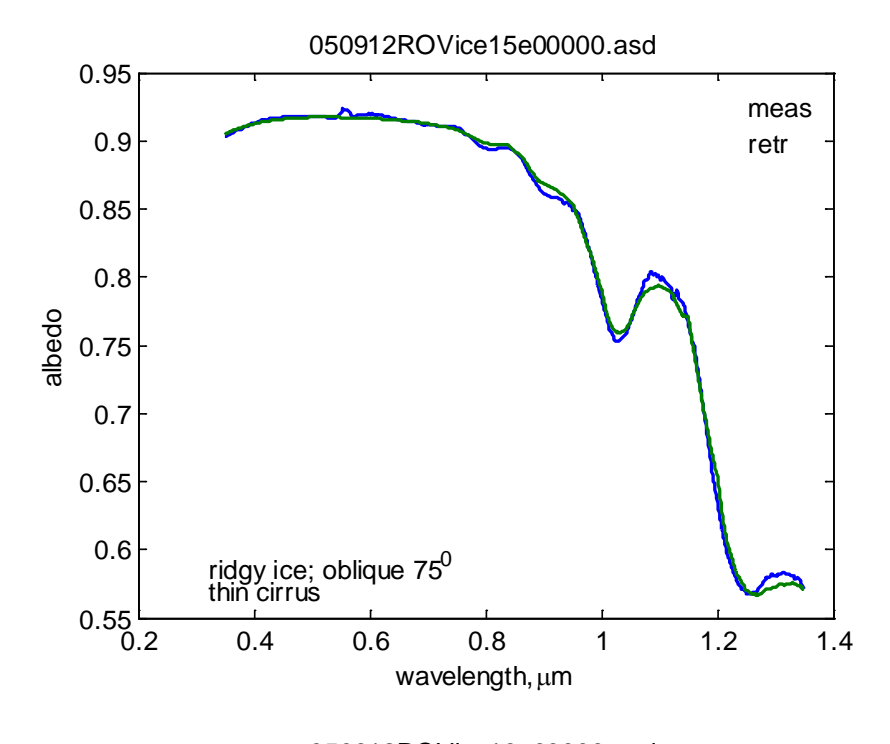


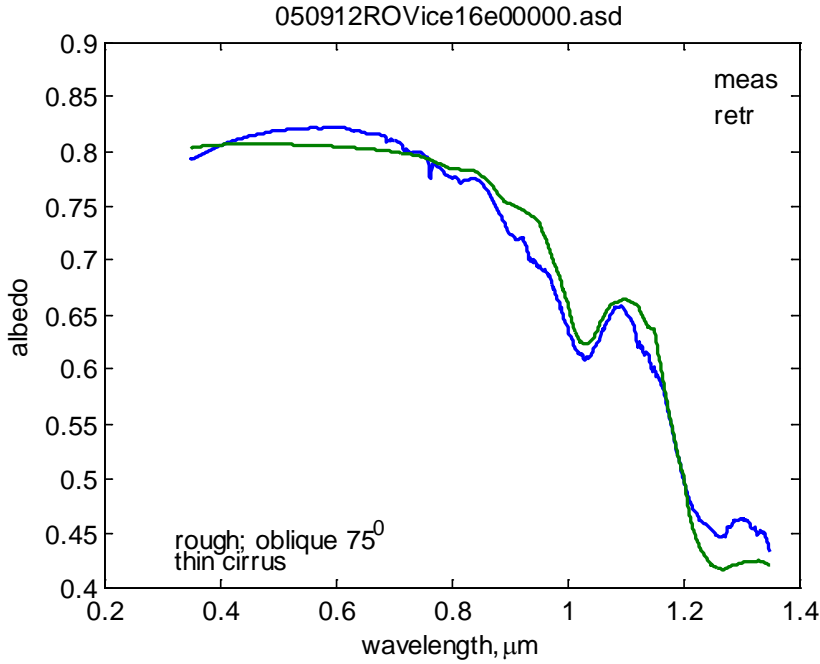


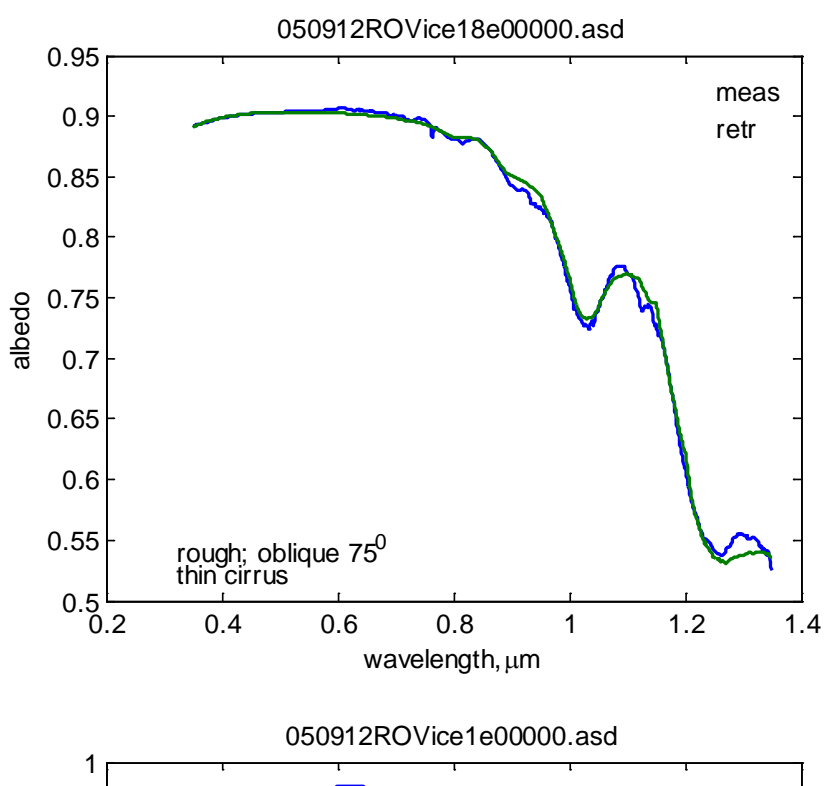


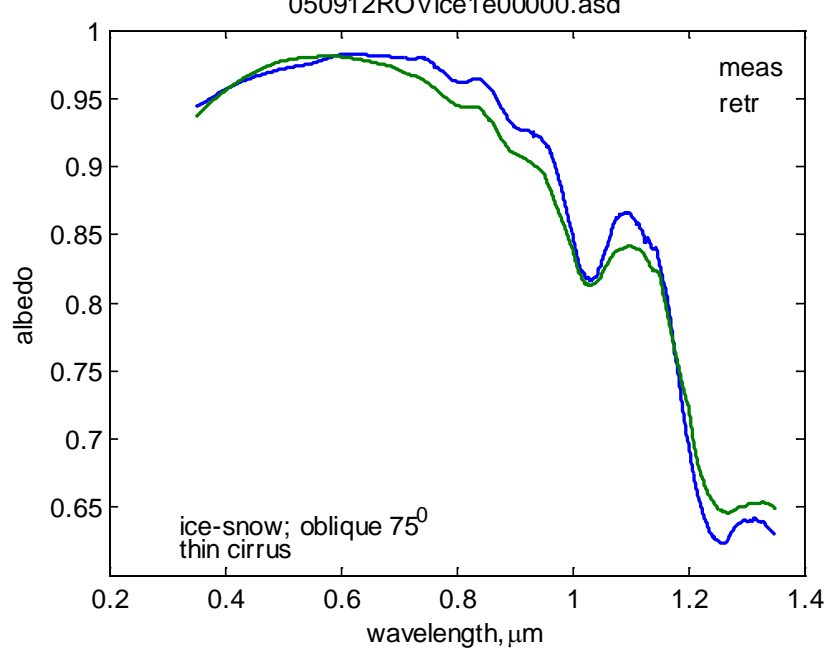


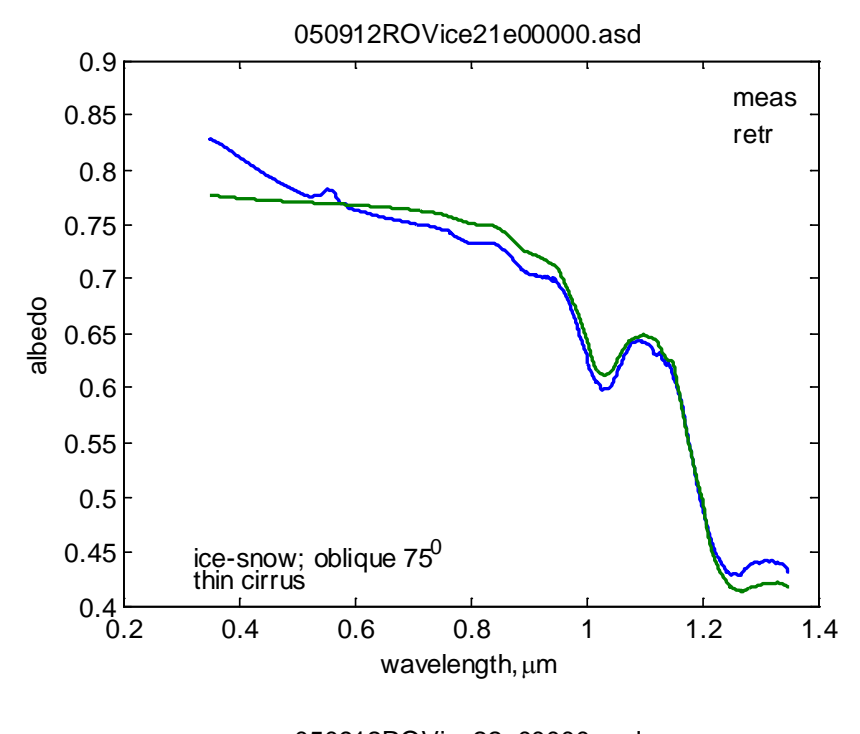


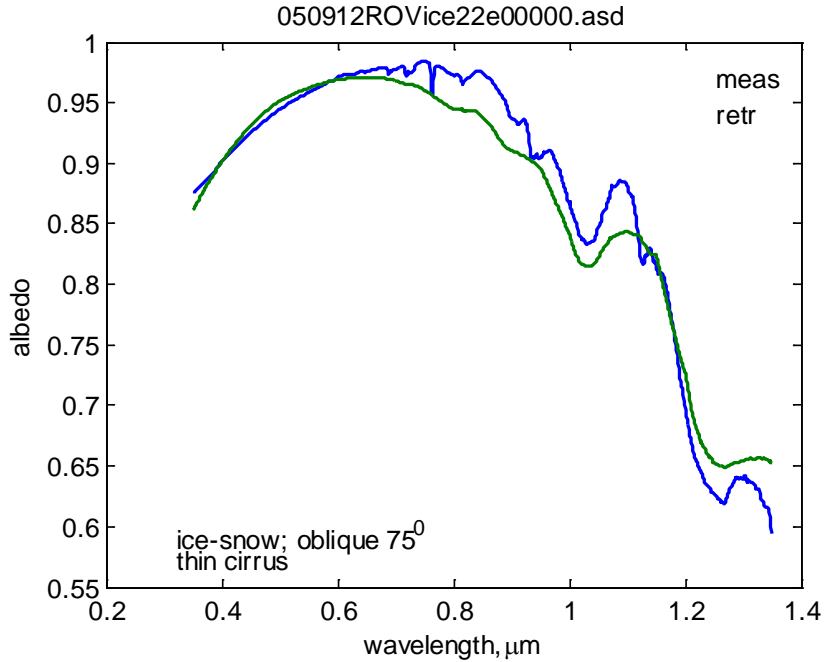


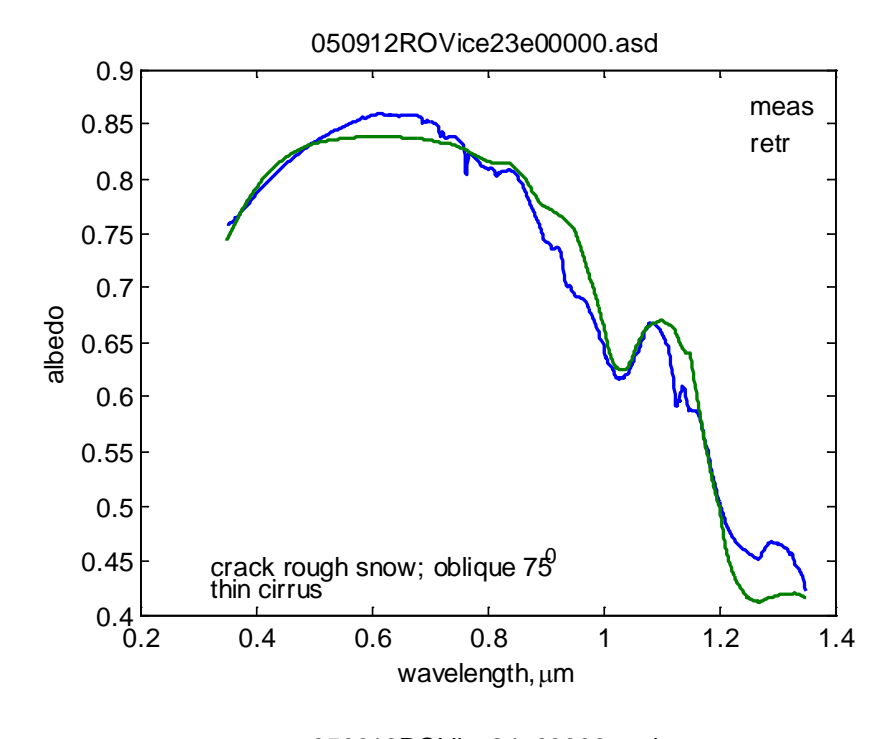


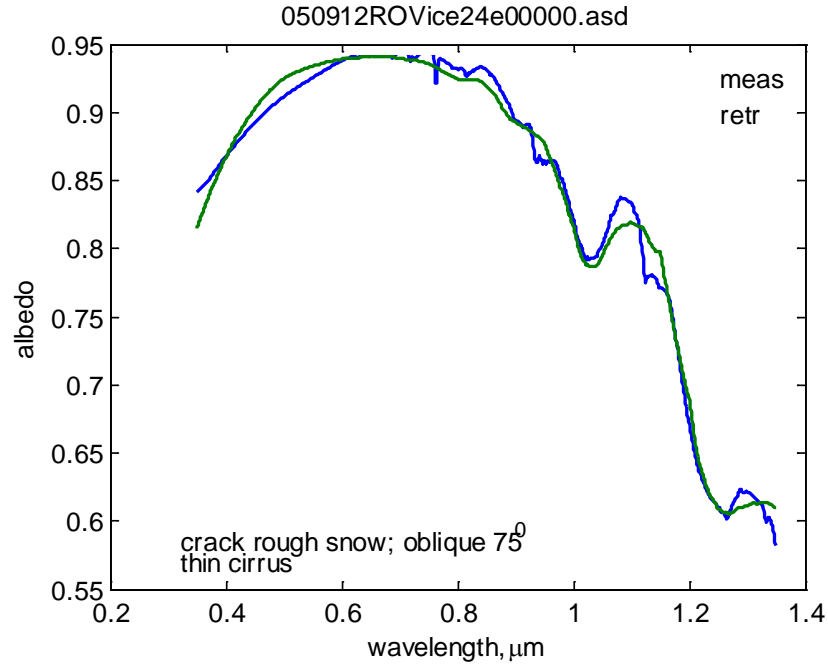


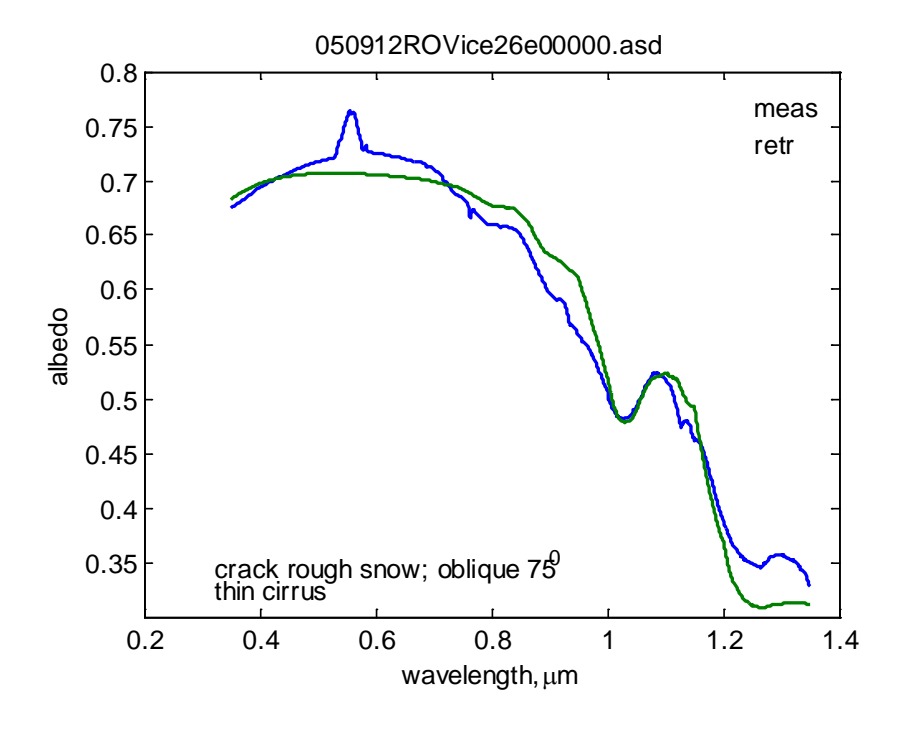


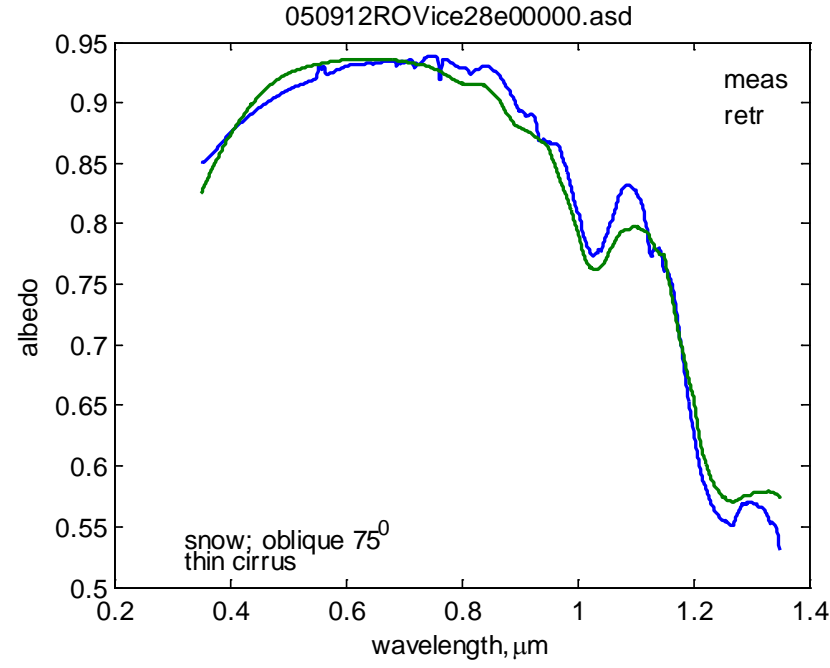


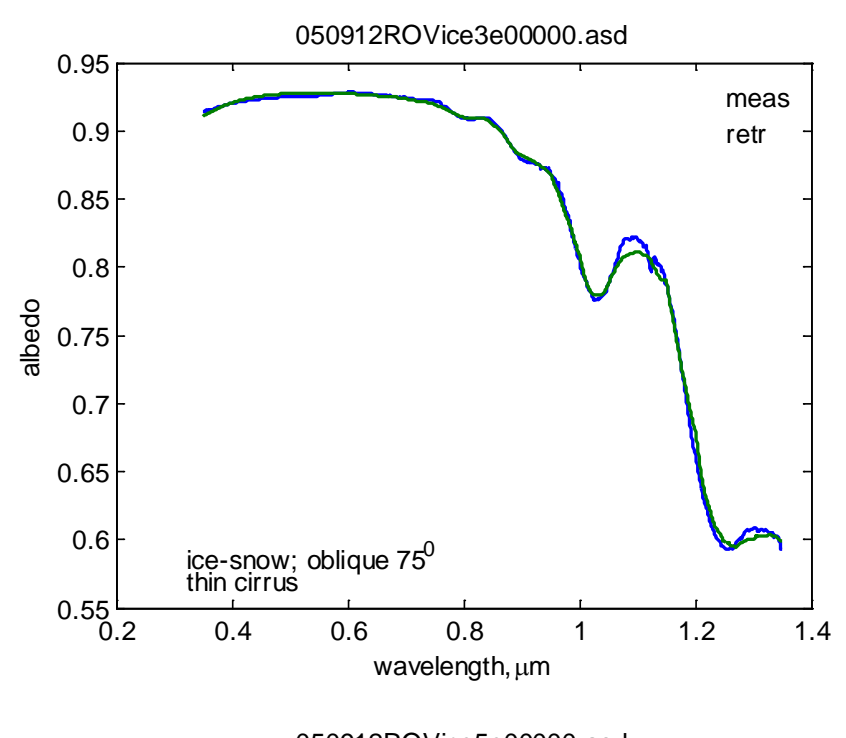


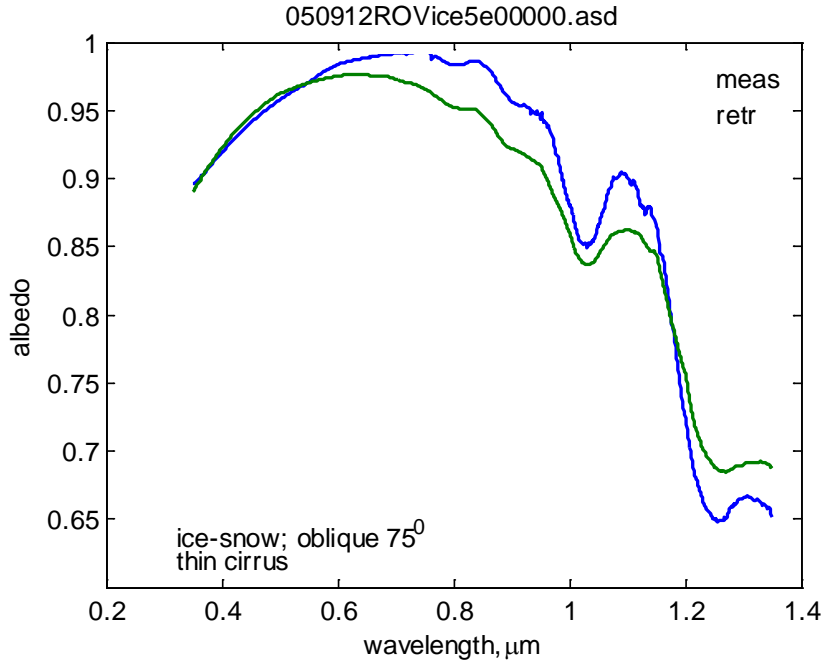


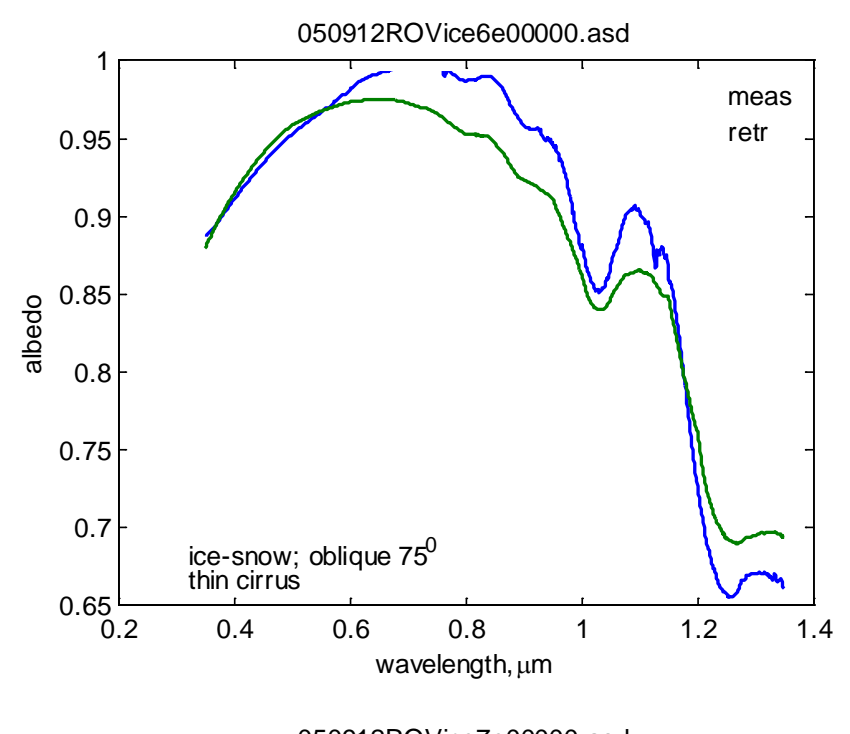


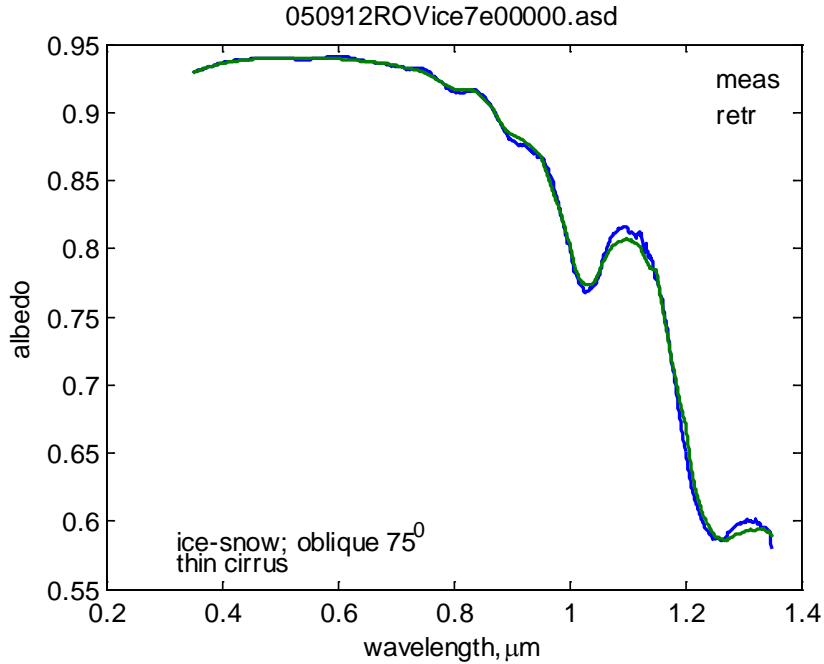


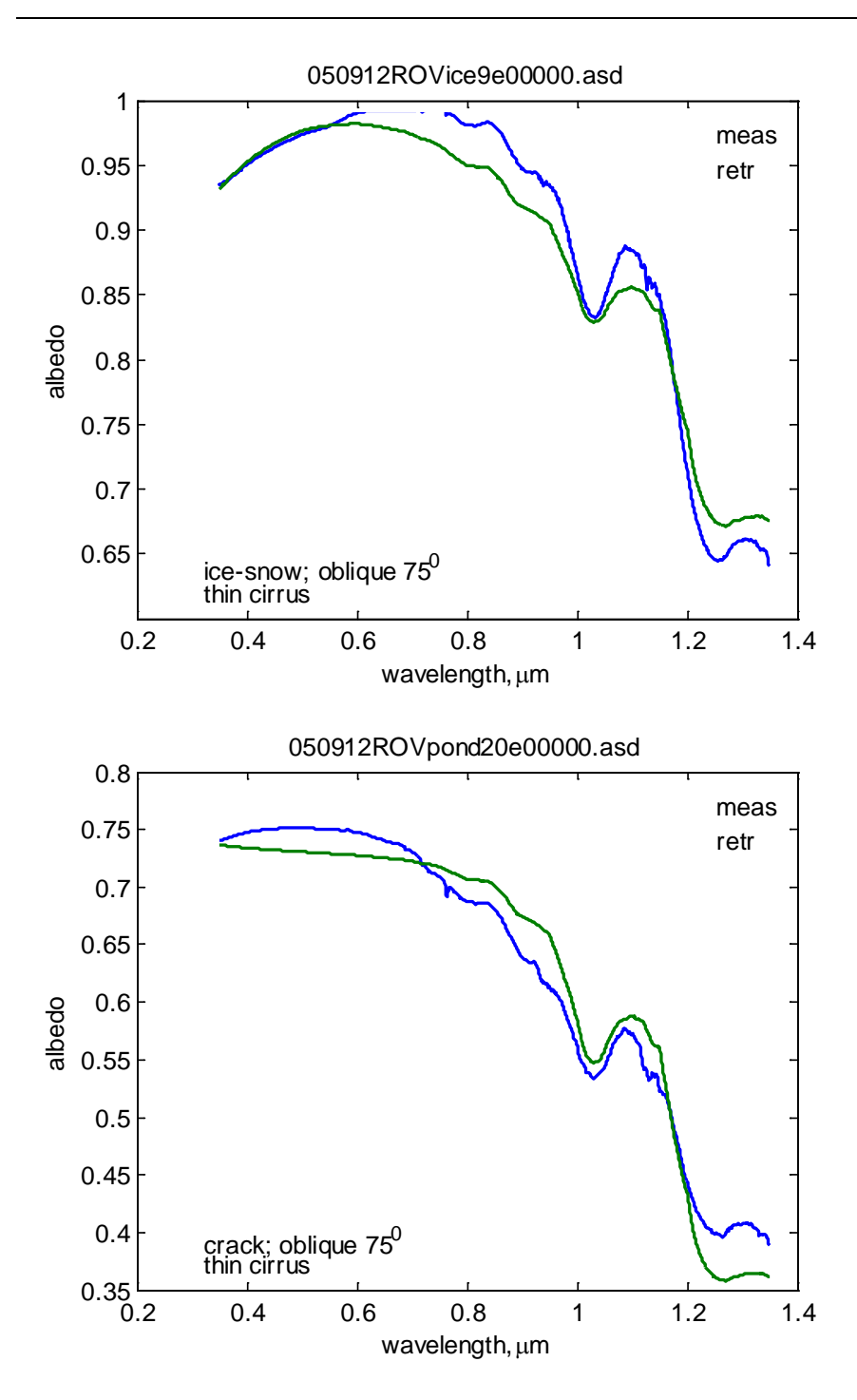




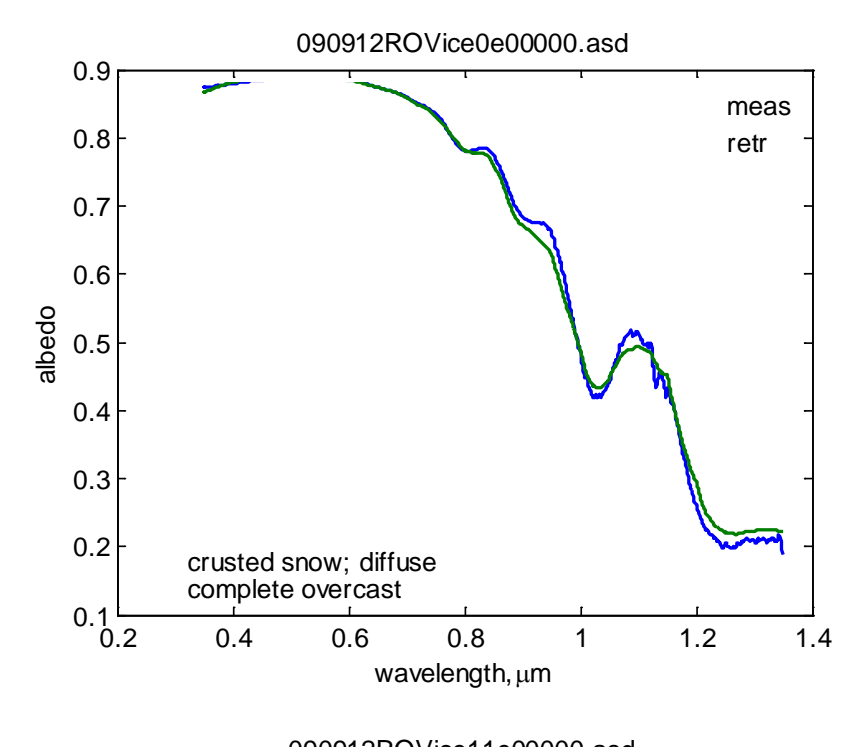


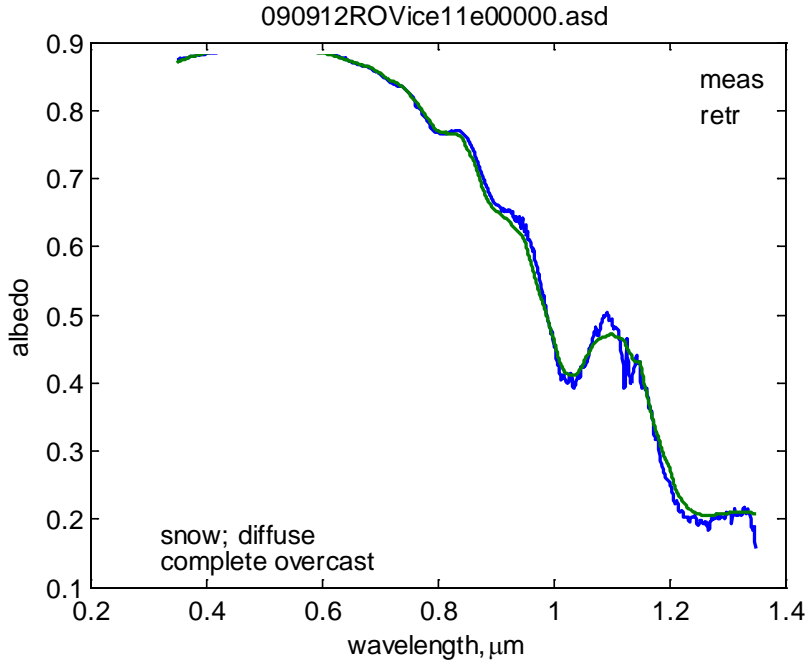


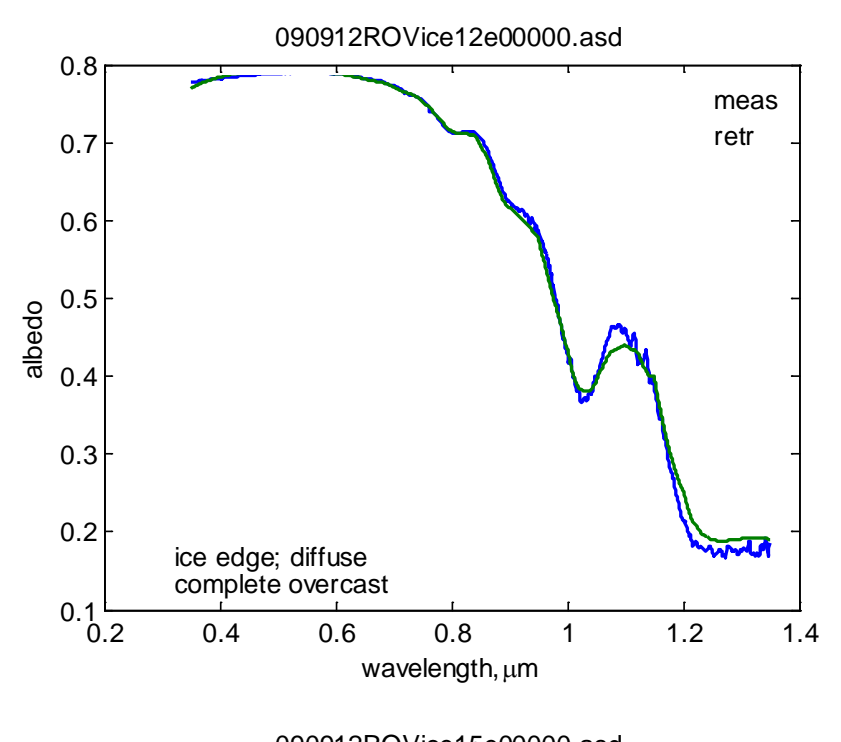


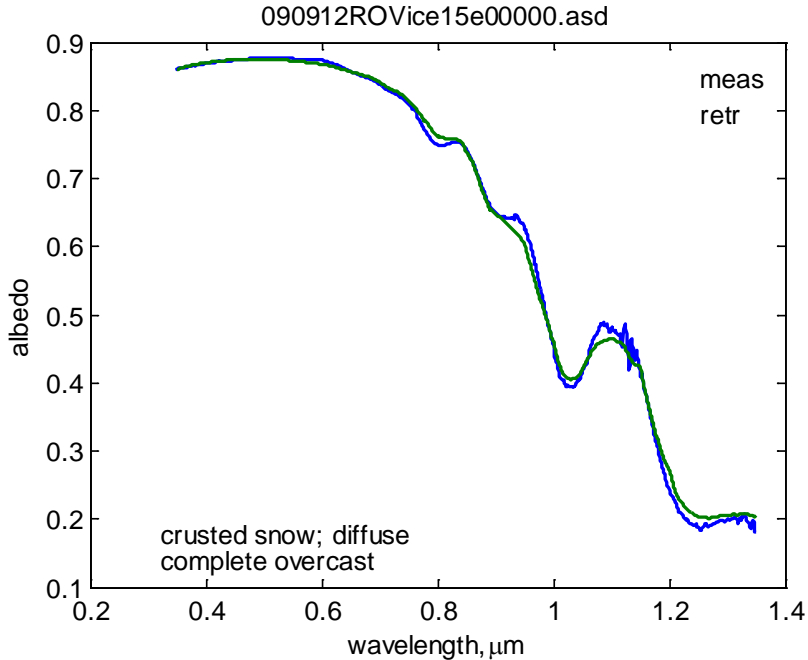


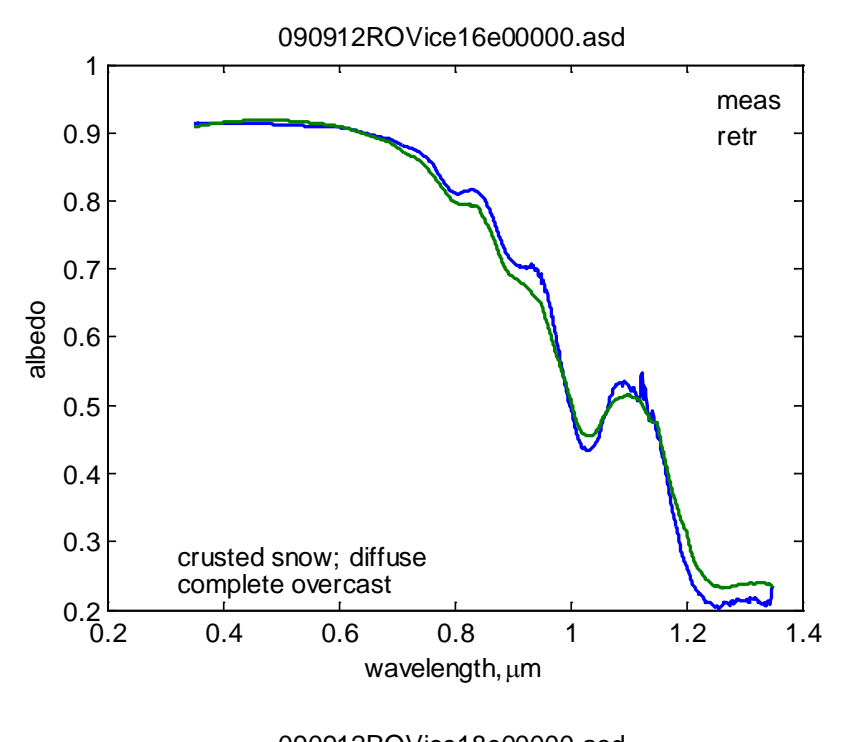
Station 6

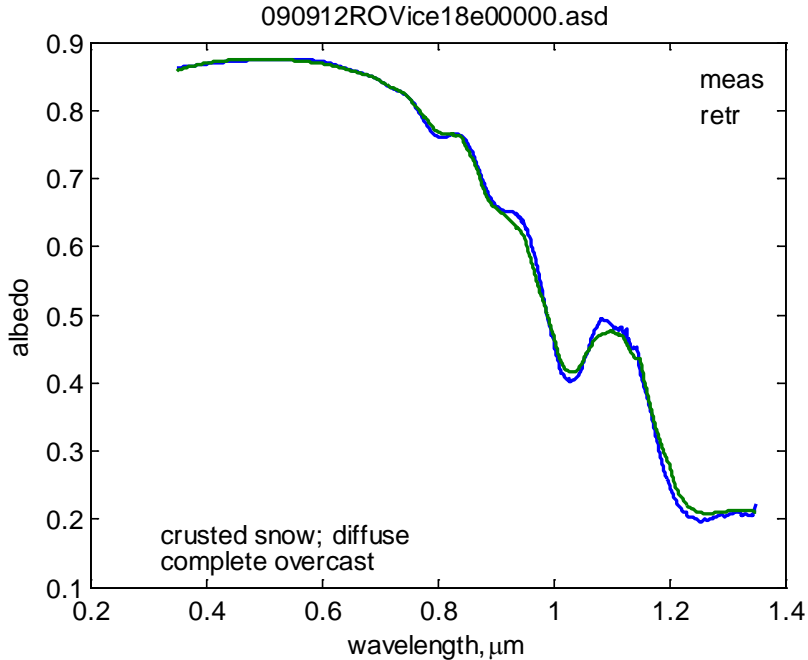


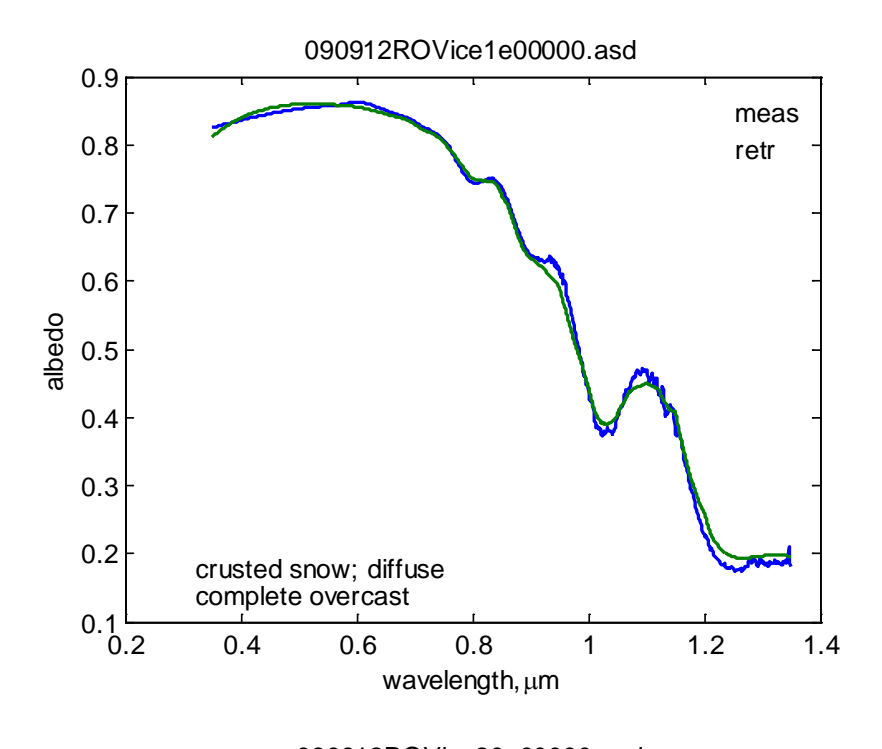


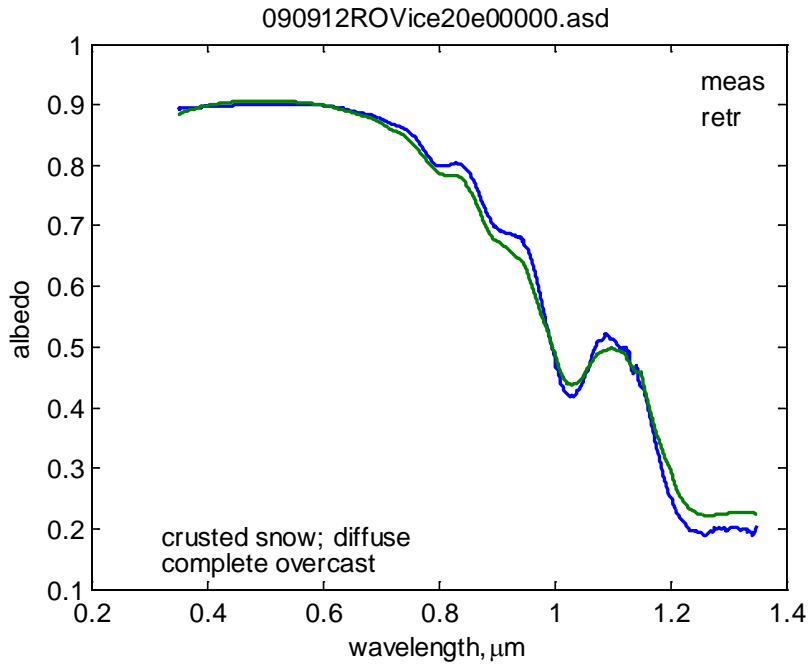


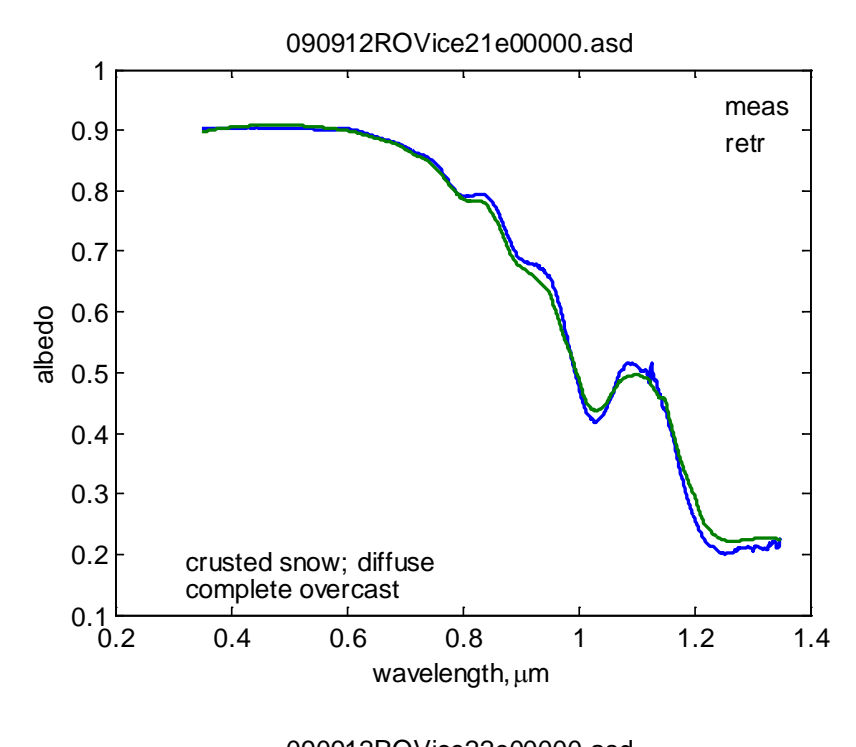


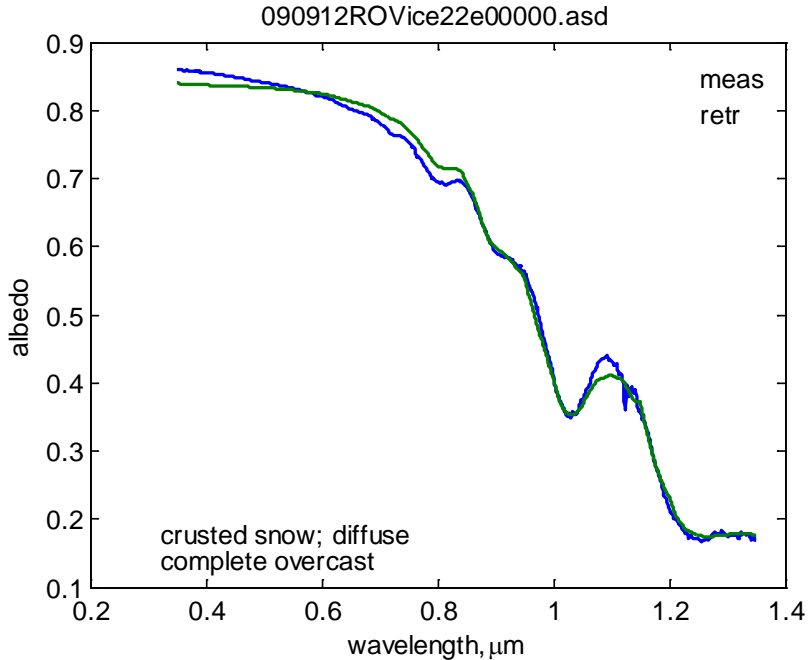


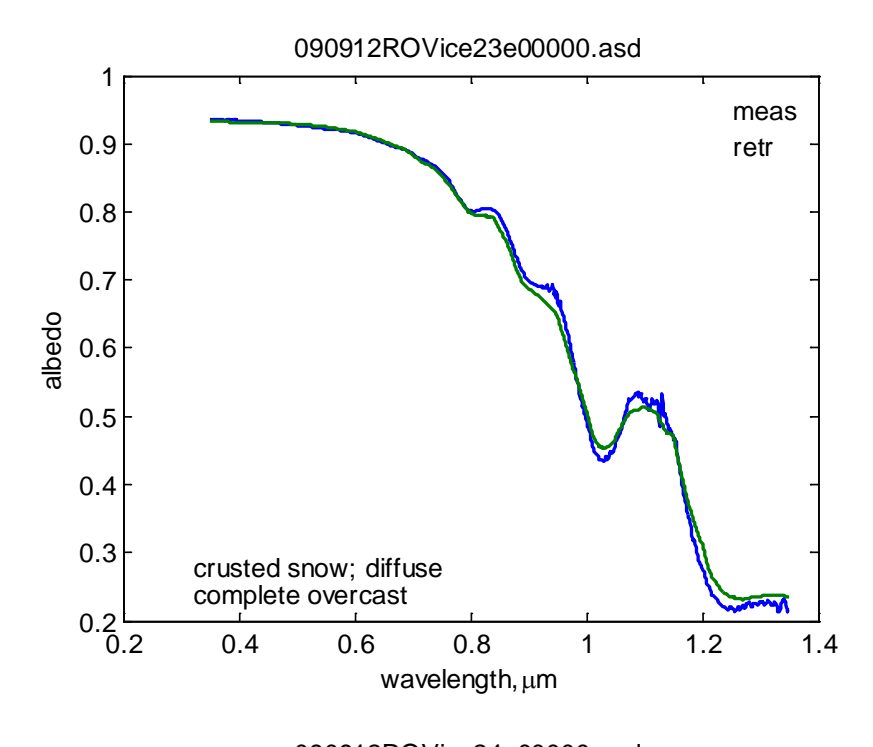


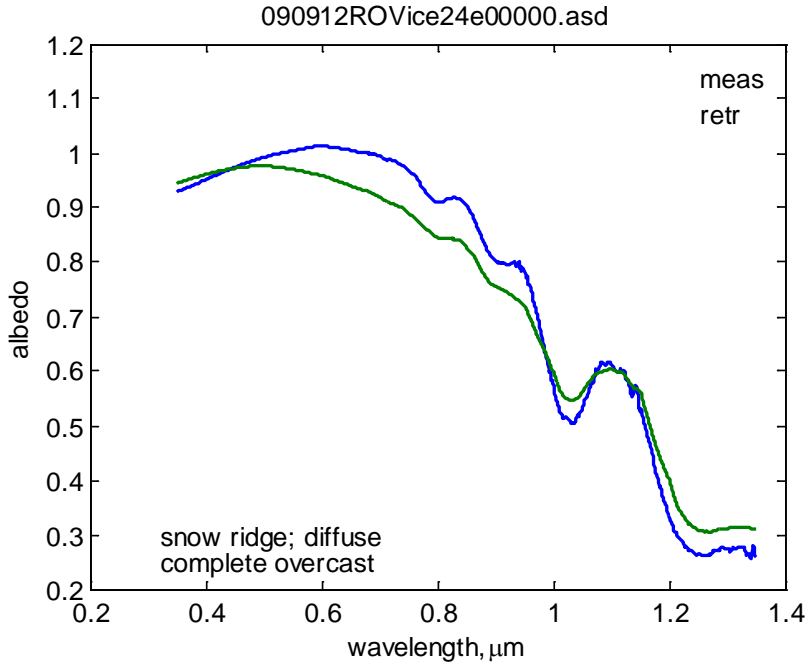


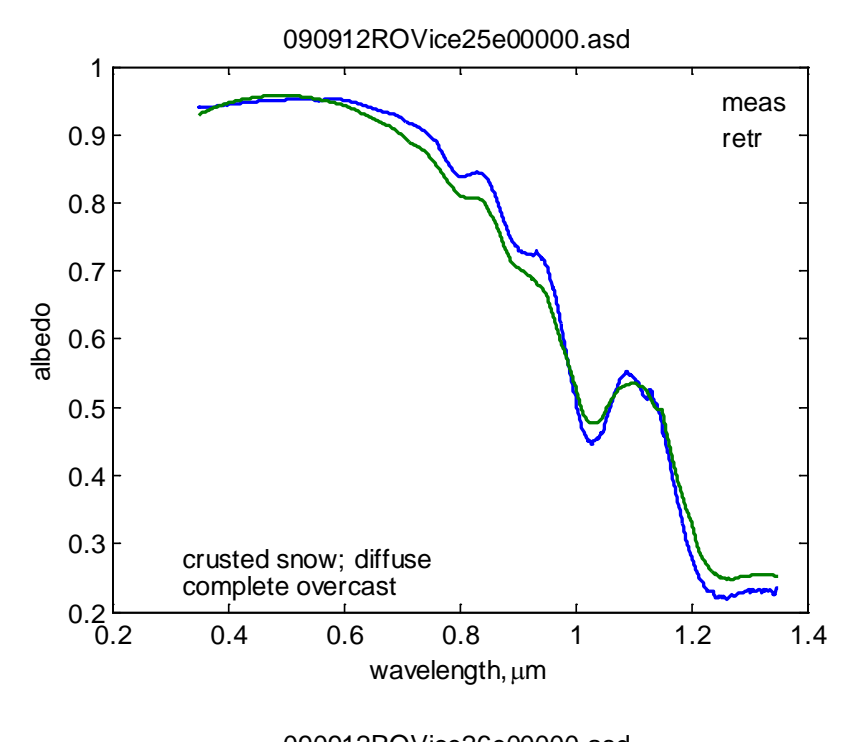


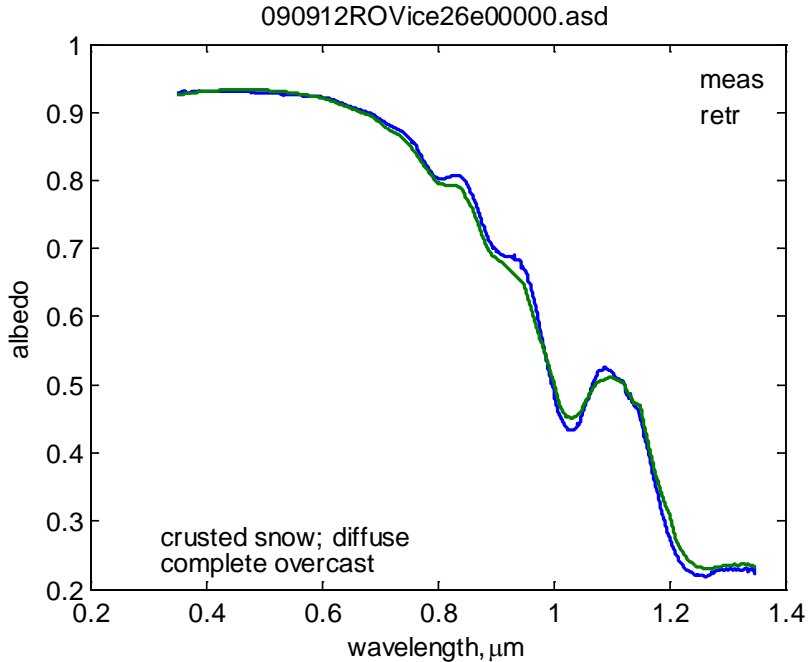


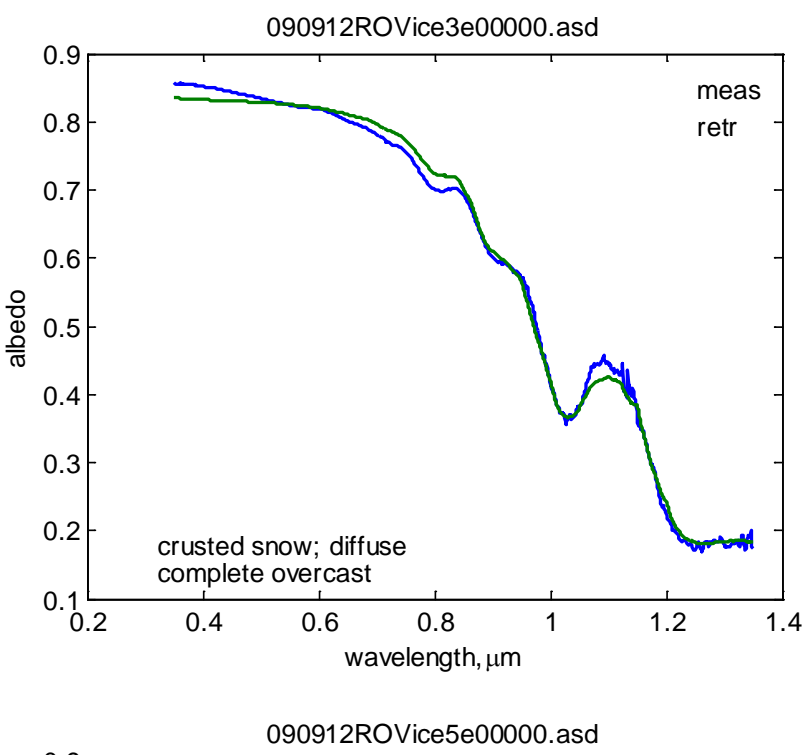


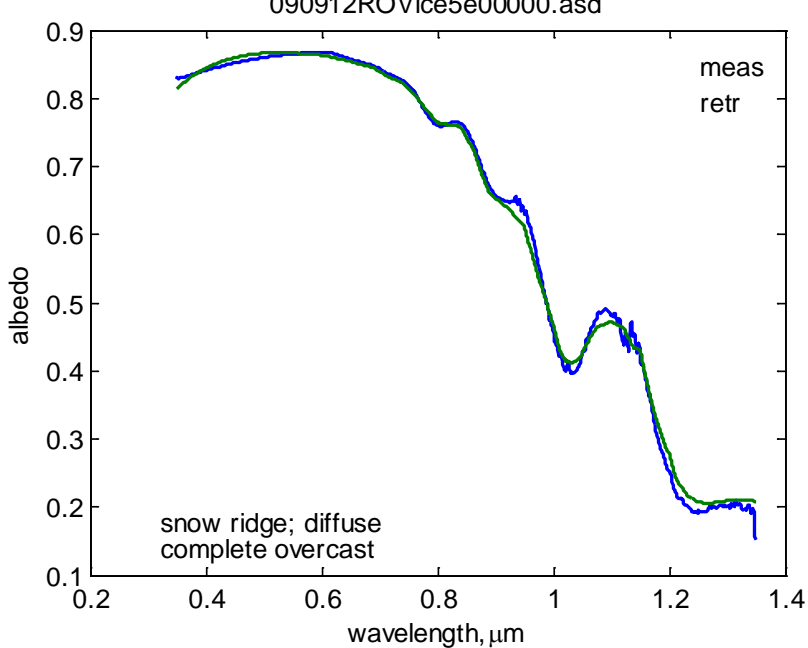


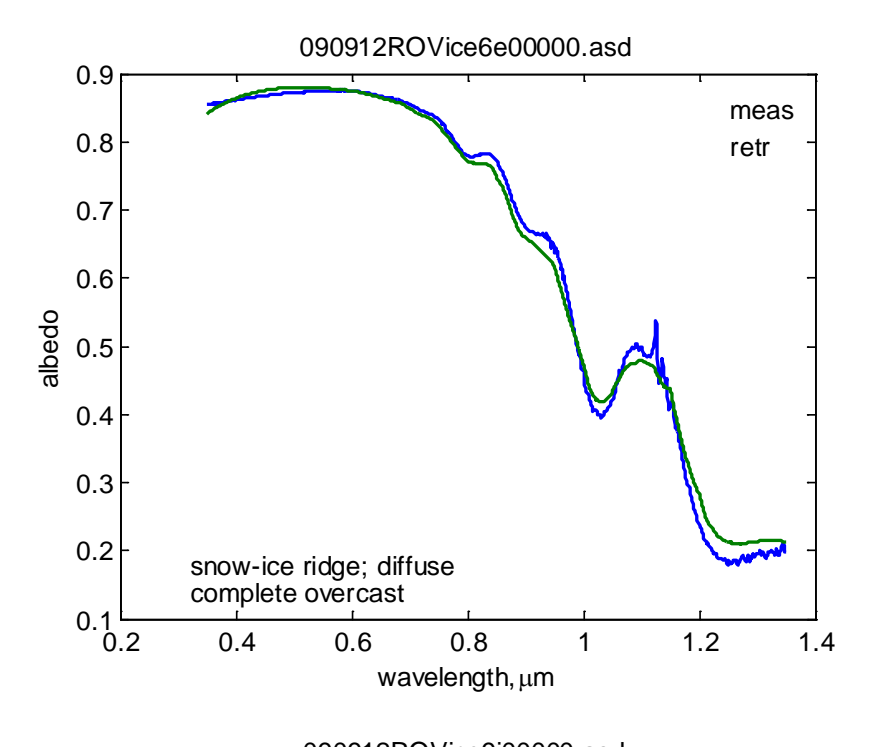


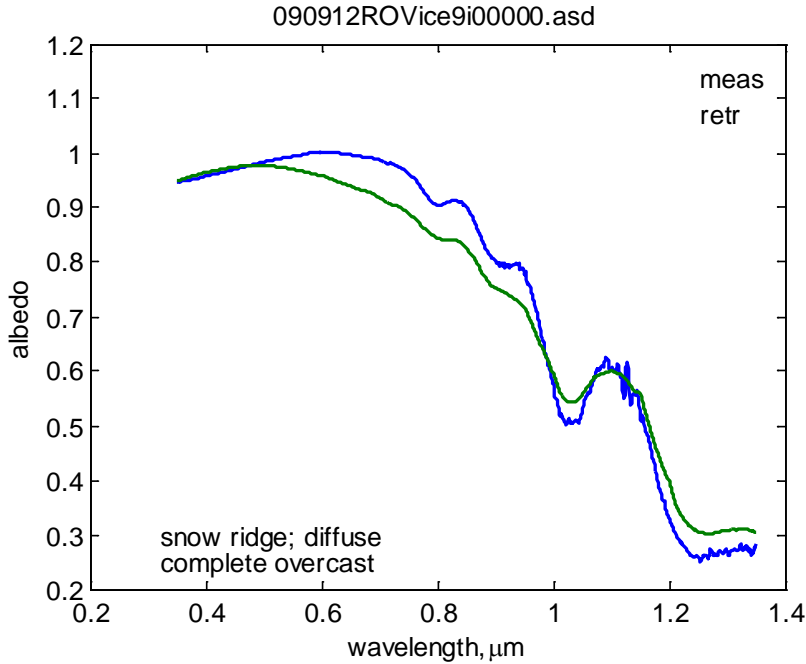


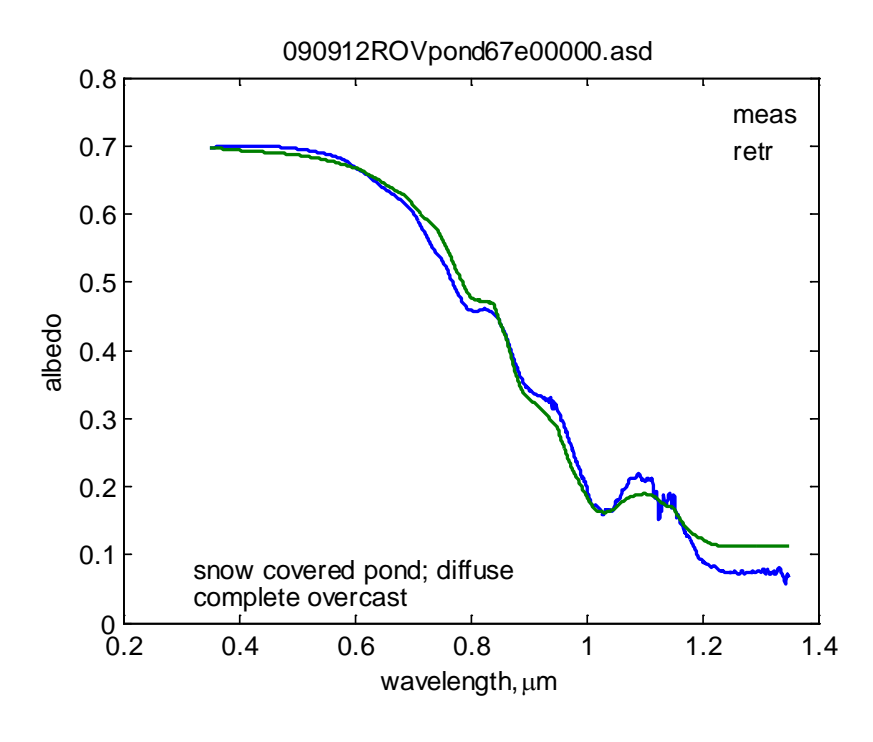


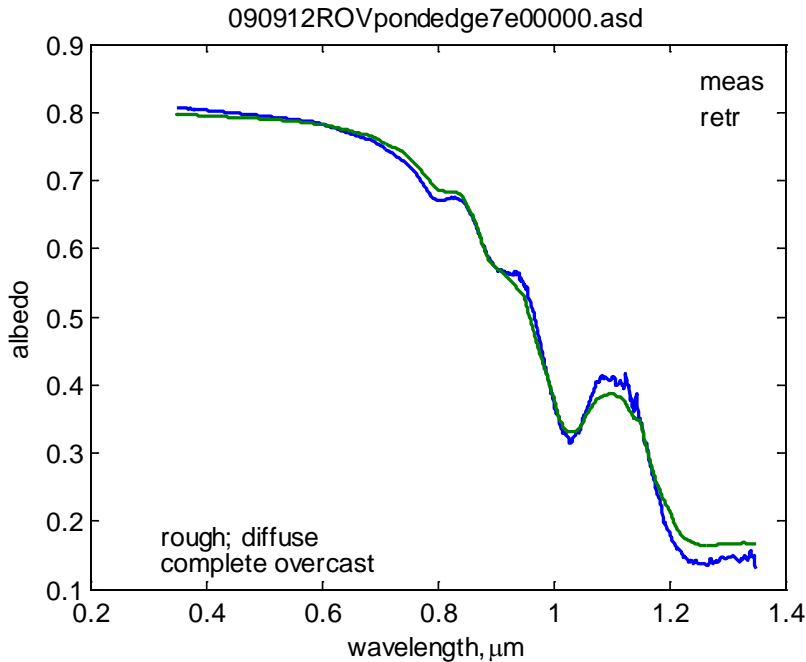






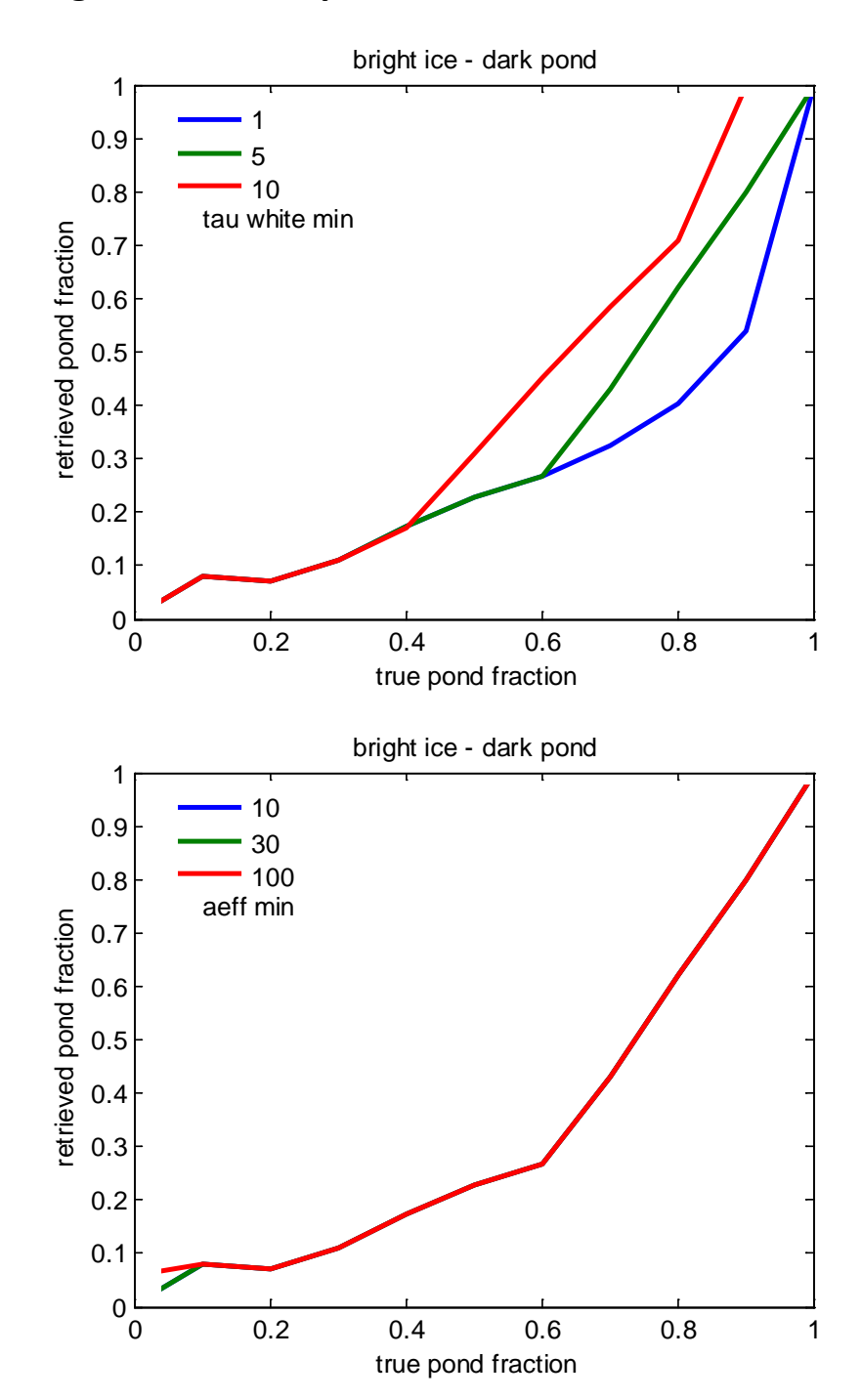


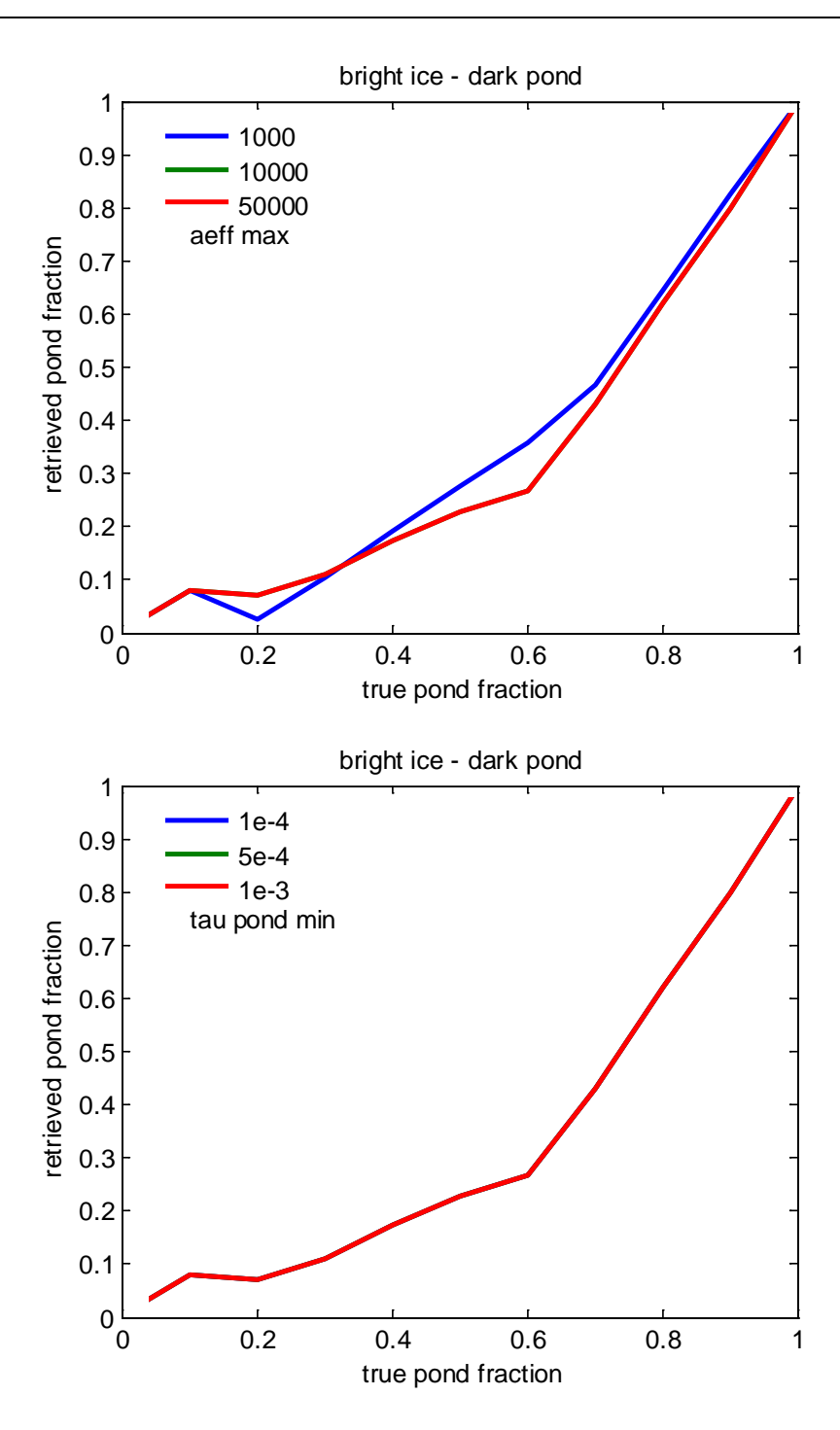


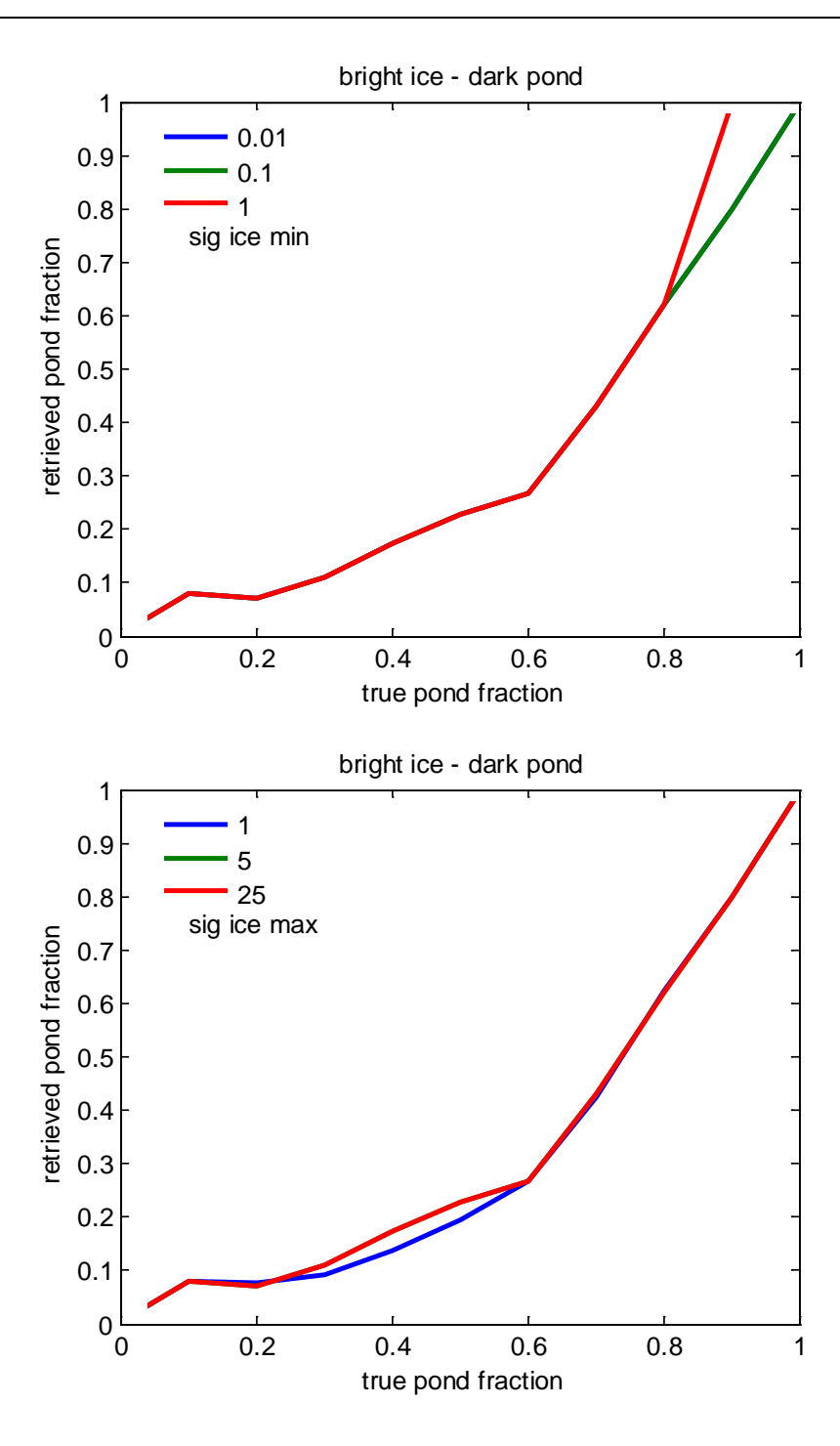


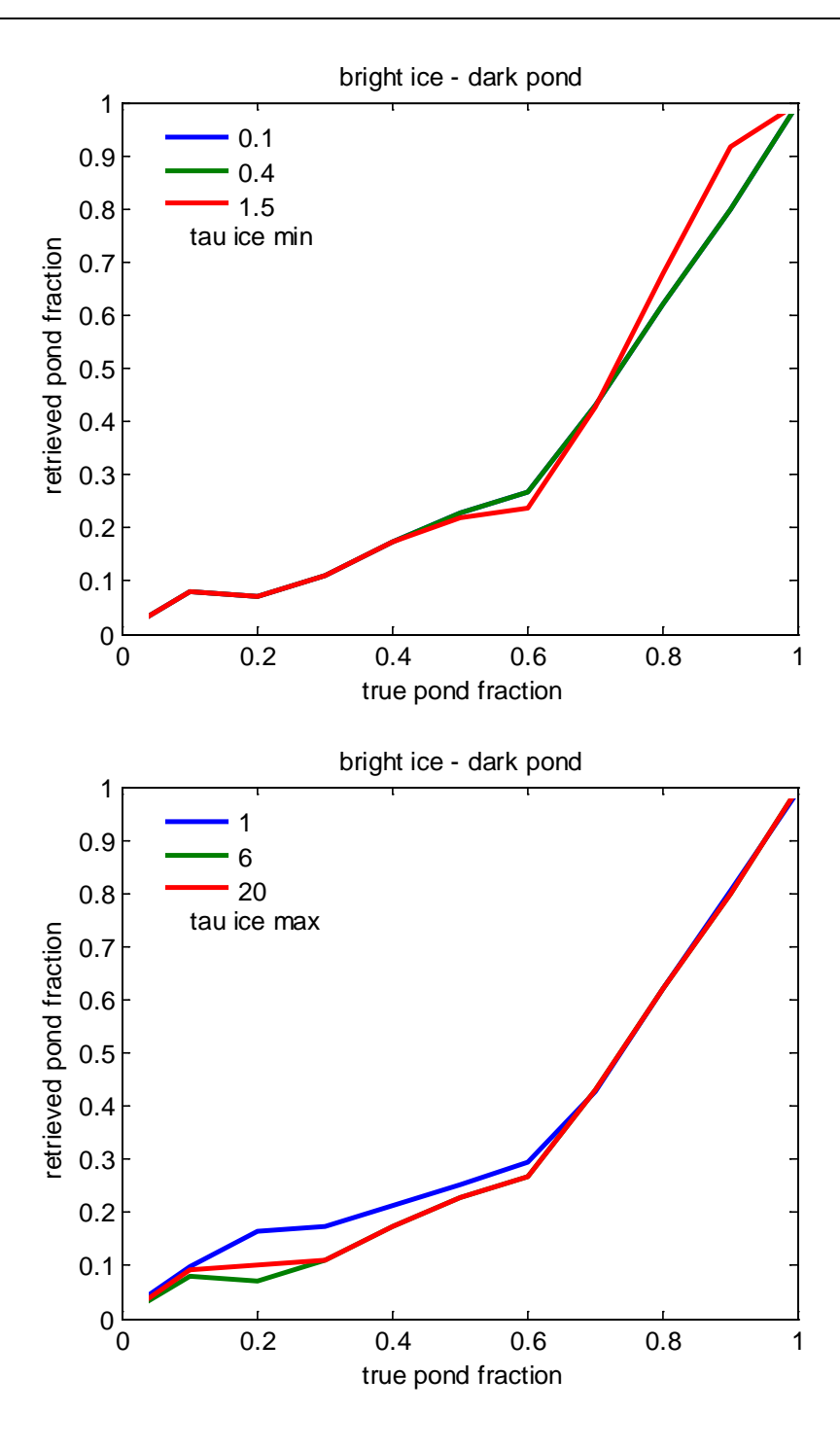
# 4 Appendix B

# Bright ice & dark pond

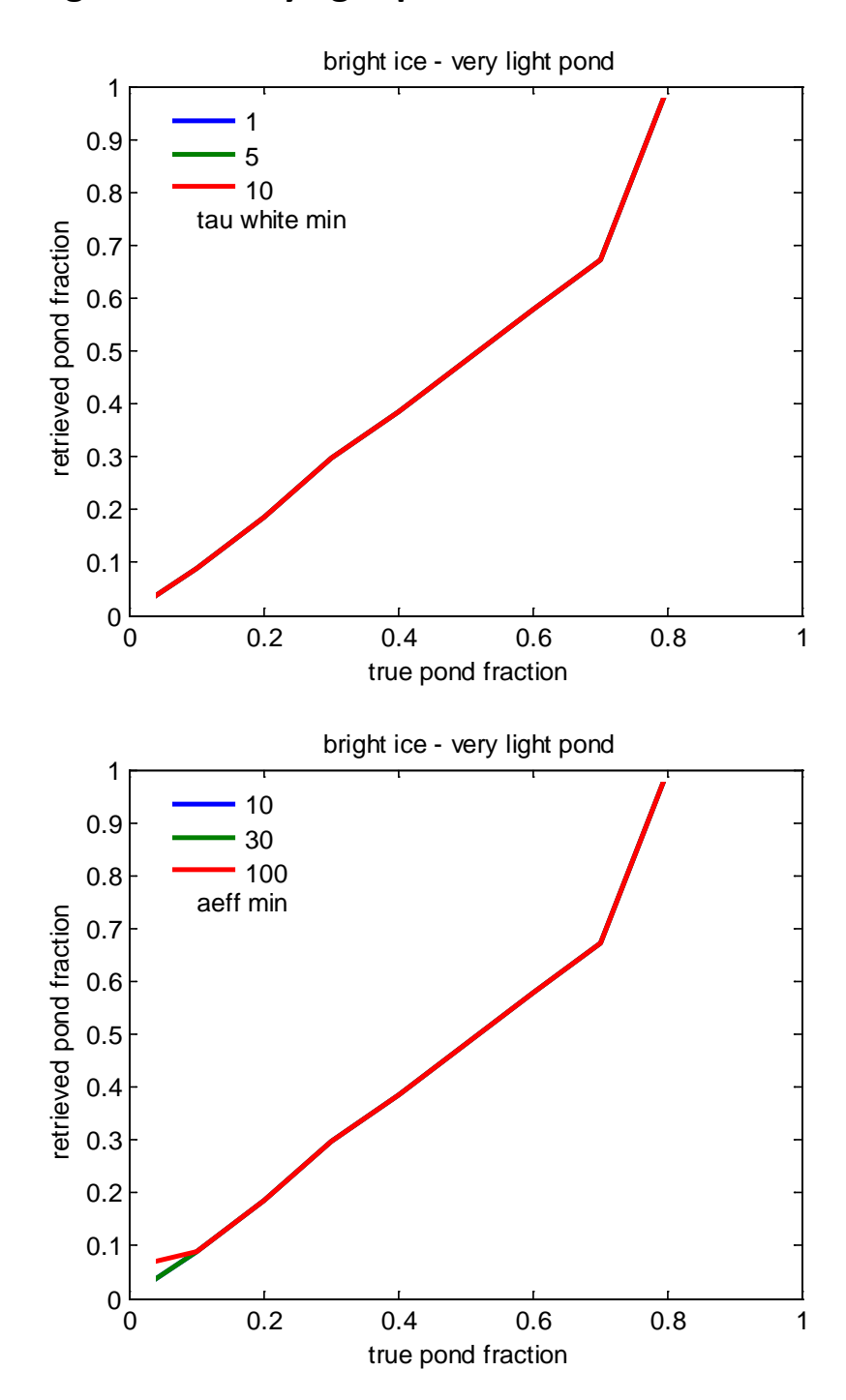


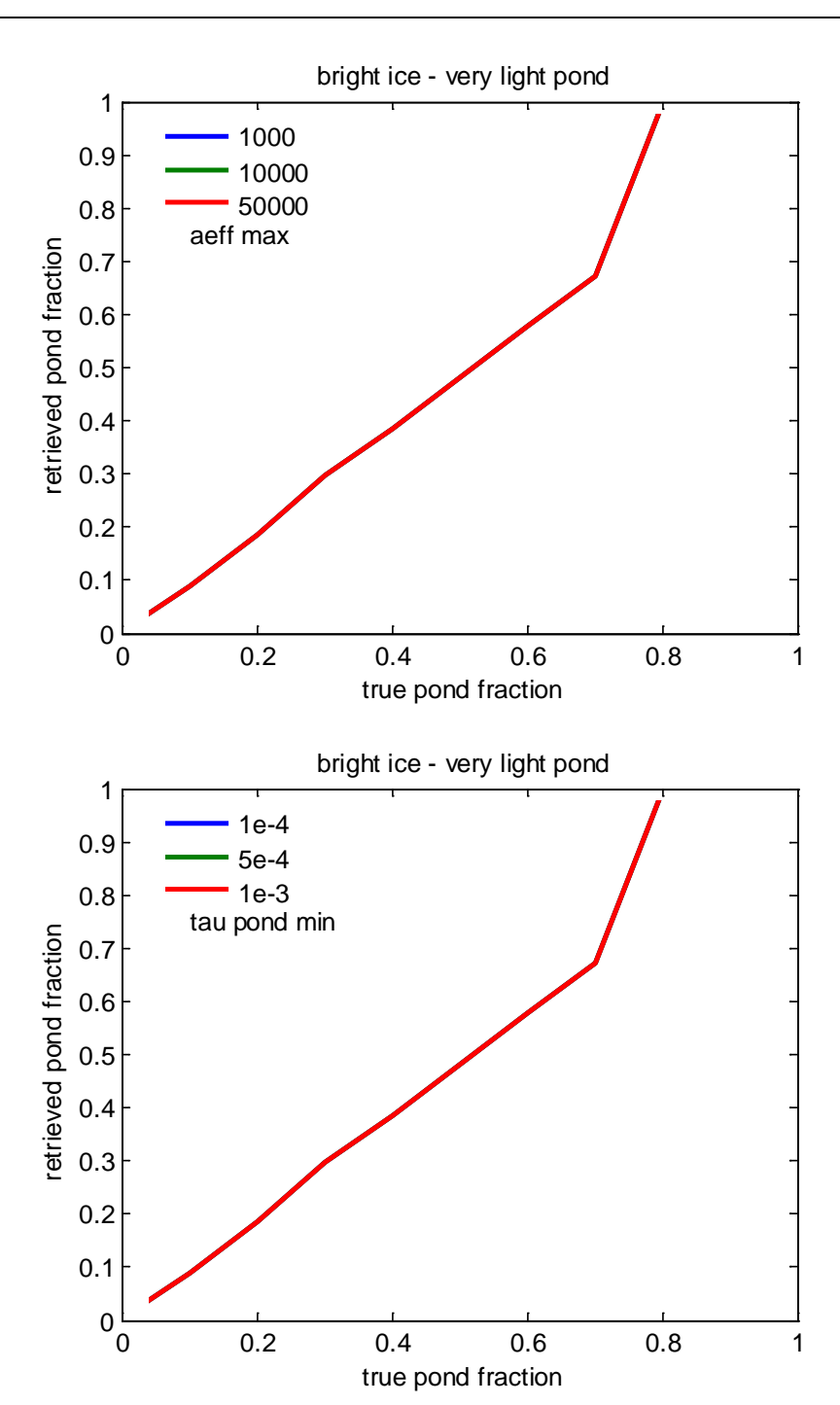


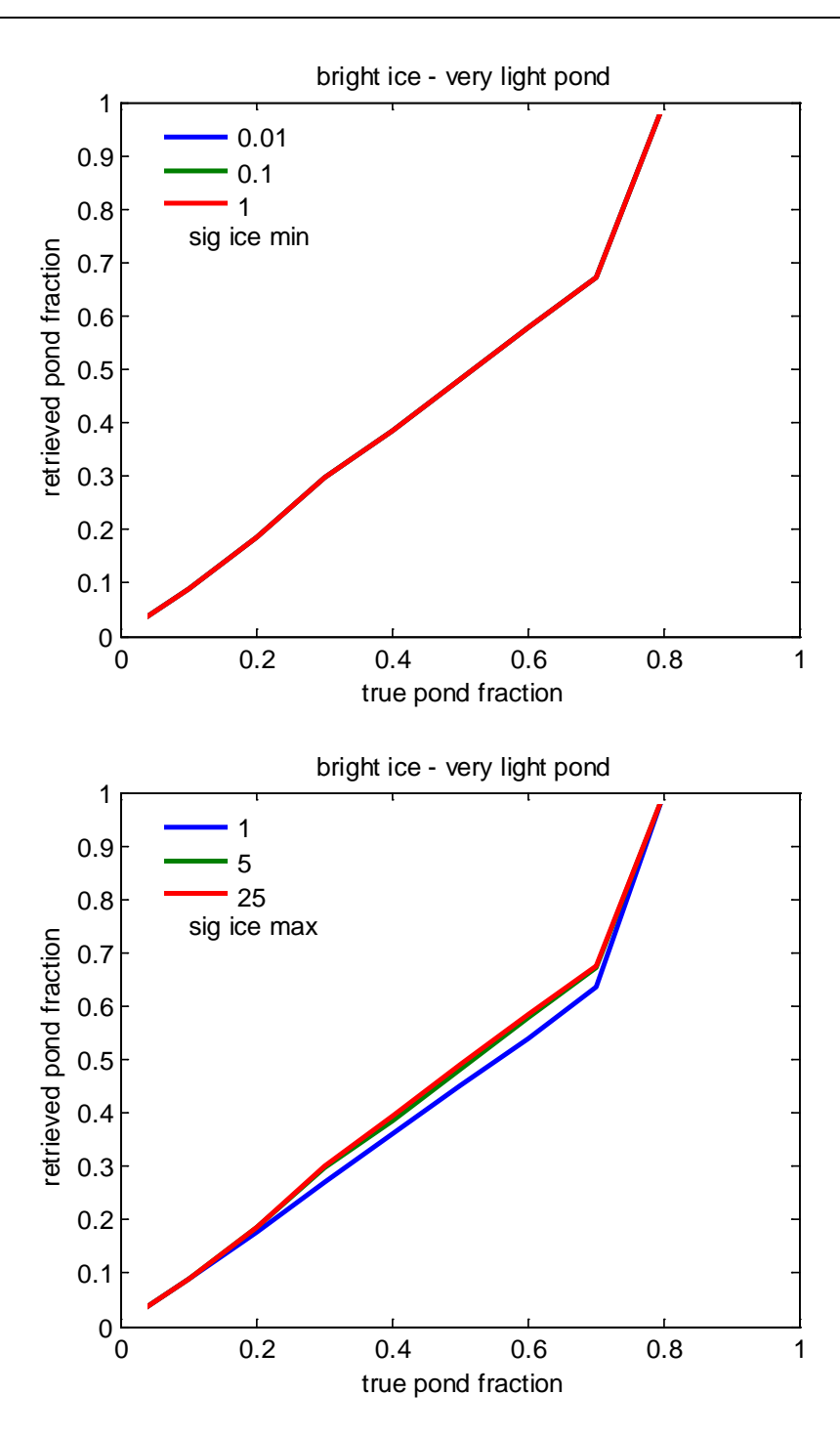


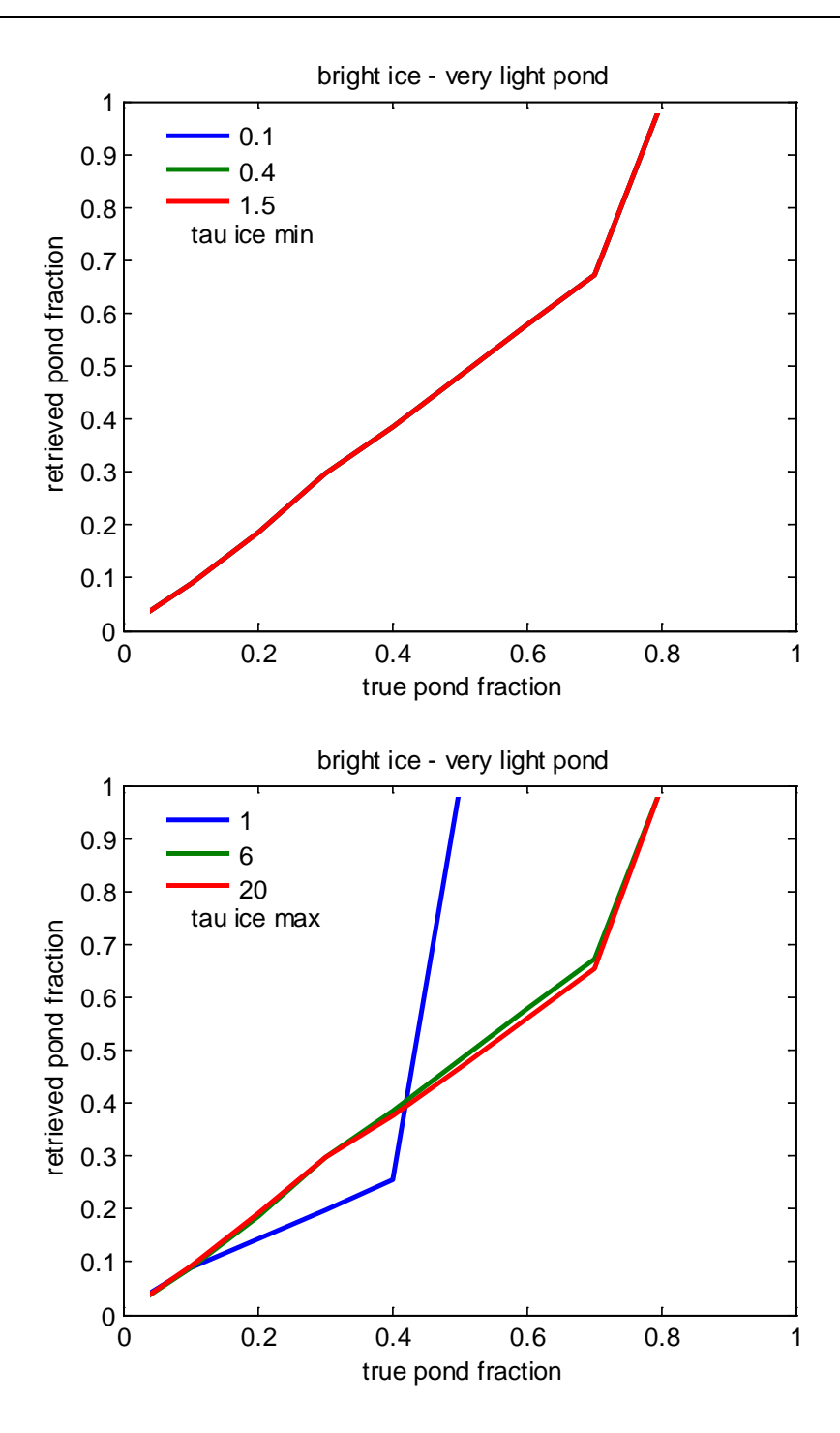


# Bright ice & very light pond

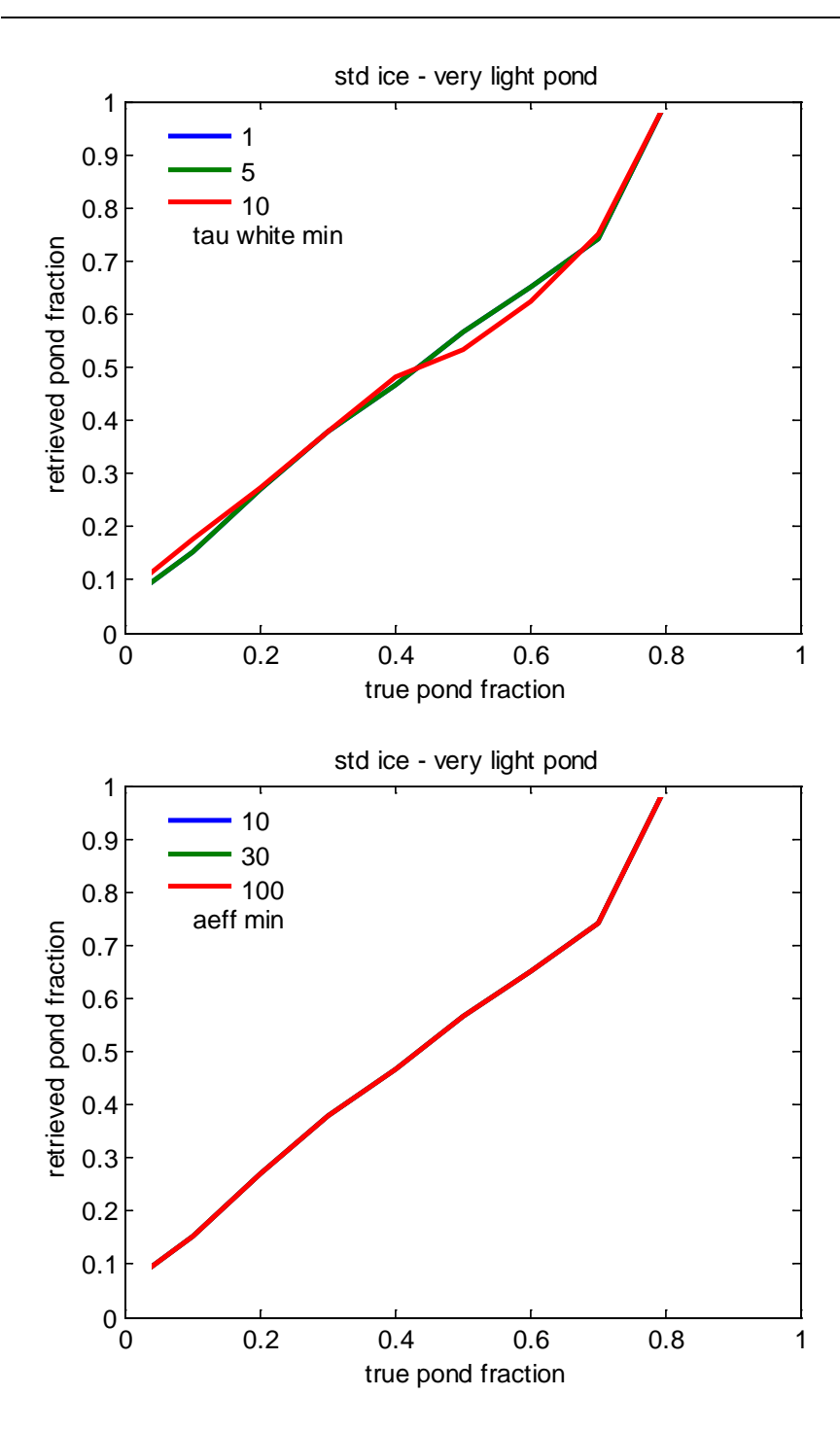


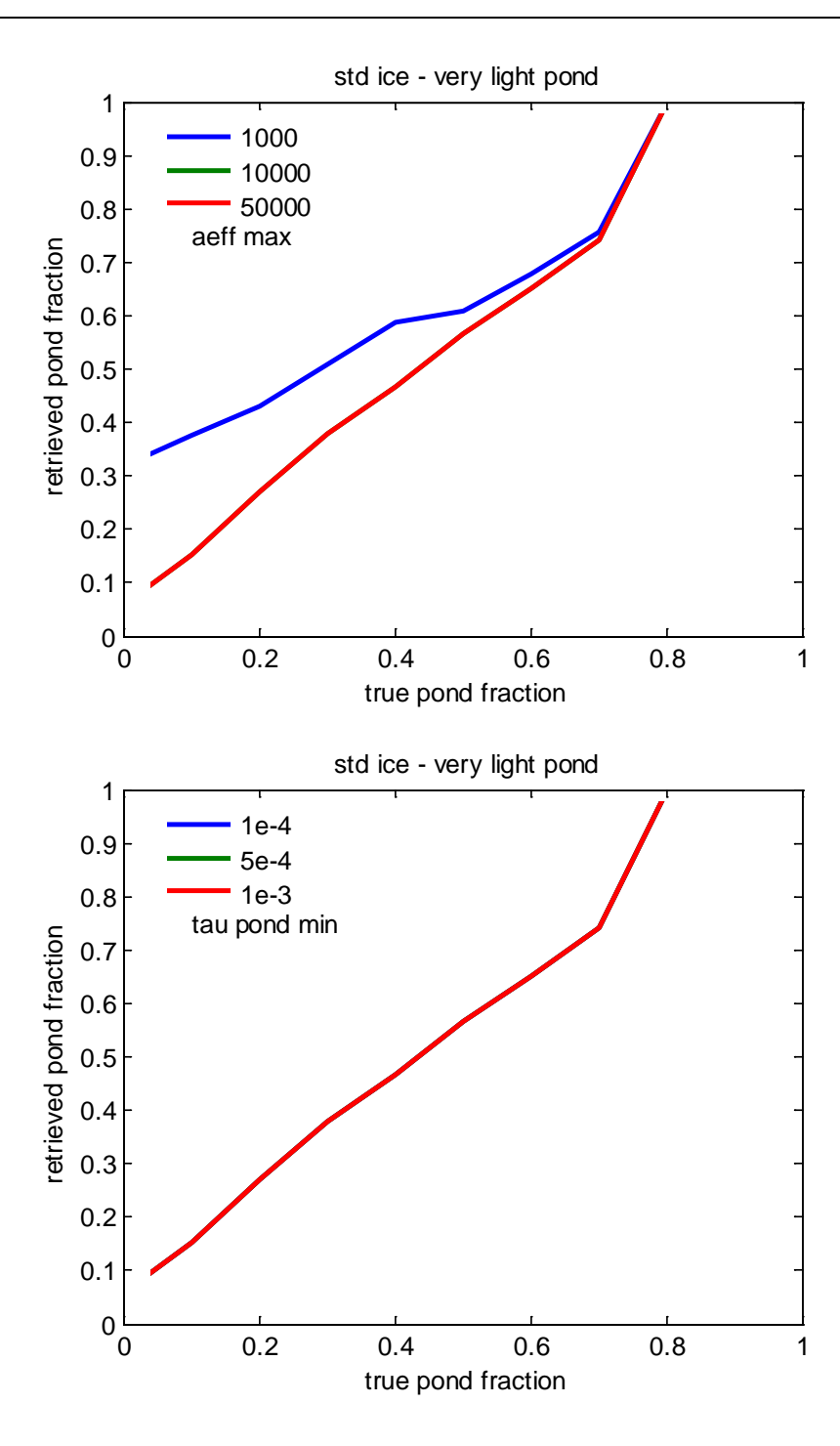


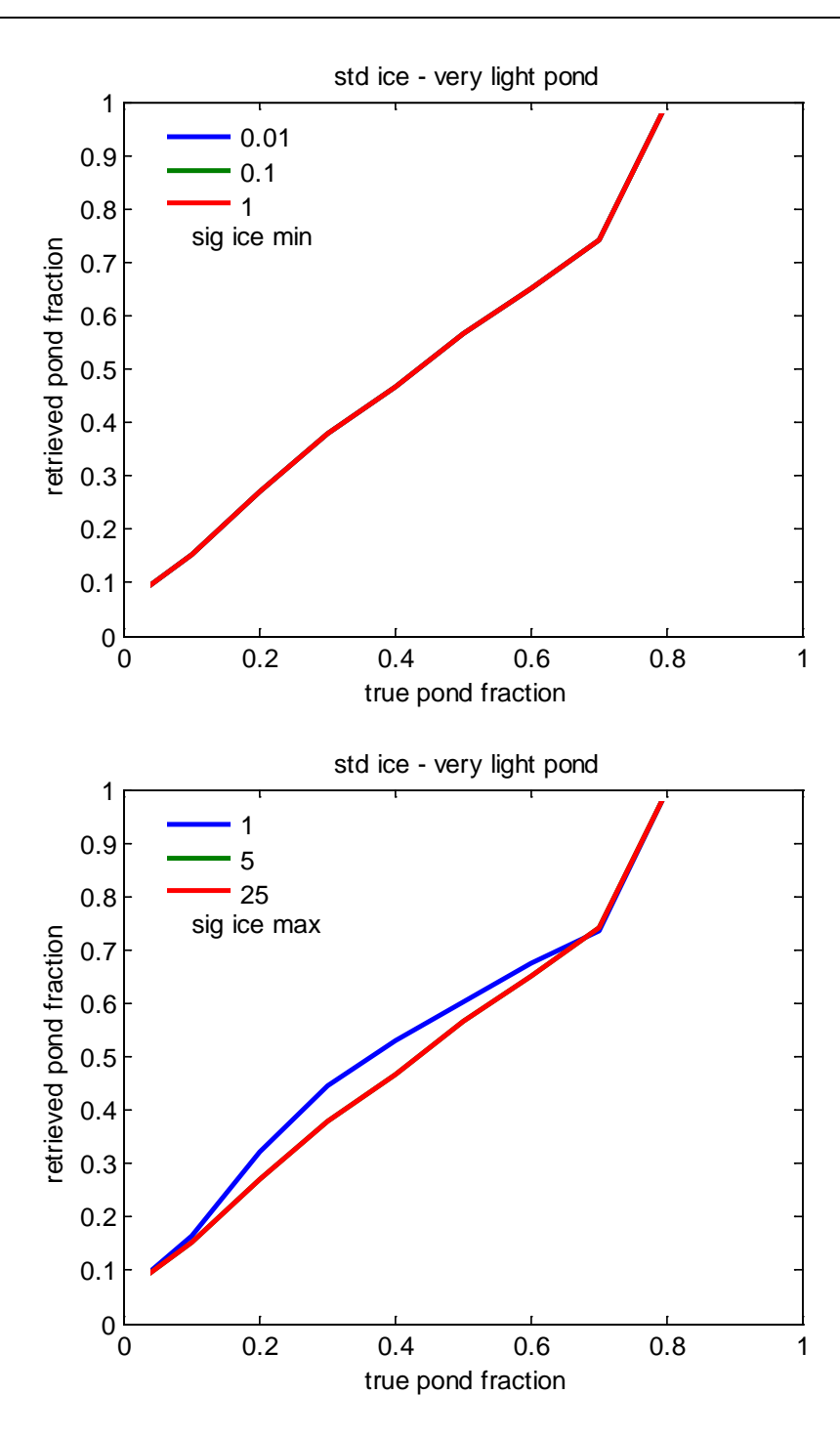


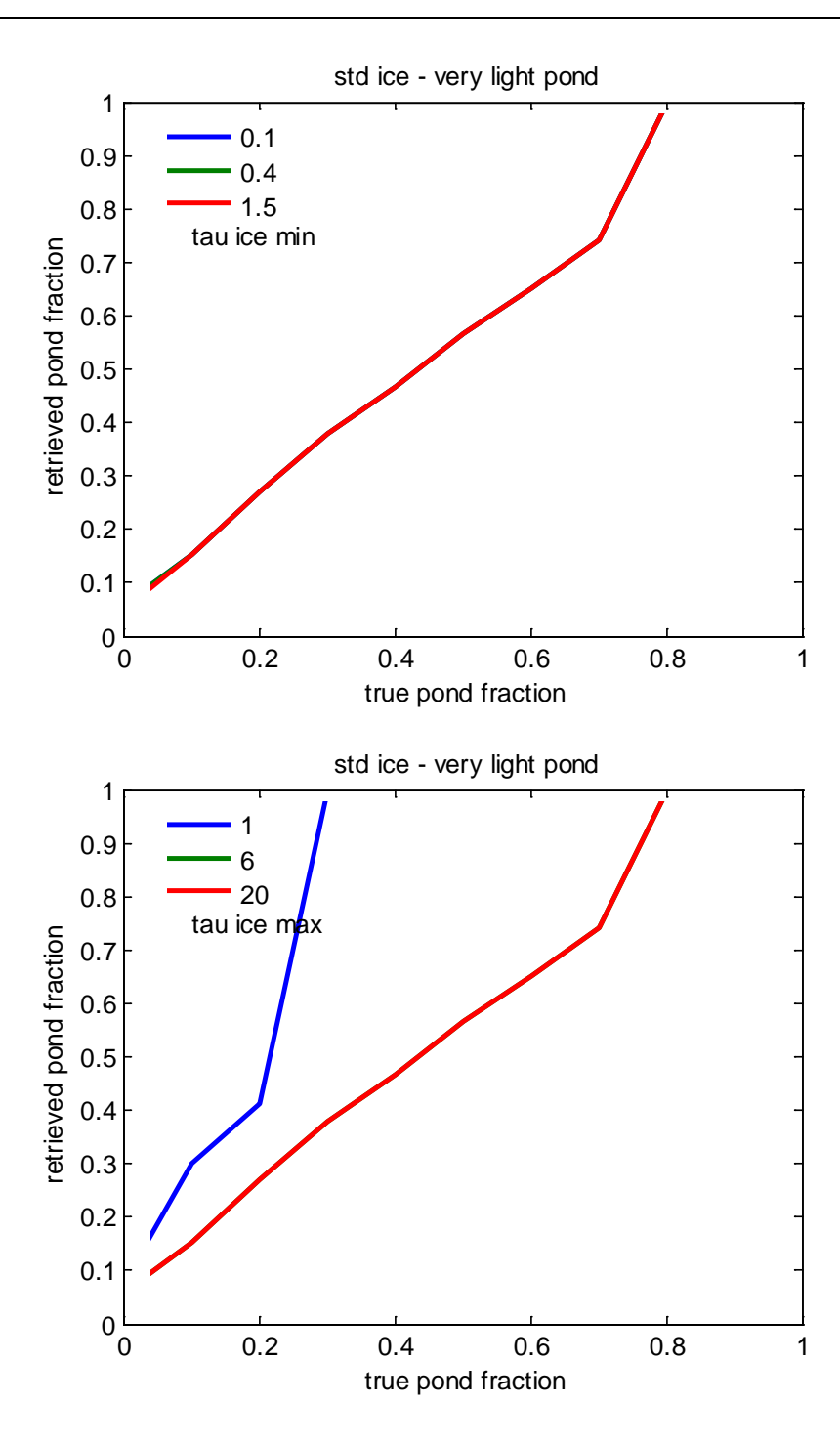


# Standard ice & very light pond

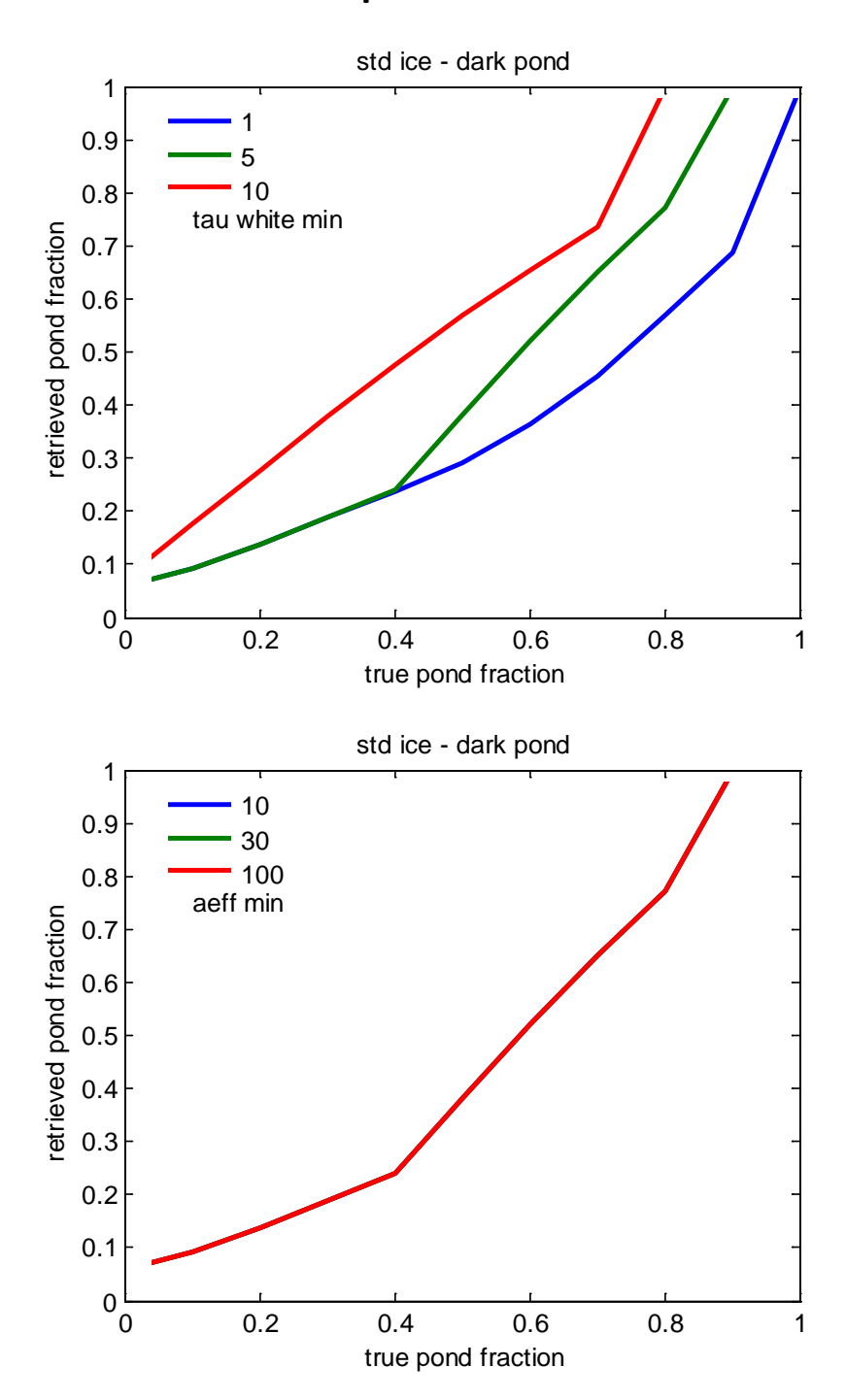


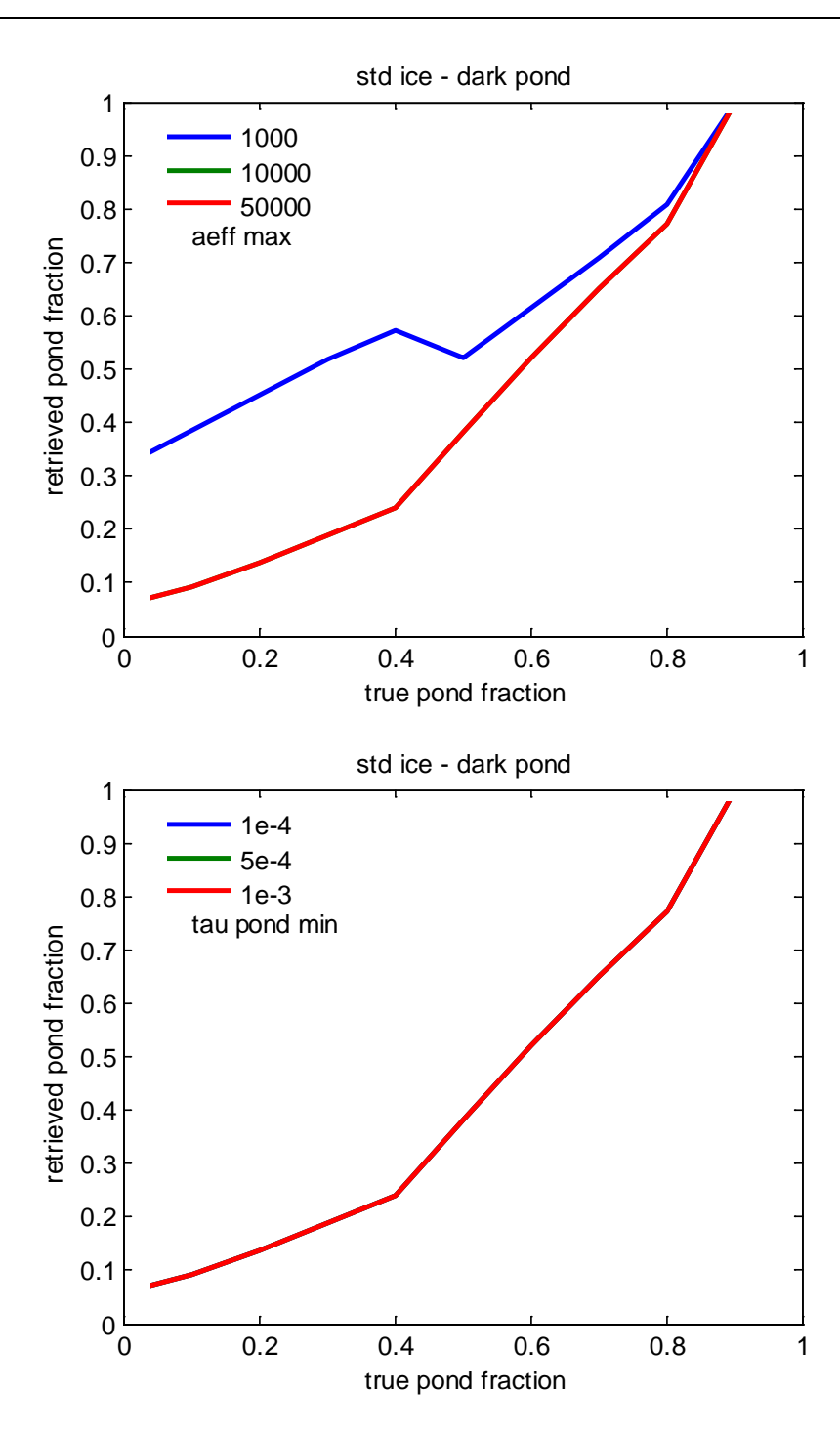


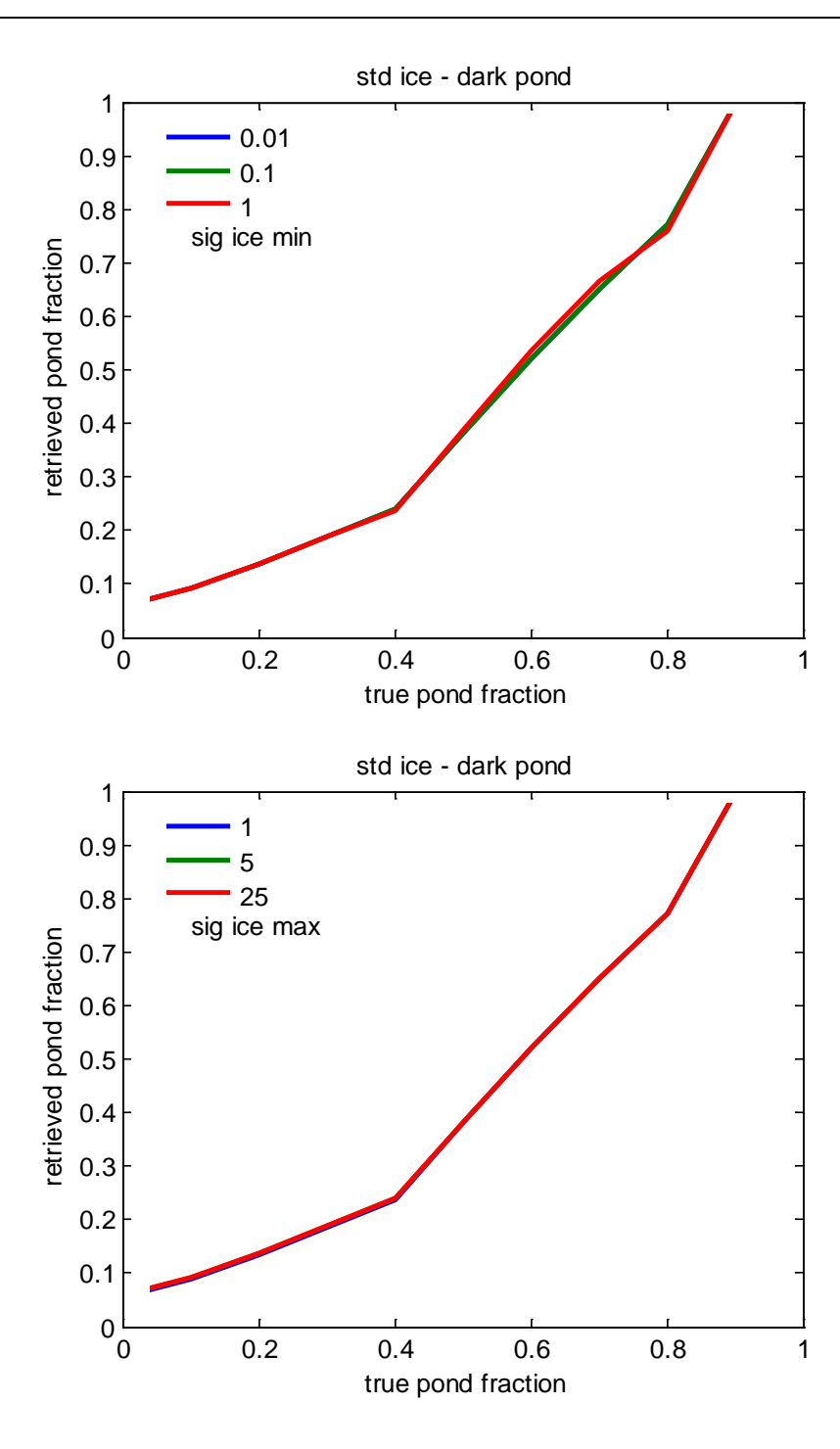


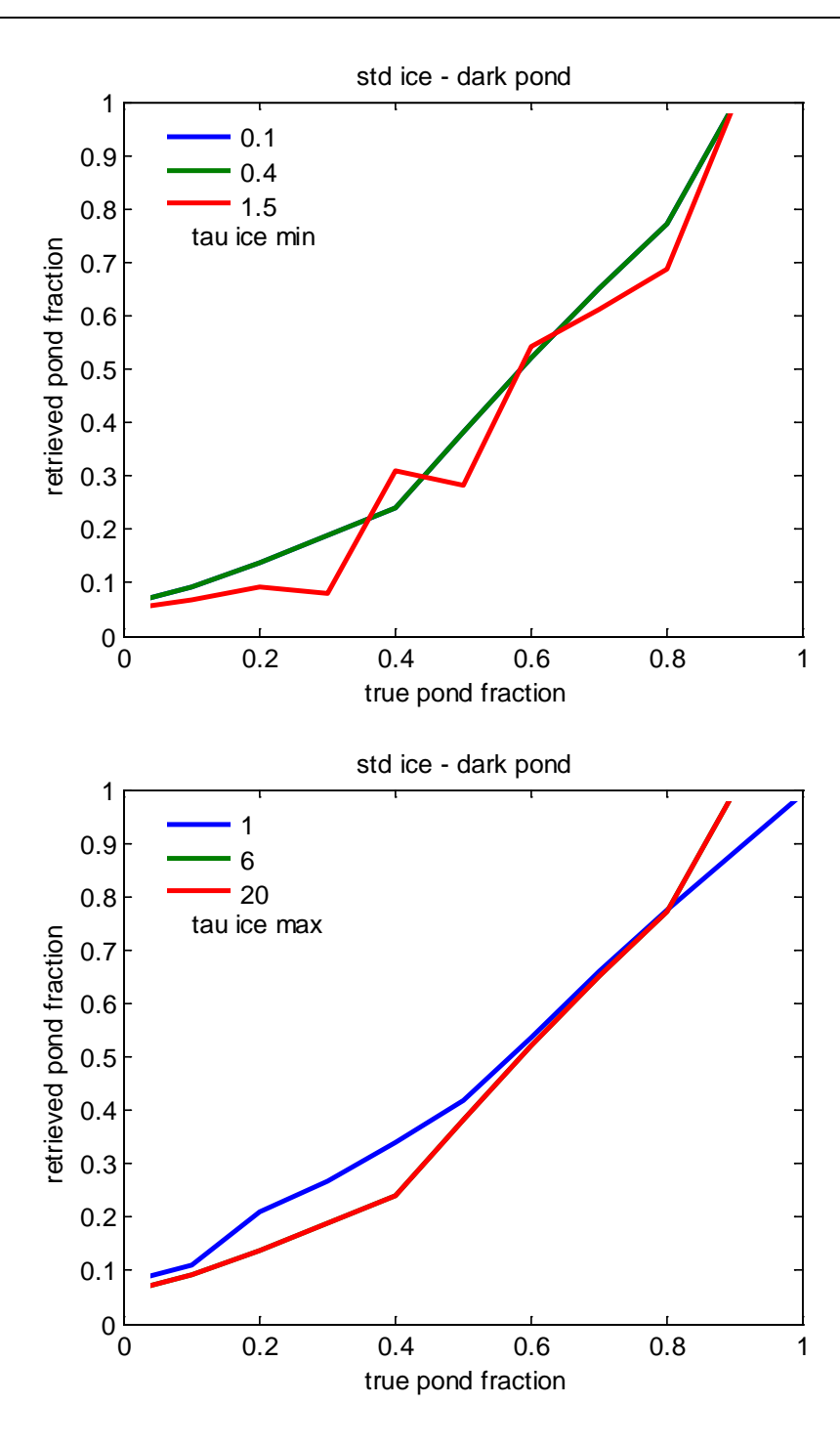


# Standard ice & dark pond

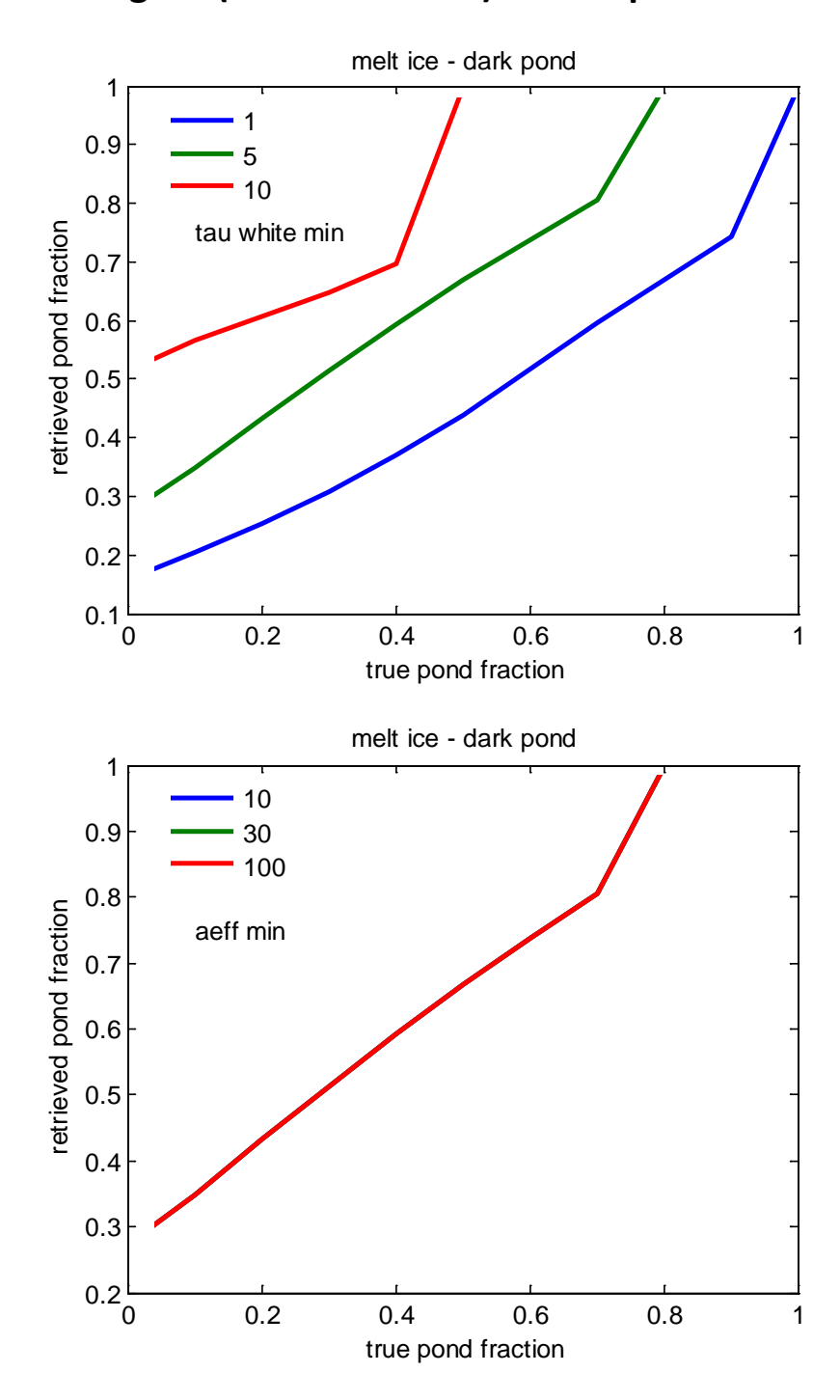


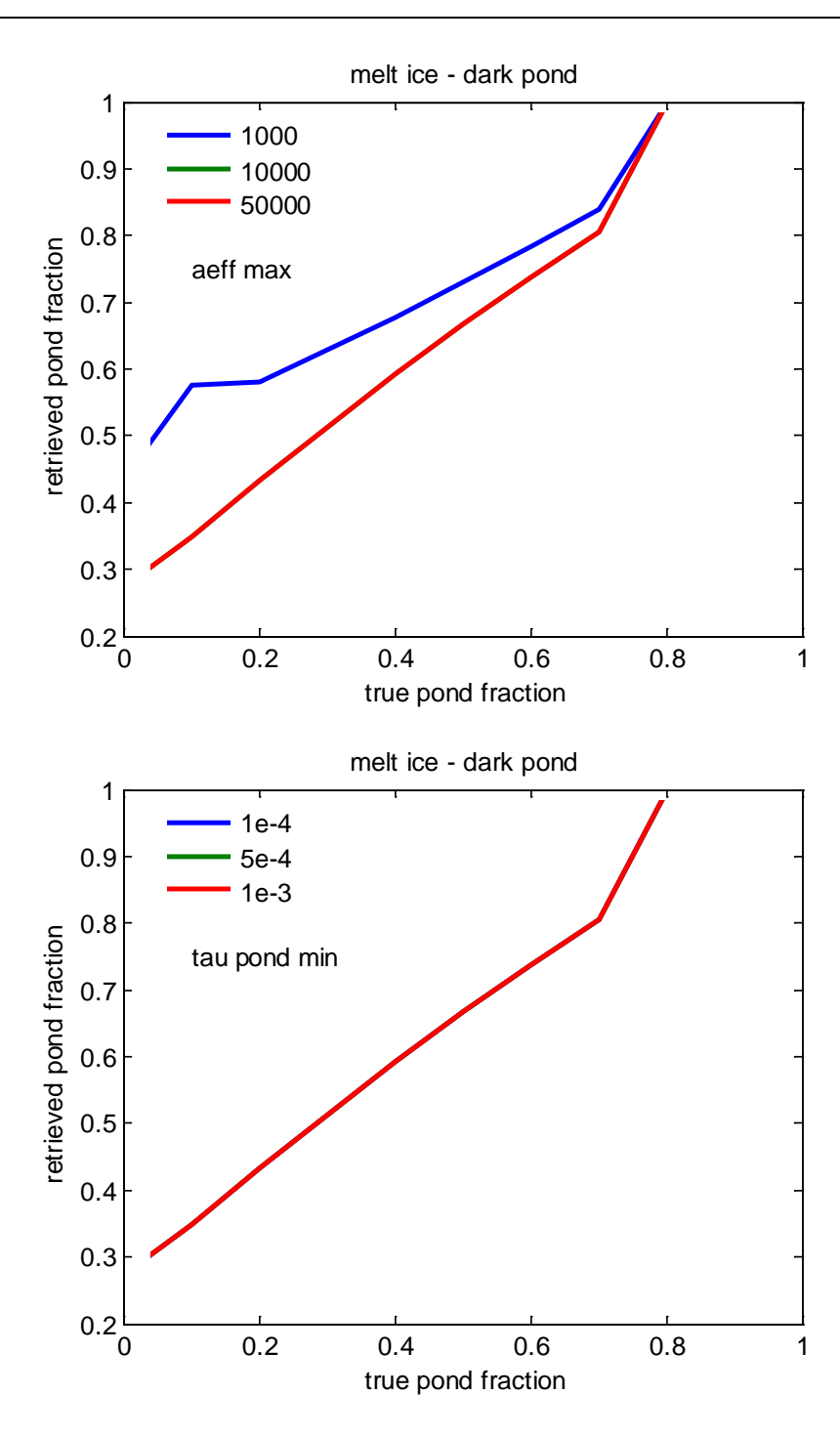


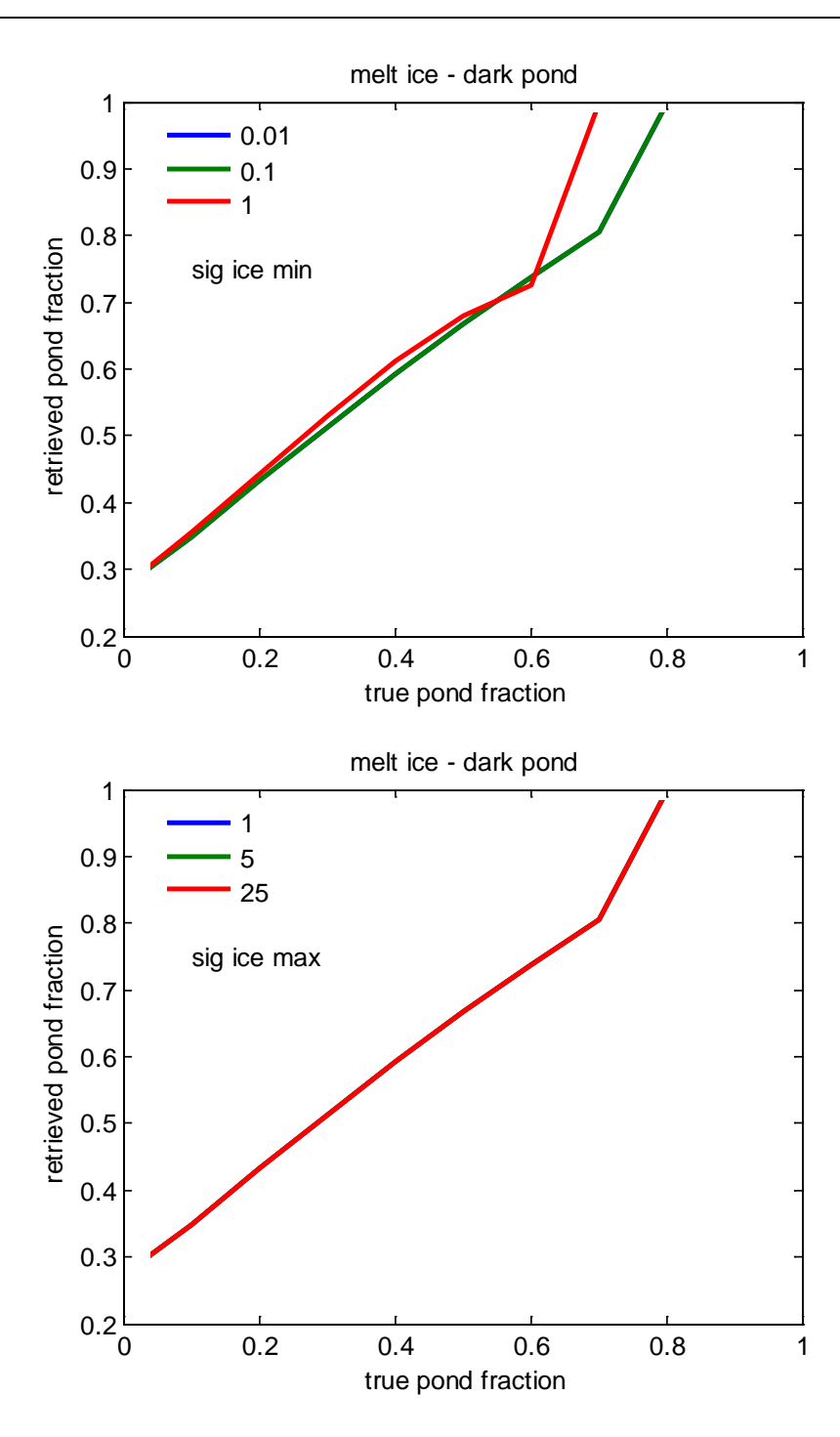


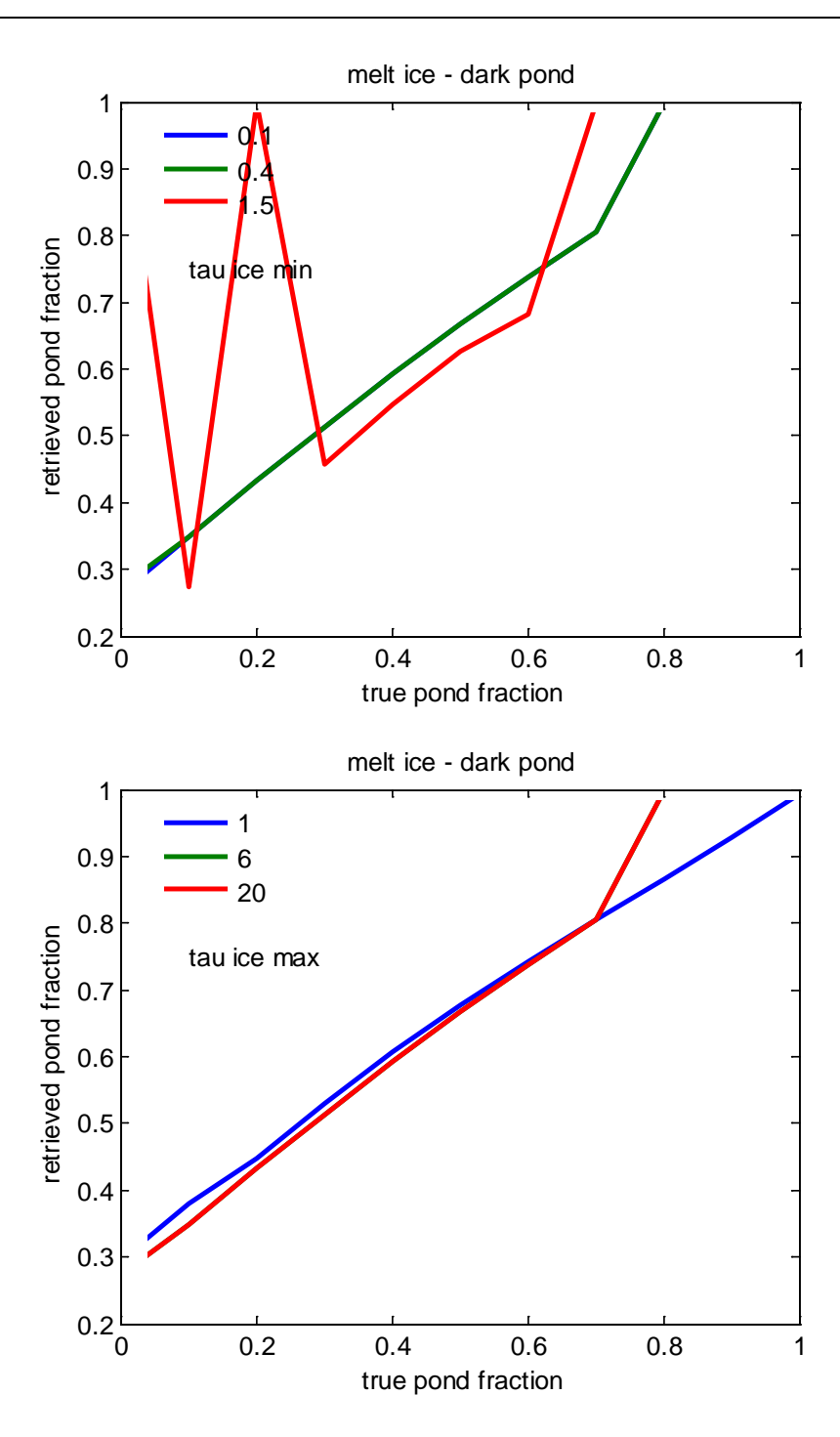


# Melting ice (outside border) & dark pond









# 5 Appendix C

This Section provides instructions for installing and running the MPD (Melt Pond Detection) software version 1.55.

## 5.1 Introduction

This document describes how Melt Pond Detection software (MPD) can be installed and run on LINUX workstations and PCs. The program can also be installed and run under Microsoft WINDOWS, but it is out of this document scope.

Software input is MERIS L1B data product preprocessed by MERIS Level 1 Radiometry Processor included in the Basic ENVISAT Toolbox for A(ATSR) and MERIS (BEAM Version 4.9+). The BEAM Radiometry Processor performs SMILE correction, equalization, radiometric recalibration, and radiance to reflection conversion of MERIS data and saves data product in HDF5 file format.

Software product is the maps of the melt ponds area fraction and spectral pixel albedo (at up to six user defined spectral wavelengths in the region of 400 -900 nm) in HDF5 file format.

MPD software incorporates a radiative transfer model to provide atmospheric correction of MERIS data and contains data banks on atmospheric aerosols, atmospheric pressure and temperature stratifications, and trace gases concentrations for building atmosphere models. Also, software uses a lookup table for fast calculations of the ice reflectance.

The different control files are used to configure MPD software run parameters. They are:

- mpd.ini sets paths to software library locations;
- mpd xSect.ini sets files with parameters of trace gases absorption in MERIS spectral bands;
- files with "\*.cfg" extension set up MPD current run configuration;
- files with "\*.ast" extension set aerosol atmosphere model stratification;
- files with "\*.clm" extension set parameters of vertical distribution of molecular-gaseous atmosphere.

The detail descriptions of control files see in section 5.

MPD has been developed in C++ and tested under LINUX (Ubuntu 64 bit, GNU C++ compiler version 4:4.6.3-1ubuntu 5) and WINDOWS (Windows 7, Microsoft Visual Studio 2010, Microsoft Visual Studio 2012).

## 5.2 New features

#### 5.2.1 New features in version 1.55

The user can assign boundary values for most parameters (tau\_white\_MIN, aeff\_MIN, aeff\_MIN, sig\_ice\_MIN, sig\_ice\_MAX, tau\_ice\_MIN, tau\_ice\_MAX) in the new [boundaries] section of the file.cfg (see section 5.1). If any parameter value is omitted in run configuration file, the default value (see section 2.2) is used. Boundary values used in the run are saved in the log file.

#### **5.2.2** New features in version 1.50

- Refinement of the MPD algorithm:
  - 1. Earlier, it was recommended to retrieve melt pod fraction only for pixels flagged as FLAG\_MELTICE (the control file parameter **melt pond mapping** was set to 0, see section 5.1, **[run]** section). The MPD software version 1.50 processes reliably pixels with the flag FLAG\_SI\_NOT\_C. Moreover, pixels flagged as TOO\_BRIGHT are also not discarded in version 1.50. They are considered as pixels with no melt ponds (S=0) and processed as snow or bright ice surfaces. It allows retrieving melt pond fraction and albedo in larger areas. To do so, the control file parameter **melt pond mapping** should be set to 1 (see section 5.1, **[run]** section).
  - 2. Starting values for iteration process are changed. Now the starting value of tau\_white\_ice depends on the measured signal in the 3rd MERIS channel.
  - 3. The most parameters have the border values: they cannot be greater than MAX value or less than MIN value.

$$aeff\_MIN = 30.$$

$$aeff_MAX = 10000.$$

tau\_pond\_MIN=0.0005

$$sig\_ice\_MAX = 5.$$

$$tau\_ice\_MIN = 0.4$$

$$tau_ice_MAX = 6.$$

4. Output file has a field Precision, defined for every pixel as the root mean square of difference between measured and retrieved signals:

$$prec = \sqrt{\frac{1}{m} \sum_{i} (R_{meas}^{i} - R_{ret}^{i})^{2}}.$$

This value is a good estimation for the albedo retrieval error (absolute):

$$A_{true} = A_{ret} \pm prec,$$

and for the relative error of pond fraction retrieval (except the case S=0):

$$\frac{\Delta S}{S} = \sqrt{\frac{m}{n}} \frac{prec}{lev},$$

where m is the number of channels used, n is the number of parameters to retrieve, and lev is the level of regularization of the pseudo-inverse matrix. In this version:

$$m = 8$$
;  $n = 7$ ;  $lev = 0.0075$ .

That is

$$\frac{\Delta S}{S} = prec * 143.$$

#### 5.2.3 New features in version 1.20

- Melt pond detection algorithm improvement:
  - 1. Restrictions on the white ice characteristics are set (the nonabsorbing optical thickness *tau\_white* cannot be less than 5 and mean chord of the ice component *aeff* cannot be greater than 10000 microns);
  - 2. Pixels in which the melt pond area fraction *S\_meltpond* is 1, not discarded. Now, these pixels are treated as the ice surface, which are completely covered with a water layer.
- The additional runtime pixel classification criterion is added. If the root-mean-square deviation of the differences between satellite measured radiances and calculated ones (taken from the last iteration of pixel processing) exceeds a threshold value (0.02) the RTF\_LOW\_PRECISION flag (see section 6) for the pixel will be set (low precision for modeled TOA radiance).
- Map of the precision of modeled TOA radiances can be included in the output (see section 5.1, [run] section and section 6).

#### **5.2.4** New features in version 1.10

- The new output product maps of spectral pixel albedo (at up to six user defined spectral wavelengths in the region of 400 -900 nm) is added (see section 5.1, [atmo] section).
- The new parameter yellow matter absorption at 390 nm is included in the melt ponds detection algorithm (see section 6).
- The additional runtime pixel classification criterion is added. The radiance coefficients provided by the absolutely white surface at the top of atmosphere are calculated and compared with satellite data for pixels. If the satellite measured value in any spectral channel is greater than calculated one, the pixel will be discarded and RTF\_TOO\_BRIGHT flag (see section 6) for the pixel will be set (such a pixel does not fit to the melting ice model).
- To distinguish the "melting ice" from "snow" the criterion  $R_{TOA}\left(865nm\right) < 0.6$  is used instead of  $R_{TOA}\left(865nm\right) < 0.4$  one. Experience shows, that when 'melt pond mapping' parameter is set to 1 (see section 5.1, **[run]** section), the criterion  $R_{TOA}\left(865nm\right) < 0.4$  looks too strong and discards too many pixels.
- The new file format for the lookup table data of ice reflectance is used. The new lookup table data file is the *Rand3\_tau10000v2.dat* file (see section 5.4).

#### 5.3 How to install

Before you start you should have the following installed on your computer:

- 1. g++ compiler.
- 2. HDF5 library (runtime and development files).

Please check, that HDF5 library INCLUDE files and LIB files are placed in the compiler default library search path and in the default shared library search path.

Unpack MPD files to the location you wish to place software. Move to *mpd/Release/* directory and run *make*. After compilation you will find *mpd* executable file in this directory. Run *make clean* to delete all intermediate files.

Make sure, that *mpd.ini* and *mpd\_xSect.ini* control files are located in the program working directory and *mpd.ini* sets up correct paths to software library files.

Type "./mpd" to run software. If the program was built correctly you will see the screen output similar to following:

```
Melt ponds detection, SIDARUS project.
mpd version 1.00, build: Jun 5 2012.
mpd usage:
  mpd -c=run.cfg inp.h5 [out.h5]
  where
  run.cfg is the mpd config file;
  inp.h5 is the MPD_INPUT file;
  out.h5 is the output file.
```

#### 5.4 How to run

The command with three arguments:

```
./mpd -c=run.cfg inp.h5 [out.h5]
```

is used to run MPD software.

Argument '-c= run.cfg' sets the name of control file to configure run parameters (*run.cfg*). If this argument is omitted, the software tries to load run parameters from *default.cfg* file, which should be located in program working directory. The description of control files to configure run parameters see in section 5.1.

Argument 'inp.h5' is the pathname of the input file. That is the MERIS L1B data product (distributed in Envisat-1 file format as "\*.N1" files) processed by MERIS Level 1 Radiometry Processor included in the Basic ENVISAT Toolbox for A(ATSR) and MERIS (BEAM Version 4.9+). The BEAM Radiometry Processor performs SMILE correction, equalization, radiometric recalibration, and radiance to reflection conversion of MERIS data. HDF5 file format should be selected to save the processed product.

Argument 'out.h5' is the pathname of the output file. If omitted, the output file name will be the input file name prefixed with "r\_" (for example, 'r\_inp.h5'). The output file format is specified in section 6.

If the program run was successful you will see the following message at the end of the screen output:

```
... saving output file OK!

Completed successfully.
```

Before exit, the program creates log file named '[output\_file\_name].log'. This file contains data on input and application configuration, runtime messages and additional statistical data.

## 5.5 Control files

To set up run parameters MPD software uses control files in INI file format. These files are simple text files with a basic structure composed of "sections" and "properties". Every property has a "name" and a "value", delimited by an equals sign ("="). The name appears to the left of the equals sign:

name=value.

Properties may be grouped into arbitrarily named "sections". The section name appears on a line by itself, in square brackets ("[" and "]"). All properties after the section declaration are associated with that section. The order of properties in a section and the order of sections in a file are irrelevant. All lines beginning with "#" are comments line and are skipped while reading (also, as empty lines).

## **5.5.1** Control file to configure run parameters

Control files with "\*.cfg" extension are used to set up MPD run configuration defined by following parameters.

# 5.5.2 [atmo] section

#### aerosol stratification file

The parameter defines the name of the control file with extension "\*.ast" to set up the aerosol atmosphere model stratification. Such control files are located in the /ast/ subdirectory of the software library. These files format is specified in section 5.2.

# atmospheric profile file

The parameter defines the name of the control file with extension "\*.clm" to set up parameters of vertical distribution of molecular-gaseous atmosphere. These control files are located in the /clm/ subdirectory of the software library. For user convenience the software library contains standard LOWTRAN models of molecular-gaseous atmosphere stratification (MidlatitudeSummer.clm, MidlatitudeWinter.clm, SubarcticSummer.clm, SubarcticWinter.clm, TropicalAtmosphere.clm, USStandard1976.clm). Also there are monthly and latitudinal dependent models, which are built using McLinden and MPI Mainz climatology data (from SCIATRAN databanks). The corresponding

filenames have the following structure: "mon{xx}lat{yy}{z]\_mcl.clm", where "{xx}" denotes the number of the month (01 = January, 02 = February, ..., 12 = December), "{yy}" denotes the latitude band (05 = 0 - 10 deg, 15 = 10 - 20 deg, ..., 85 = 80 - 90 deg), and "{z}" denotes the hemisphere (n = Northern Hemisphere, s = Southern Hemisphere).

The "\*.clm" files format is specified in section 5.3.

**H2O** 

03

02

04

NO<sub>2</sub>

NO<sub>3</sub>

If the parameter value is set to 1, the absorption of the corresponding atmospheric trace gas will be taken into account. Set the parameter value to 0 to exclude absorption of the gas from calculations.

#### Earth's surface elevation

This parameter defines the mean surface height above sea level in km. All the parameters of molecular-gaseous atmosphere will be calculated only for layers above this value. Allowed value range is [0 .. 8km].

#### new precipitable water

If the parameter value is empty, the water vapor amount defined by assigned climatological mode is used. The user can set new precipitable water amount (allowed value range is [0.1 .. 10] g\*cm-2). However, the relative vertical distribution of water vapor remains unchanged.

#### new ozone amount

If the parameter value is empty, the ozone amount defined by assigned climatological model is used. The user can set new ozone amount (allowed value range is [0.1 .. 1] atm\*cm). However, the relative vertical distribution of ozone remains unchanged.

## 5.5.3 [MERIS\_data] section

channel #1

channel #2

channel #3

channel #4

channel #5

channel #6

channel #7

channel #8

These parameters are the numbers of MERIS bands used in melt ponds detection algorithm. They should be ordered from #1 to #8 with band wavelength increasing. Allowed values range is [1 .. 15].

# 5.5.4 [run] section

## melt pond mapping

This parameter sets up the melt ponds mapping algorithm. Allowed values are:

0 – pixels over snow or ice (pixels with flag FLAG\_SI\_NOT\_C) are processed;

1 – pixels over melting ice (pixels with flag FLAG\_MELTICE) are processed.

# 5.5.5 [albedo] section

albedo\_1

albedo\_2

albedo\_3

albedo\_4

albedo\_5

albedo\_6

These parameters define wavelength values for spectral albedo computation. If assigned wavelength value is in the range of [400.0 .. 900.0] nm the map of pixel albedo at this wavelength will be calculated and included in output file.

# 5.5.6 [RAY\_preferences] section

# depolarization factor

The parameter defines the depolarization factor for molecular scattering matrix, allowed value range is [0..09].

#### vector computation

If the parameter is set to 0, the scalar algorithm is used while calculating light scattering parameters in the atmosphere; else the polarization effects are taken into account.

#### harmonics number

It is the number of azimuthal harmonics, which are taken into account while performing light scattering calculations. Allowed value range is [1 .. 14].

## 5.5.7 [save] section

#### output flag

This parameter allows the user to include additional data in output file. Allowed values are:

```
0 (or empty) - no additional data;
```

- 1 maps of TOA reflections for MERIS bands used in melt ponds detection algorithm, maps of the cosines of the Sun and sensor zenith angles, and the map of Sun-viewing azimuths;
- 2 maps of intermediate parameters, calculated in melt pond detection algorithm:
  - white ice nonabsorbing optical thickness;
  - mean chord;
  - yellow matter absorption at 390nm;
  - melt pond optical depth;
  - transport scattering coefficient of the underlying ice;
  - optical depth of the underlying ice.
- 3-1 and 2 together;
- 4 the map of the precision of modeled TOA radiances;
- 5-1 and 4 together;
- 6 2 and 4 together;
- 7 1, 2, and 4 together.

# full size tie point grids

If the parameter value is 0, latitude and longitude Geolocation SDSs from input MERIS file are simply copied to the output file, else the latitude and longitude SDSs interpolated to the full scene resolution are saved.

#### detailed Log file

If the parameter value is non-zero the detail information about radiative transfer calculation procedures will be included in the log file.

#### atmo model file

This parameter specifies the name of the file to save the detailed tables with stratification of microphysical and optical characteristics of the atmosphere model. If empty, no file created.

## 5.5.8 [boundaries] section

tau\_white\_MIN
aeff\_MIN
aeff\_MAX
tau\_pond\_MIN
sig\_ice\_Min
sig\_ice\_MAX
tau\_ice\_MIN
tau\_ice\_MAX

These parameters define boundary values for *tau\_white*, *aeff*, *tau\_pond*, *sig\_ice*, and *tau\_ice*. If any parameter value is omitted in run configuration file, the default value (see section 2.2) is used. Boundary values used in the run are saved in the log file.

# 5.6 Control file to set aerosol atmosphere model stratification

Control files with "\*.ast" extension are used to set aerosol atmosphere model stratification. The atmosphere model includes up to three different aerosol layers. Their parameters are set up in the sections (from top layer to bottom layer) [sol\_layer3], [sol\_layer2], [sol\_layer1]. Every section contains the following parameters:

#### aerosol type

This parameter value is the name of the aerosol list file. This file contains the list of all databank files on optical properties of the given aerosol type. If aerosol type=NULL (or/and green optical thickness=0) there is no aerosol in the layer.

#### altitude

This is the aerosol layer upper border height above Earth's surface elevation, in km. Allowed value range is [0.1 .. 50] km. The layers should be ordered by altitude ([sol\_layer1] is the lowest one) and thickness of each layer should not be less than 1km.

#### green optical thickness

This is the aerosol layer optical thickness at wavelength 550nm. Allowed value range is [0 .. 10]. If green optical thickness=0 (or/and aerosol type=NULL) there is no aerosol in the layer.

# 5.6.1 [atmo] section

#### **ALFA**

The parameter defines the exponent of aerosol vertical profile in the lower aerosol layer ([sol\_layer1]). Allowed value range is [0 .. 2] 1/km.

#### **MRV**

This is meteorological range of visibility in km. Parameter is not used in current code version.

# 5.7 Control file to set model of molecular-gaseous atmosphere

Control files with extension "\*.clm" are used to set parameters of vertical distribution of molecular-gaseous atmosphere. These files are located in the /clm/ subdirectory of the software library and define following parameters.

# 5.7.1 [air\_density] section

#### **Pres**

This is the name of the atmospheric pressure stratification model file ("\*.pres" files located in the /mol/ directory)

Т

This is the name of the atmospheric temperature stratification model file ("\*.T" files located in the /mol/ directory).

# 5.7.2 [atmospheric\_gases] section

**H2O** 

03

02

CO<sub>2</sub>

CH4

NO2

CO

NO3

**OCIO** 

These parameters define the names of the corresponding trace gases stratification model files, located in the /mol/ directory. There is no CO2, CH4, CO, and OCIO absorption (or it is negligible) in MERIS bands. So, stratification model files of these trace gases are not used in the current code version.

# 5.8 mpd.ini control file

The *mpd.ini* control file is located in program working directory and sets up paths to software library files. In the current code version the only **[libs]** section contains following parameters:

#### **PathToAstLib**

This is path to directory for control files to set aerosol atmosphere model stratification (files with "\*.ast" extension).

### **PathToClmLib**

This is path to directory for control files to set parameters of vertical distribution of molecular-gaseous atmosphere (files with "\*.clm" extension).

## **PathToMolLib**

This is the path to the /mol/ directory.

#### **PathToSolLib**

This is the path to the /sol/ directory.

## **PathToGxsLib**

This is the path to library files with parameters of trace gases absorption in MERIS spectral bands.

#### **PathToAngDat**

This is the pathname of the file with the current angle scale of the aerosol databanks. That is the \_Angle.ang file in the /sol/ directory.

## **PathToIceDat**

This is the pathname of the file with the spectral properties of the indices of refraction for ice. That is the *Ice2007.ri* file in the */dat/* directory.

#### **PathToWtrDat**

This is the pathname of the file with the spectral properties of the indices of refraction for water. That is the *Water.ri* file in the */dat/* directory.

## **PathToIceTab**

This is the pathname of the file with the lookup table data for ice reflectance. That is the Rand3\_tau10000v2.dat file in the /dat/ directory.

# 5.9 Mpd\_xSect.ini control file

The *mpd\_xSect.ini* control file is located in program working directory. The parameters of only **[channels]** section set names of the files with parameters of trace gases absorption in corresponding MERIS spectral bands.

# 5.10 Output file

The output file specification is the same as BEAM used to save the row data products in HDF5 file format. Following groups and datasets can be present in the output file:

```
/
/bands
/bands/S_meltpond
/bands/Precision
/bands/albedo_1
/bands/albedo_2
/bands/albedo_3
/bands/albedo_4
```

```
/bands/albedo_5
/bands/albedo_6
/bands/flags_cl
/bands/flags_rt
/bands/R_1
/bands/R_2
/bands/R_3
/bands/R_8
/bands/R_10
/bands/R_12
/bands/R_13
/bands/R_14
/bands/mu
/bands/mu0
/bands/azimuth
/bands/aeff
/bands/sig_ice
/bands/tau_ice
/bands/tau_pond
/bands/tau_white
/bands/yma390
/flag_codings
/flag_codings/flags_cl
/flag_codings/flags_rt
/tie_point_grids
/tie_point_grids/latitude
/tie_point_grids/longitude
```

/ - the root group contains the following global attributes:

```
format - the sign of the file type (MPD_OUTPUT);

version - the version of file format specification;

producer – the name of the program that created the file;

nbands - the number of datasets which present row data in different spectral bands;

raster_width - the scene raster width in pixels;

raster_height - the scene raster height in pixels.

/bands group contains datasets with the full scene resolution. They are:
```

/bands/S\_meltpond - the map of the melt ponds area fraction, dimensionless;

/bands/albedo\_{N}- ({N} is an index of spectral albedo map) up to 6 datasets with maps of spectral albedo at user defined wavelengths , dimensionless;

/bands/flags\_cl - the classification flags set up by melt pond pixel mapping;

/bands/flags rt - the runtime flags returned by the melt pond detection algorithm;

If the bit 0 (the least significant bit in the byte) of the 'output flag' parameter in the configuration file is set to 1, the /bands group also contains:

/bands/R\_{N}— ({N} is the number of MERIS channel) 8 datasets with maps of TOA reflections for MERIS bands used in melt ponds detection algorithm, dimensionless.

/bands/mu – the map of the cosines of sensor zenith angels, dimensionless;

/bands/mu0 – the map of cosines of the Sun zenith angels, dimensionless;

/bands/azimuth – the map of the Sun-viewing azimuths, radians.

Also, if the bit 1 of the 'output flag' parameter in the configuration file is set to 1, the /bands group additionally contains the datasets with intermediate parameters calculated in melt pond detection algorithm:

/bands/aeff - the map of the stereological mean chord of the ice component, microns;

/bands/sig\_ice - the map of the transport scattering coefficients of the underlying ice, 1/m;

/bands/tau\_ice - the map of the optical depths of the underlying ice, dimensionless;

/bands/tau\_pond - the map of the melt pond optical depths, dimensionless;

/bands/tau white - the map of the white ice nonabsorbing optical thickness, dimensionless;

/bands/yma390 – the map of the yellow matter absorption at 390nm, 1/m.

If the bit 2 of the 'output flag' parameter in the configuration file is set to 1, the /bands group additionally contains the dataset:

/bands/Precision – the map of the precision of modeled TOA radiances.

/flag\_codings group contains the groups with flag coding description:

/flag\_codings/flags\_cl – the group attributes give the coding of classification flags:

FLAG\_NO\_DATA - pixel data is out of range;

FLAG\_WATER - pixel is valid, not coastline and over water;

FLAG\_BRIGHT - pixel is over cloud/snow/ice;

FLAG\_SI\_NOT\_C - pixel is over snow/ice and not over cloud;

FLAG\_MELTICE - pixel is over melting cloud free ice.

/flag\_codings/flags\_rt – the group attributes give the coding of runtime flags:

RTF\_LACK\_OF\_ITERATIONS - pixel with weak convergence;

RTF\_NO\_CONVERGENCE - no convergence in singular value decomposition;

RTF\_NOT\_PROCESSED - pixel is not processed;

RTF\_TOO\_BRIGHT - pixel does not fit to the melting ice model;

RTF\_LOW\_PRECISION - low precision for modeled TOA radiance.

/tie\_point\_grids group contains the datasets which provide less sample data than full scene resolution datasets in the /band group. The group contain following datasets

/tie\_point\_grids/latitude - the latitudes of the tie points (WGS-84), positive N, degree;

/tie\_point\_grids/longitude – the longitudes of the tie points (WGS-84), Greenwich origin, positive E, degree.